NTNU

Norwegian University of
Science and Technology

Effects of extreme precipitation and drought on the performance of filter medias for stormwater treatment

Henrik Winther Solemslie

Master's Thesis
Submission date: June 2017
Supervisor: Tone Merete Muthanna, IBM
Co-supervisor: Aamir Ilyas, IBM

Norwegian University of Science and Technology
Department of Civil and Environmental Engineering

Abstract

People are moving to the cities, and the climate is becoming more extreme. The growing urbanisation of the world population is causing massive expansion of new urban areas. These areas are filled with impervious surfaces generating large amounts of polluted runoff. In accordance with the low impact development strategy, municipalities are working towards returning urban runoff to its pre-development flow, volume, and purity. This is done with local retention, reduction, and treatment of urban runoff, before it is released to recipients. The pollution in urban runoffs originates mainly from traffic. It comes in both particulate, and dissolved form. The particulate pollutants have for a long time been removed through sedimentation basins. Among the dissolved pollutants are toxic metals such as zinc, lead, copper, and nickel. In the dissolved state these metals are both more bio-available, and more difficult to treat than in the particulate state. One of the most commonly used techniques of removing dissolved toxic metals are by adsorption on an active and commercially available filter media. These filter medias are often expensive, and the removal of dissolved toxic metals are therefore often discarded because of the cost of instalment and maintenance. Therefore, more research is being done to find new alternative adsorption material. New materials need to have documented, not only their removal rate of pollutants, but also that their removal rate are not affected by the extreme climate of the future. At the Department of Civil and Environmental Engineering, at the Norwegian University of Science and Technology, four alternative adsorption materials such as charcoal, pine bark, olivine, and bottom ash coated with iron oxide were selected for testing. The objectives of this thesis was to investigate how these alternative adsorption materials would be affected by extreme precipitation events and drought. The testing was conducted in pilot scale column experiments. In a continuous order, these materials experienced the hydraulic loads of three intensities and four different return periods precipitation events each - 5-minutes, 45-minutes, 180-minutes intensities, and 10-years, 50-years, 100-years, and 200-years return periods. In addition, the material was subjected to four dry periods of 7 to 34 days, interrupted by extreme precipitation events between the dry periods. Samples were taken both during the extreme precipitation simulations and 24 hours after each simulation. The results show that the extreme precipitation events had catastrophic effect on the pine bark and charcoal. The olivine and bottom ash, however, were hardly affected with a stable high removal rate throughout the whole experimental period.

For a filter covering 1 % of the catchment and in combination with a particle removal step, a design depth of 5 cm of either olivine or bottom ash with iron oxide will suffice for removing toxic metals from urban runoff.

Sammendrag

Mennesker flytter til byene, og klimaet blir mer ekstremt. Den voksende urbaniseringen av verdensbefolkningen forårsaker massiv utbygging av nye byområder. Disse områdene er fylt med tette flater som genererer store mengder forurenset avrenning. I samsvar med blå-grønn strategi, arbeider kommunene med å returnere urban hydrologi til slik den var før utbygging. Dette innebærer avrenningsvolum, hastighet, og renhet. Dette gjøres med lokale tiltak for fordrøyning, reduksjon og behandling av avrenningen. Forurensning i urban avrenning stammer hovedsakelig fra trafikken. Den kommer både i partikulær form, og oppløst form. Den partikulære forurensninger har lenge blitt behandlet med sedimentasjonsbasseng. Blant de oppløste forurensninger finnes giftige metaller som sink, bly, kobber, og nikkel. I oppløst tilstand er disse metallene både mer bio-tilgjengelig og vanskeligere å behandle enn i partikulær form. En av de meste brukte metodene for behandling a oppløste gifte metaller er ved adsorpsjon på et aktivt, og kommersielt tilgjengelig, filtermedium. Disse filtermediene er ofte dyre, og behandling av giftige metaller i oppløst form blir derfor ofte unnlat på grunn av kostnadene for etablering og vedlikehold. Derfor foregår det mye forskning for å finne et nytt alternativt adsorpsjonsmateriale. Nye materialer må ha dokumenter, ikke bare deres adsorpsjonsrate for giftige forurensninger, men også hvordan fremtidens ekstreme klima vil påvirke adsorpsjonsraten. Ved Institutt for bygg- og miljøteknikk, ved Norges teknisk-naturvitenskapelige universitet, ble fire alternative adsorpsjonsmaterialer kull, furu bark, olivin, og bunnaske dekket med jernoksid valgt for videre testing. Målet med denne oppgaven var å undersøke hvordan disse alternative adsorpsjonsmaterialene ville bli påvirket av ekstreme nedbørshendelser og tørke. Testingen ble utført i pilotskala kolonneeksperimenter. I en kontinuerlig rekke eksperimenter ble hvert materiale utsatt for nedbørssimuleringer av tre intensiteter og fire forskjellige returperioder – 5 minutter, 35 minutter, 180 minutter intensiteter og 10-års, 50-års, 100-års, og 200-års returperioder. I tillegg ble materialene tørket i fire perioder på mellom 7 og 34 dager, avbrutt av ekstreme nedbørshendelser mellom hver tørkeperiode. Prøver ble tatt både under simulering av ekstremnedbør, og 24 timer etter hver simulering. Resultatene viser at ekstreme nedbørshendelser hadde katastrofal påvirkning på furu bark og kull. Olivin og bunnaske ble derimot ikke påvirket og hadde en stabil høy adsorpsjonsrate gjennom hele forsøksperioden.

For filter som dekker 1 % av nedbørsfeltet, og i kombinasjon med tiltak for fjerning av partikler, vil en filterdybde på 5 cm av enten olivin, eller bunnaske med jernoksid være tilstrekkelig for å fjerne giftige metaller fra urban avrenning.

Preface

This master thesis was written at the Department of Civil and Environmental Engineering at the Norwegian University of Science and Technology during the spring of 2017. The master thesis was done under the subject TVM 4905.

I would first like to thank my co-supervisor Aamir Ilyas. He has been a tremendous help throughout the whole process. I would also like to thank my supervisor Tone Muthanna for good talks and guidance. From the lab I would like to thank Carlos Monrabal for great talks, and my fellow students at Verkstedsloftet for making the last years a lot better.

As I'm writing this I've already left Trondheim and started work in Oslo. So, I would finally like to thank Trondheim for the last 10 years of my life. Never did I think it would be possible to experience the amounts of fun I've had while living in Trondheim. Where ever I end up in life I will always have a special place in my heart for Trondheim, and the time I spent there. To quote the lyric of Odd Nansens "Hjemve": Naar æ tænke paa ka godt du ga mæ e de' som æ læste dekt! Which translate to «When I think of all the good things you gave me, it's like I'm reading poetry».

Henrik Winther Solemslie

Oslo, June 11th, 2017

Table of content

List of Figures

List of Tables

List of Abbreviations

AADT	Average annual daily traffic
Al	Aluminium
As	Arsenic
Ba	Barium
C	Outlet concentration
C_0	Inlet concentration
Ca	Calcium
Cd	Cadmium
Cl	Chlorine
cm	centimetre
Co	Cobalt
Cr	Chromium
Cu	Copper
EC	Electrical conductivity
EQS	Environmental Quality Standard
Fe	Iron
GAC	Granular activated carbon
ha	hectare
Hg	Mercury
HLR	Hydraulic loading rate
ICP-MS	Inductively coupled plasma mass spectrometry
K	Potassium
LID	Low impact development
m	meter
mg	milligram
Mg	Magnesium
mL	milliliter

mm	millimeter
Mn	Manganese
Mo	Molybdenum
µS	microSiemens
Na	Sodium
Ni	Nickel
No	Number
NOM	Natural organic material
P	Phosphorus
PAH	Polycyclic aromatic hydrocarbons
Pb	Lead
RP	Return period
rpm	Revolutions per minute
S	Sulphur
s	second
Sb	Antimony
Si	Silicon
SIM	Simulation
SOC	Synthetic organic compound
SUDS	Sustainable urban drainage systems
t_C	Time of concentration
TIC	Total inorganic carbon
TOC	Total organic carbon
V	Vanadium
W	Tungsten
WSUD	Water sensitive urban design
Zn	Zinc

1. Introduction

With the growing urbanization of the world populations, the ever-increasing urban runoff has become an important challenge for municipalities. The worlds population is concentrated in the cities where an increasing need for new housing causes the need to develop new areas. This causes a continue increase in impervious areas such as road ways, parking lots, and roof tops. When rain falls on impervious surfaces it flows overland until it reaches a drain or a pervious area to infiltrate. As the runoff from large areas gather at small point of drainage or infiltration, a small precipitation event may appear as large problem because of the accumulated volume.

In addition, the changes in climate are causing the precipitation events to become more intense. This will again increase the hydraulic load on the drainage and infiltration sites.

In Norway the need for proper stormwater management have become imminent during the last decade. The practices used by the municipalities are slowly evolving from old gray solutions, usually in pipes underground, to local blue-green solutions. Blue-green solutions use above ground installments to detain, retain, infiltrate, and treat urban runoff. This is done to lessen the hydraulic load on wastewater treatment plants and receiving bodies of water. As urban runoff may contain large amounts of pollutants, it is very important to treat the runoff before releasing it to the receiving waters, or infiltrate it to the groundwater. Examples of such runoffs are runoffs from highways, and washing of tunnels, which has a high concentration of toxic metals. This runoff may be treated in filter strips, along the side of the road, with filter media which removes particles and toxic metals. In this case there would be additional adsorption material specifically targeted toxic metals, while the rest of the media consist of sand [1].

Like all new technologies, it is challenging to have entrepreneurs and municipalities embrace it. To help convince them it is important to make the new solutions as economical as possible. For example, filter strips the cost of filter media is important because of the amount needed. Therefore, there are continues search to find new, low cost, alternative filter medias. At the Department of Civil and Environmental Engineering, at the Norwegian University of

Science and Technology, four alternative filter medias such as charcoal, pine bark, olivine, and bottom ash coated with iron oxide were selected after laboratory testing [2, 3]. These medias were chosen to specifically target toxic metal pollutants in highway runoff. The removal mechanism used by these materials is adsorption on the material surfaces.

As the climate changes, the alternative filter medias will have to endure more extreme precipitation events. These events will become shorter, more intense, and what is considered a 20-year return period event today, may be considered a 4-year return period event in 50 years [4]. Heavy hydraulic load may have unwanted effect on filter materials. Chemical and physical aspects may change, and large desorption events of toxic metal may occur. Such events may have critical effect on the biology of the recipient, and may render the filter useless, in the best case scenario, and a bio-hazard in the worst case. Other aspects that may affect the performance of filter media is intermitting drying and wetting. Adsorption happens on the surface in a wet environment. If prolonged dry-periods the chemical environment may be changed before the next precipitation event. Intermitting drying and wetting may bring oxygen to the surface which may deteriorate the material. This, in combination with removal of moisture on the surface may increase or decrease its performance as filter media.

Since filter media may be installed in permanent urban infrastructure it is very important to investigate how any new filter material may react to future extreme climate. Both extreme precipitation event, and intermitting drying and wetting should be well documented before the filter media are permanently installed.

While adsorptive materials, as described above, are usually used in combination with sand or soil, it is also important to investigate the performance of the new materials without sand. In this thesis, the performance of four novel adsorption materials have been tested during and after extreme precipitation events and drought. The materials were tested in a pilot scale column study which would provide data on their potential real life performance.

1.1 Objectives

The objectives of this theses have been as followed:

- To simulate extreme precipitation events, and droughts to evaluate the performance and environmental impacts of selected media
- To conclude and provide insights about resilience, environmental risks and design guidance for the infiltration based treatment system

2. Theory

2.1 Global urbanisation and hydrology

The world has during the last century started the transition from a rural population, to a population focused more and more in the urban areas. In 2014 the United Nations published that 53 percent of the world's population lived in cities. In 1950 the number was 30 percent, and they predict that in 2050 the number will increase to be 66 percent [5]. The urbanisation of the population, and the development of the necessary land has a large impact of the general hydrology in the area. The introduction of impervious areas such as: roofs, and pavements, instead of vegetation causes a heavy reduction in the rainwater infiltration and groundwater recharge, the same for urban streams base flow [6]. The impervious area increases the runoff which can cause large impacts on the environment [7], such as flooding downstream [8]; increase in sediment, nutrients, and toxic metals concentration decreasing the water quality [9-12]; streambank and downward erosion [13-15]; and the aquatic biota [16]. The hydrological impact of urbanization can generally be illustrated by Figure 1, adapted from [17].

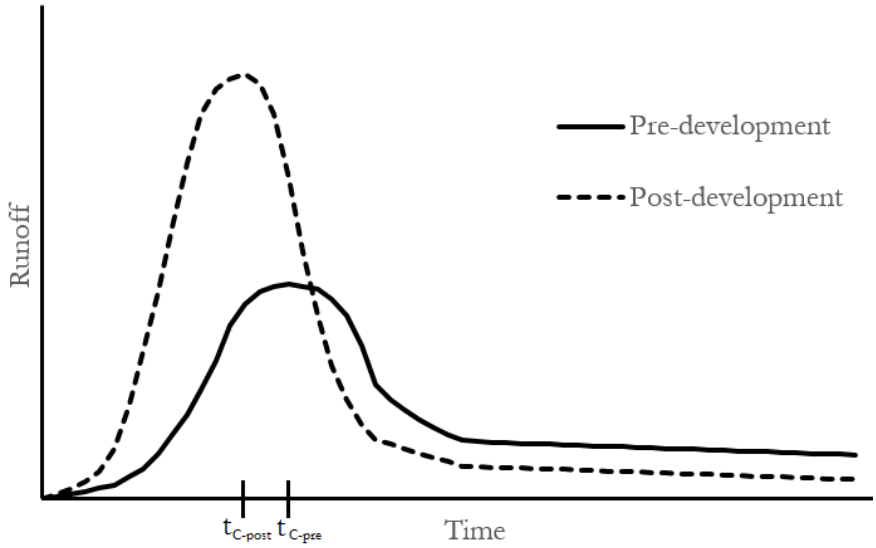

Figure 1. Schematic illustration of the pertinent impacts of urbanisation on hydrology at the catchment scale, adapted from [17].

From Figure 1 one can see that the volume increases drastically, but also that the time of concentration (t_C) decreases with urbanization.

2.1.1 Changes in channel structure

The hydrological changes in an area also lead to structural changes in the connected rivers, streams, and channels. This causes, in addition to streambank and downward erosion, simplification of habitat and removal of sediments [13-15]. There are two main mechanisms that cause these changes. The first is the increase in frequency and volume of flows. This causes a higher shear stress which increases the mobility and transportation of sediment [18]. The second is the lack of new coarse sediment. The impervious surfaces of the catchment, and often the channel itself, produces mostly fine, suspended, sediments [19]. The result of this is urban streams and channel floors consisting of a growing portion of fine sediments, while the coarse sediments are transported downstream. The increase in shear stress also increases the probability for channels migration. This is rarely popular in urbanized areas so the riverbanks are modified with a lining, often rocks or concrete. These modification removes another source of coarse sediments. Combined with the lack of other sources due to urbanization, and the loss of other habitat areas such as wood debris, the urbanization of the channel leads to greatly diminishing habitat quality [20]. Such alteration of urban streams separates them from natural floodplains. This does not only affect the exchanges between the stream and the riparian zone, but also important processes such as the riparian zone facilitating denitrification [21, 22].

2.1.2 Ecological degradation

An earlier review by Walsh *et al.*[23] from 2005 shows a list of consistently observed consequences of urbanization including a loss of organic matter, sensitive species, and an increase in toxicants and nutrients. These consequences start to show at a very small percentage of impervious area in the total catchment area. Earlier reports show that urbanization of as little as 10 % of the total catchment affects the ecosystem significantly [24]. Other more recent studies have found degradation to start at a much earlier level of imperviousness, a study by King *et al.*[25] shows that approximately 80 % of the declining groups of organisms does so between 0, 5% and 2,5 % catchment imperviousness.

2.1.3 Water quality

The water quality is highly affected by the change in hydrology and urbanization of the catchment. There are two major mechanisms causing this (i) the land use and human activity causes an increase of pollution generated and (ii) the increased runoff from the impervious areas increases the mobilization and transportation of the pollutants [6]. There are a number of different pollutants in the urban stormwater including toxic metals, sediments, nutrients, polycyclic aromatic hydrocarbons (PAHs,) and pesticides [26]. Passeport *et al.*[27] found that the nutrient concentration and loads can be adequately predicted by analysing the catchment area; percentage of impervious area and natural surroundings, and rain depth. Another study by Hatt *et al.*[28] found that the percentage of impervious catchment directly connected with the receiving water through a constructed drainage system was more accurate.

2.2 Metal pollution in urban areas.

In urban areas the metal content, of stormwater runoff, is of a particular concern. The metals are not degraded by the environment, and are thus subjects to accumulate in soils, and the flora and fauna. The metal pollution can also cause toxic shock in the short-term due to temporarily high concentrations, and give long-term impact due to mass accumulation and long-term exposure [29]. Road traffic has many sources of toxic metals, as illustrated in Figure 2, which are transported in the stormwater during precipitation events. Earlier research from 1987 found that for some toxic metals, i.e. copper (Cu), the total load contributed to the stormwater by the road is more than 75 % [30]. Comparing this to the relatively small percentage of total area the road occupies, the contribution is significant. A later study from Sweden in 2001 found that for the total metal emission the traffic contributed about 40 % of copper (Cu), 90% of cadmium (Cd); more than 99 % of both chromium (Cr) and nickel (Ni), 80 % of zinc (Zn), and 85 % of lead (Pb) when pavement and galvanized goods were included [31].

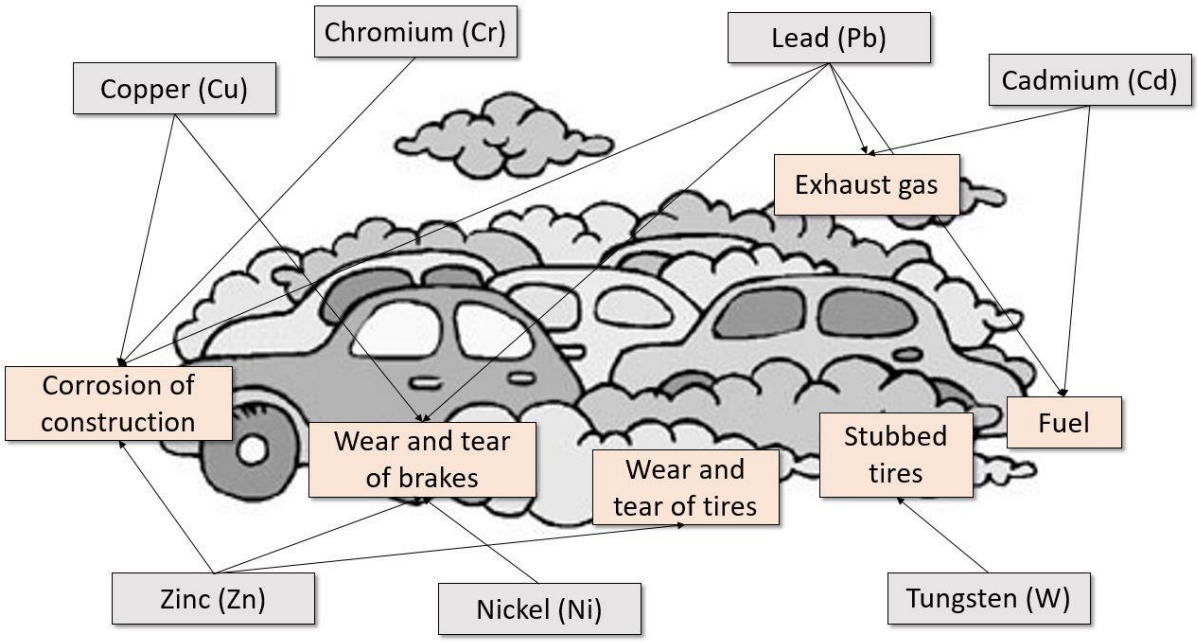

Figure 2. Toxic metal emission from traffic, modified by [32].

Another study by Davis *et al.*[33] in 2001 presented a different result which showed that other sources in urban areas had significant contribution to metal concentrations. For Pb they found that the building wall material contributed between 12 % and 79 %, dependant on building material and whether it was measured in residential or commercial area. Traffic was still the highest contributor of Cu (47 % - 55 %) in residential areas, while in commercial area the roof runoff contributed 75 % of the Cu. The contribution of sources of Zn varied considerably with the building material. In areas with brick buildings the wall represented 59 %, while in areas with vinyl buildings the walls represented only 4 %, and the roof contributed 8 % of Cu. In commercial areas with various materials the roof runoff contributed 45 % of the Zn contents in the runoff. Table 1 presents data on estimated toxic metals in the wastewater from Stockholm[34]. Along with the surfaces and materials, atmospheric deposition is also an important source of metals in dense urban areas with heavy traffic.

Table 1. The contribution in % from difference sources as given in [34].

Source	**Pb [%]**	**Cu [%]**	**Zn [%]**	**Ni [%]**
Buildings	-	72-77	65-67	-
Traffic	70-73	22-38	28-30	30
Atmospheric deposition	27-30	7-8	5	70

2.2.1 Toxic metal sources in traffic

Among pollutants sources in traffic the brake linings are believed to contribute Cd, Cu, Pb, iron (Fe), antimony (Sb), and Zn [33, 35, 36]. Even though the pollution from traffic exhaust has drastically decreased after the ban of Pb in petrol [37, 38], one may still find exhaust emission of Cd, Cr, Cu, Ni, and Pb [36, 39-41]. The wear of vehicle tyres is another major contributor for especially Zn [33, 36, 42-44], but also a contributor to the emission of several other metals e.g. Cd, cobalt (Co), Cr, Ni, and Pb [33, 43, 45]. In colder climates, where studded tires are used, the wear of the road pavement have a large emission contribution. The content of this emission is dependent on the content of the binding material (bitumen), and stone material used. Studies done in Sweden found the pavement to contain Cd, Cr, Cu, mercury (Hg), Ni, Pb, Zn, and vanadium (V) [46] and that, on the average, each car with studded tires causes 10-30 g/km emission from wear of the asphalt [47]. The wear of the studded tires is also a small source of tungsten (W) pollution [48].

Another pollution source which is unique to colder climates is the accumulation of pollutants in snow in the vicinity of the roads. Runoff from snowmelt, along heavy trafficked roads, have been found to have concentrations of Pb, Cu, Cd, and Zn with two orders of magnitude higher than stormwater runoff [49].

2.3 Estimated metal loads and limits for highway runoff

In this thesis, the focus has been on four metals e.g. Pb, Ni, Zn, and Cu. An estimate of the pollution concentrations of these elements can be seen in Table 2. This was proposed by Lindholm[50] in 2003 and is the most used estimation in Norway.

Table 2. Estimated concentration of different toxic metals at different traffic load, represented by annual average daily traffic (AADT) [50].

Road [AADT]	**Pb [µg/L]**	**Cu [µg/L]**	**Zn [µg/L]**	**Ni [µg/L]**
5 000	13.5	38	62	1.2
30 000	31	72	197	4.4

These numbers were verified by an estimation proposed by Amundsen and Roseth[51] as seen in Table 3.

Table 3. Estimated concentration of different toxic metals at different traffic load [51].

AADT	**Pb [µg/L]**	**Cu [µg/L]**	**Zn [µg/L]**	**Ni [µg/L]**
5 000	13.5	38	62	1.2
15 000	20.5	59	116	2.45
30 000	31	72	197	4.4
60 000	52	85	359	8.3
100 000	80	94	575	13.5

As for the percentage of particle-bound and dissolved metals a study by Maniquiz-Redillas *et al*.[52] found that for a single precipitation event the ratio of dissolved vs. particle-bound metals was for Cu, Pb, and Ni between 2-6.2 and for Zn 0.29 at time of concentration.

2.3.1 Emission limits for road runoff

There are at the time of this thesis no national limits of toxic metal concentration in road runoff in Norway. Other entities have come up with limits which can be used as guidance for Norwegian treatment goals. A study from Sweden, based on several studies conducted in Stockholm in the 1990s, proposed classification of pollution concentrations. The study proposed 3 classes of concentration for pollutants, as seen in Table 4.

Table 4. Stormwater metal concentration divided into 3 classes[38].

Metal	Unit	Low concentration (Class 1)	Moderate concentration (Class 2)	High concentration (Class 3)
Pb	µg/L	<3	3-15	>15
Cu	µg/L	<9	9-45	>45
Zn	µg/L	>60	60-300	>300
Ni	µg/L	<45	45-225	>225
Cd	µg/L	<0.3	0.3-1.5	>1.5
Hg	µg/L	<0.04	0.04-0.2	>0.2
Cr	µg/L	<15	15-75	>75

When setting limits for discharge concentrations of target metals, the receiving body of water has to be taken into account. Very often the recipient has unique limits, but a proposal for limiting stormwater values have been defined for several municipalities in Sweden, as seen in [53]. The limit values are meant as guidance for investigating the tolerance limit for each recipient.

Table 5. Proposed discharge limits for different recipients [53].

Substance	Unit	Smaller lakes, watercourses, and bays		Larger lakes and sea	
		Direct discharge	Discharge to sub-basin	Direct discharge	Discharge to sub-basin
Pb	µg/L	8	10	10	15
Cu	µg/L	18	30	30	40
Zn	µg/L	75	90	90	125
Ni	µg/L	15	30	20	30
Cd	µg/L	0.4	0.5	0.45	0.5
Hg	µg/L	0.03	0.07	0.05	0.07
Cr	µg/L	10	15	15	25

A study done by Meland *et al.*[54] in 2016 used results from an analysis, done by Huber *et al. [55]*, of 294 measurements of road runoff from six continents to suggest concentrations for road runoff in different scenarios. The results can be seen in Table 6. In addition, the Norwegian Miljødirektoratet [56, 57] has suggested that treatment may be needed if the metal concentration exceed 10 times the annual average (10xAA) stated by the Environmental Quality Standard (EQS) from the Water Framework Directive [58]. The EQS also has listed a maximum allowed concentration (MAC) in the runoff.

Table 6. Concentration of metals from different types of roads with different AADT [54]. *All the units are in µg/L.*

		EQS			Road: AADT 5 000-15 000			Road: AADT < 15 000			Road: AADT > 15 000			Highway: AADT < 30 000			Highway: AADT > 30 000			Urban Highway AADT > 30 000		
Metal	**Fraction**	**AA**	**MAC**	**10xAA**	**Av.**	**Min**	**Max**	**Av.**	**Min**	**Max**	**Av.**	**Min**	**Max.**	**Av.**	**Min**	**Max.**	**Av.**	**Min**	**Max.**	**Av.**	**Min**	**Max.**
Pb	Tot.	-			62	2	152	32	3.7	136	79	6	380	64	2.5	230	32	4.4	90	33	1.4	220
	Dis.	1.2	14	12	-	-	-	0.9	0.13	2.8	3.9	0.5	7	1.3	0.01	3.1	13[a]	13[a]	13[a]	3	0.8	7.4
Cu	Tot.	-	-	-	54	6	180	65	7	280	105	26	288	61	13	140	84	23	430	64	13	274
	Dis.	7.8	7.8	78	20	3.3	56	16	2.7	65	26	6.8	57	23	5.7	64	35	4	100	36	4.1	151
Zn	Tot.	-	-	-	212	25	940	285	23	1000	474	120	1940	306	32	1760	385	53	2210	338	21	2234
	Dis.	11	11	110	76	15	314	68	7.9	258	113	51	262	77	5	191	204	8.6	577	217	11	2118
Ni	Tot.	-	-	-	13	8.4	17	16	3.8	35	21	4.1	55	23	6	73	29	4	83	19	2	93
	Dis.	4	34	40	4.7	3.1	6.3	0.9	0.5	1.3	11	9.5	12	.	.	.	14	4	27	15	1.9	29
Cd	Tot.	-	-	-	2.7	0.3	13	3.2	0.06	37	5.6	0.67	25	1.8	0.05	9	2.6	0.14	12	4.1	0.06	35
	Dis.	0.08	0.45	0.8	0.7	0.14	1.8	0.2	0.01	0.5	0.6	0.25	0.9	0.5	0.02	2.6	1.4	0.5	3	1.3	0.1	3.8

a) *concentrations are perceived as highly uncertain*

Comparing Table 6 with the concentrations suggested by Lindholm *et al*. in Table 2 and Amundsen and Roseth in Table 3 these values are substantially higher. The EQS limits in Table 6 are lower than the limits set by Riktvärdsgruppen in Table 5. The reason for this may be because the EQS has to fit a larger set of scenarios, while Riktvärdsgruppen made their suggestion based on their local situation.

2.4 First flush

During the start of the precipitation event, the debris, and deposits accumulated on the road surfaces are washed off by the runoff [59, 60]. This is generally called as the “first flush”. The first flush phenomenon has been well documented by several reports [60-65]. Lind *et al*.[66] in 2001 investigated the runoff from 2 sites in Lindköping, Sweden. The first site was a highway with an AADT of 17 900, the second site was a light regulated urban road with an AADT of 11 500. After a 3 day dry period they found that, for both sites, the first 30 % of the runoff contained 50-60 % of the total mass of Zn, Cu, Pb, Ni, Co, Cd and arsenic (As).

2.5 Low Impact Development (LID)

Low impact development, or LID, is an environmental engineering strategy which was first introduced by Prince George's County, Maryland, USA in the early 1990s [17] and it seeks to limit the impacts of urban development on a local level. LIDs, similar to sustainable urban drainage systems (SUDS) in the United Kingdom [67], and water sensitive urban design (WSUD) in Australia [68, 69], are environmental engineering practices that implement low-scale hydrological control and pollutant treatment to compensate for the effect urban development has on hydrology and water quality. All the three practices, except for different names, share a similar approach [6]:

1. In a sustainable manner, manage the urban water cycle. Both surface water, ground water, erosion, and flooding of waterways needs to be considered.
2. The flow regime should be returned, or maintained as closed to its natural level as possible.
3. For both surface, and ground water: protect, and if possible, restore the water quality.
4. For the receiving water: protect, and if possible, restore the health of the receiving water.
5. View urban stormwater as a water resource, and conserve this resource.
6. Enhance the aesthetics of the community by incorporating stormwater management measures.

The main tools that LID uses to maintain or replicate the pre-development hydrology and water quality are enhanced infiltration and evapotranspiration. This reduces off-site runoff and maintains adequate ground water recharge [17]. The technology used in stormwater management mainly developed for two applications: Treatment of water quality, and mitigation of changes to the hydrology. Two of the main types of technology for both of these applications are infiltration-based (swales, infiltration trenches, filter strips, basins, unlined bioretention units), and retention-based technologies (wetlands, ponds, vegetated roofs, filters, lined bioretention units). These technologies can be used at the end of the catchment, or closer to the sources. Even though these technologies are widely used separate, research have found that the key to successfully achieve a natural flow regime is to both use retention to handle flow peaks and overall volume, and infiltration to make up for loss of infiltration due to impervious areas [70].

2.6 Infiltration and filtration units.

Infiltration and filtration units are often depressed areas in the landscape, which receive runoff from upstream impervious areas. The units often consist of layers of filter media and an overflow weir. Filtration units have under lining and underdrain. If covered with a vegetation layer they are called biofiltration units [71]. They are typically used locally and have a significant storage capacity. For filter units the underdrain may be elevated to facilitate a saturated zone in the base for denitrification and to increase the storage capacity [1]. By decreasing the flow and volume, infiltration units help return the hydrology to its natural cycle as pre-development, see Figure 1 [72]. Incoming runoff is filtrated through layers of media and percolated to the ground water. An infiltration unit typically consists of a storage volume, for pooling, between 15 and 30 cm of depth, and a layer of filter media (sand/soil/organic mixture) for removing particles and other pollutants. Additionally, various adsorbent materials may be used to target specific pollutants. When designing a infiltration unit one needs to design both an inlet for the runoff and a pathway for the overflow for larger precipitation events with larger runoff than the capacity of the infiltration unit [73]. For infiltration units, the hydraulic conductivity of the underlying soil should not be lower than 13 mm/h [74]. If that is the case, an underdrain should be considered [71]. The main filtration of the runoff is done by the filter media, where sediments, particles, nutrients, toxic metals, and other pollutants are removed through different mechanisms from the runoff [75]. For bioretention units the vegetation layers help slow down the runoff, traps sediments, and helps remove nitrogen from the runoff [76, 77]; prevents clogging of the filter media [78]; and increases the evapotranspiration[79]. There are many different unit processes treating the runoff in infiltration units. The pollutants are removed by the chemical, and physical properties of the filter media. In total the infiltration unit reduces the runoff volume, pollutant load, peak flow; and increases groundwater recharge [72].

2.6.1 Existing design guidelines for infiltration ditches in Norway

In an report made for Rogaland County/Jæren water areas in 2013. COWI proposed an infiltration ditch design for roadside ditches as seen in Figure 3 [56].

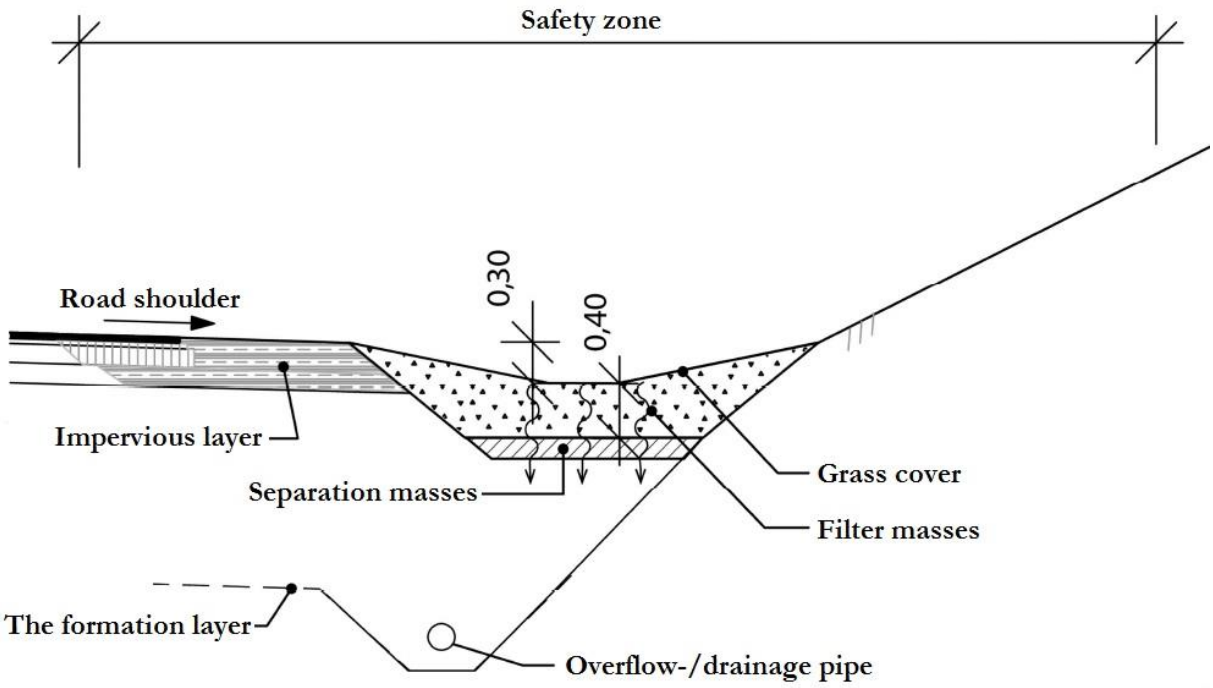

Figure 3. Infiltration ditch along a major road [56].

While their proposed design for urban infiltration trenches can be seen in Figure 4.

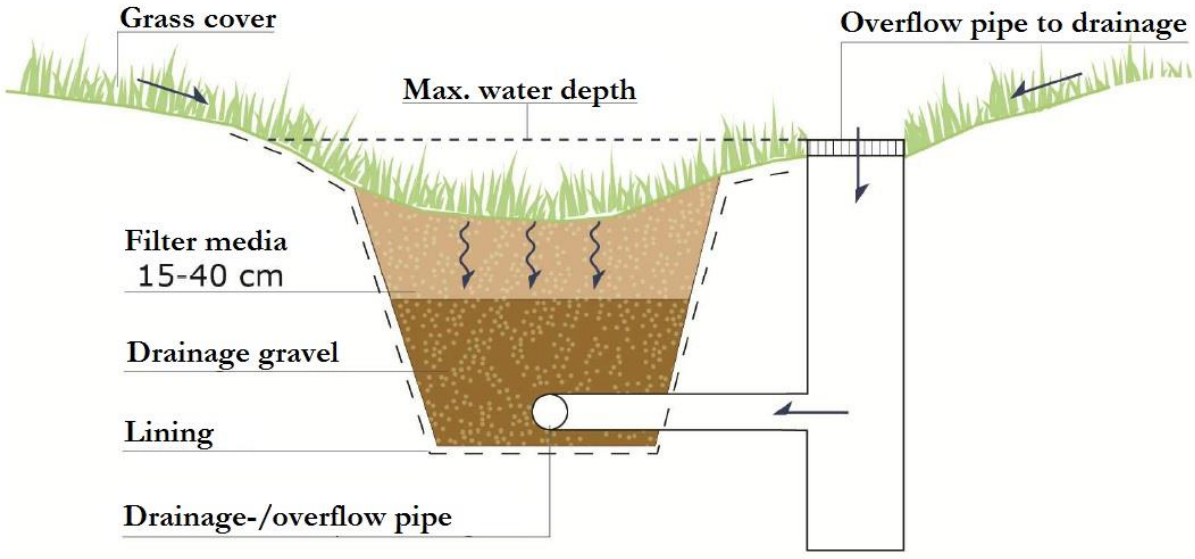

Figure 4. Filtration in urban areas

This guideline does not mention which filter media should be used, but recommends that the filter masses should remove 60-80 % of the toxic metals. It does not specify if the removal is dissolved, particle-bound, or total metal content. However, there are no existing guidelines for

the use of the alternative adsorption material. The novelty of alternative adsorption medias may explain the lack of guidelines. Research done by Ilyas *et al.*[80] have shown that using 35 cm of clean quartz sand with uniform particle sand on top of 5 cm of alternative adsorption materials such as charcoal, olivine, pine bark, and bottom ash stabilized with iron oxide, removed most of the dissolved metals. In their research they used a top layer of sand to remove to particle bound metal and some dissolved. At the bottom they had a layer of alternative adsorption material to help remove any remaining dissolved metal.

2.7 Alternative adsorption materials

2.7.1 Adsorption mechanism

Adsorption is defined as a mass transfer operation in which substances present in a liquid phase are adsorbed or accumulated on a solid phase and thus removed from the liquid [81]. Adsorption to a media surface is illustrated in Figure 5.

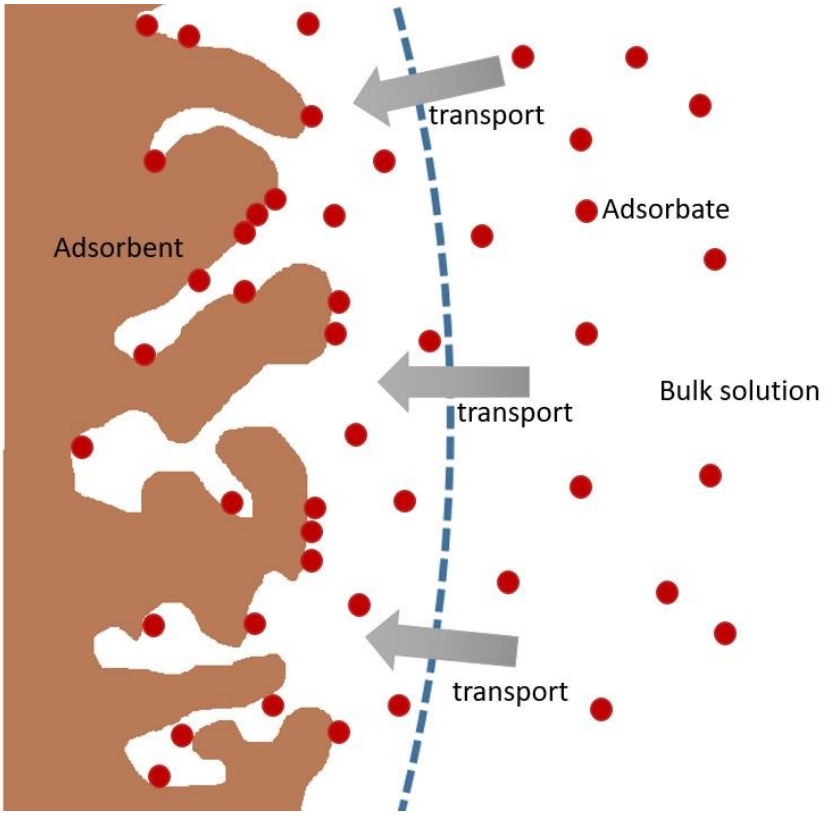

Figure 5. Adsorption to media surface.

The substance which adsorbs upon a solid is called adsorbate. The solid, to which the substance binds, is called the adsorbent. Desorption is when the adsorbate is released back into the bulk solution [82]. There are two types of adsorption, and depending on the forces between the adsorbent and adsorbate, they either undergo physical (physisorption)-, or chemical adsorption (chemisorption). Physical adsorption, which is the most common type used in water treatment, uses nonspecific binding mechanisms such as van der Waals forces, and vapour condensation. Physical adsorption is reversible, where the adsorbate adsorbs and desorbs in response to the bulk solution concentration. In chemical adsorption the adsorbate is bound to the adsorbent by covalent or ionic bond. These electron exchanges are only possible in a monolayer. Chemical

adsorption is typically not reversible. In addition is ion exchange which are driven by electrical attraction between adsorbate and adsorbent, this is also reversible [81, 82].

2.7.2 Charcoal

Charcoal is a commercial available adsorption material, and is thus more expensive than other alternative adsorption materials with a cost approx. >60-170 $/kg [2]. The activation process starts with a pyrolytic carbonization, where volatile components are released and graphite is formed. The subsequent, or parallel activation causes the carbon to form a porous structure. This is done by different processes which removes specific carbons from an opening of closed porosity. Charcoal utilized in water treatment is activated by an endothermic thermal process. This process uses a gaseous activation agent, usually a steam, at a temperature usually between 850 °C to 1000 °C. Charcoal has a pore diameter ranging from 10 to 300 µm. Charcoal is much used in water treatment plant for it adsorption affinity for natural organic matter (NOM) and synthetic organic compounds (SOCs) such as solvents, fuels, and pesticides [81]. An earlier study has found the zero charge point (pH_{zpc}) of charcoal based adsorbents to be at pH 7.2 [83]. If the runoff has a higher pH the conditions would favour a cathodic adsorption. A study by Shim *et al.*[84] have found that the concentration of different active groups on the pore surface are important for charcoals adsorption capacity of Cu and Ni. For pH below the pH_{zpc} the lactone group is important, while the total acetic groups are important for $pH>pH_{zpc}$. This affects Cu and Ni differently, e.g. for pH below 8 Cu has a numerous times higher adsorption than Ni. A breakthrough experiments done by Ilyas *et al.*[80] with charcoal and clean sand found the affinity of charcoal to be Cu>Pb>Zn>Ni. The end-of-life treatment of charcoal will most likely be a specialized landfill, even though it may be regenerated with acid treatment [2].

2.7.3 Bottom Ash

Bottom ash (BA) is a secondary waste product from coal combustion, or as in Norway, municipality waste incineration furnaces [85]. Bottom ash is very cheap as it is a waste product, and it has been found to have very good adsorption capability towards toxic metals [2, 86-88]. For bottom ash leaching of environmental toxic components is a risk. As bottom ash is produced by burning solid waste, the content of the chemical constituents in ash may differ particularly

from place to place. A study has been done of the contents of bottom ash from 14 different incineration furnaces in Norway, and the results can be seen in Table 7 [89].

Table 7. Mean concentration of different components in bottom ash from 14 Norwegian incineration furnaces [89].

	TIC	TOC	Cl	S	Sb	As	Pb	Ba	Cd	Cu	Hg	Cr	Mo	Ni	Zn	Mn
Conc.	0.55	0.81	0.25	6100	120	38	2100	1450	6.5	5000	0.04	500	14	190	5000	1500
Unit	%			mg/kg												

TIC – Total inorganic carbon, Cl – chlorine, S – sulphur, Ba – barium, Mo – molybdenum, Mn – manganese.

Ilyas *et al.*[80] have found that coating the bottom ash with iron oxide (10 w%) stabilises the surface, and reduces the leakage by 16-97 % for Zn, Cu, Ni, and Pb. During a long-term experiment over 75 days, a column filled with 5 cm BA-iron oxide and 35 cm of clean sand had a removal rate of > 98 % for Pb, Cu, Ni, Zn for the whole experiment. End-of-life cost of bottom ash is very cheap as it will not increase with the use as adsorption material. It would become part of the existing disposal system, for example filling old coal mines. This costs between 60 and 110 $/kg and is cheaper than regular landfill (±167 $/ton waste) [2].

2.7.4 Pine Bark

Pine Bark is the waste product of saw mills. It is produced in large quantities, and is an interesting low-cost alternative adsorption material. Bark is a waste product produced by the forest industry, and is thus very cheap. Pine Bark may have a large surface area despite a large particle size. This is due to adsorption happening inside the pores in the material, rather than outside on the surface as other adsorbents. The adsorption on pine bark have been attributed to the presence of compound such as lignin, polysaccharides, and tannin on the surface [90]. Pine bark is found to have a very large adsorption capacity for cations at low concentrations [91]. A long-term column study has been done by Ilyas *et al.[80]* to investigate pine barks removal capacity of Pb, Cu, Zn, and Ni from synthetic stormwater. Their study found that Pine Bark has a much higher affinity for Pb and Cu, which had high removal rate throughout the experiment.

The removal rate of Zn and Ni decreased rapidly and Ni was found to be the regulating component for the estimated lifetime of the filter. This agrees with the earlier research which found the affinity of pine bark towards toxic metals to be is the following order: Pb>Cd>Cu>Ni [92]. As Pine bark is an organic material there is a concern about biodegradation and release of carbon. Leakage of carbon, increase the total organic carbon (TOC) content in the runoff which is of concern. Pine bark has a very low end-of-life cost as it is organic and can be incinerated. In Scandinavia it is estimated to cost 35-48 $/ton pine bark to incinerate [2]. This is much lower than landfill disposal.

2.7.5 Olivine

Olivine is one of the most common minerals on earth, and is a magnesium iron silicate ($[Mg, Fe]_2SiO_4$). The granulated olivine is a commercially available product and is produced by first crushing olivine to powder. Then subsequently packing it to granulates with the use of a binder (typically a type of cement). Olivine have been shown to have good adsorption capabilities towards the toxic metals focused on in this thesis [2, 80, 93-95]. Even though the olivine is plentiful, it still needs processing before applying it for adsorption, which makes is more expensive than other alternative adsorption materials. The end-of-life costs equal to that of bottom ash. Considering cost it should be combined with a prolonged service life as shown by Ilyas *et al.*[80] In their research they found Olivine to have much better adsorption capacity over time, than both pine bark and charcoal. A study done for the Norwegian Statens Vegvesen have found that weathering of minerals containing olivine may be a source of nickel leakage [96]. This should be monitored when using olivine as adsorption material

2.8 Extreme precipitation

As the global temperature is expected to increase due to climate change, it is expected to affect the temporal and spatial distribution of precipitation [97-99]. The increase in temperature will allow more water vapour to be contained in the atmosphere. This is expected to cause a change in precipitation events, toward the more intense and short-term. Intense precipitation events, combined with impervious areas, will cause a large runoff generated very quickly. This will increase the runoff at the time of concentration (see Figure 1), which will again cause large problems downstream.

A study done by Larsen *et al.*[4] have found that for Sweden a 60-minutes intensity, 20-years return period precipitation event today, will represent a 4-years return period precipitation event in 50 years. Another study by Olsson *et al.*[100] have found that 30-minutes intensity, 10-years return period precipitation events, in Sweden, will increase 6 % before 2040, 15 % before 2070, and 23 % before 2100. Consequences of intense precipitation events can be seen after a precipitation event which happened August 13th, 2007, in the city of Trondheim, Norway. This event had a duration of 5 minutes and was given a return period of over 100 years. This 5-minutes intensity event caused flooding of more than 100 basements, resulting in tremendous damages [101]. Partly because of this event, a research was commenced by Hailegeorgis *et al.*[102] to update the IDF curves of the city of Trondheim. This was done to make more reliable prediction about major storm events. Their research concluded that future urban water infrastructure should be able to handle precipitation events equal to today's 5-180 minutes intensity precipitation events with return periods of 2-100 years.

2.8.1 Filter performance during extreme precipitation events.

Because of this development towards shorter, more intense precipitation events, it is important to investigate how the removal capability of adsorption material is affected by the extreme hydraulic load, but also intermitting wetting and drying periods. For the wetting and drying a study was done by Hatt *et al.*[103] They found that for, unvegetated, soil based filter media the removal capacity of toxic metals was not affected by the dry periods. On the contrary, the removal rate increased because of the drying period. Although much of the runoff will go to the overflow during extreme precipitation events, because of insufficient hydraulic conductivity of

the filter, it is important to investigate the performance of the adsorption material after an extreme precipitation event. From the runoff during the event much of the first flush might be treated by the filter; therefore, it is also important to investigate the performance during a period of extreme hydraulic load. Lastly, the Norwegian Environment Agency have stated a prioritizing of robust treatment alternatives, which can withstand different and uncertain climate changes [57].

3. Material and Methods

In this chapter the material, and the methods used to carry out these experiments, will be presented.

3.1 General overview

This experiment had three parts, using the same experimental setup, as seen in Figure 6. The setup had eight columns filled in pairs with the alternative adsorption materials: Granulated charcoal; bottom ash mixed with iron oxide, olivine, and pine bark. Throughout the experiments the columns were fed with synthetic stormwater, containing dissolved Zn, Ni, Pb and Cu (2mg/L each). In the first part, metal removal rate was estimated by pumping a base flow equal to a hydraulic load of 30 mL/min which was equal to approximately precipitation event with 1440 minutes intensity and 2-years return period. For the last two parts; one column with each material was used in simulations of the hydraulic load of extreme precipitation events at Risvollan in Trondheim, Norway. A fictional catchment of $1m^2$ was used for each column. The other columns had a constant base flow of 30 ml/min as a reference. The second part had simulations of 10- to 200-years storms with 5- to 180-minutes' intensities in consecutive order. Each simulation was started at noon, and at end of the simulation the columns were reset to a base slow of 30 mL/min, until noon the next day. The third part simulated 10- to 200-years storms with 45 minutes intensity with increasingly longer drying period between each simulation. The simulation columns were only run with the hydraulic load from the extreme precipitation event, while the reference column was run for 24 hours. Based on the hydraulic conductivity of the columns the maximum hydraulic loads were calculated. The fictional catchment was given a geometry which gave a constant runoff over sufficient time to pass the precipitated water through the column when the hydraulic load was higher than the hydraulic conductivity. Regular samples were taken from the outlet on the bottom of the column and analysed for pH and electrical conductivity (EC). The discharge flow was measured with a graduated cylinder and stopwatch before each sampling. The samples were filtered through 0.45

µm filter and preserved with acid before the metal content was measured with ICP-MS. The samples were stored at -4 °C when needed.

Figure 6. Experimental setup. 1 m^3 tank with synthetic stormwater down to the right. Pumps above it with tubing going from the tank to the columns lined to the left.

3.2 Filter column preparation

3.2.1 Adsorption material

The bottom ash used in this experiment had previously been collected at the Heimdal incinerator, which is the main incineration centre of Sør Trøndelag County, Norway, as described by Luz [95]. The bottom ash was sieved through a 12.9 mm sieve and mixed manually with 10 w% iron oxide. The iron oxide was produced by Sigma-Aldrich. The olivine used was produced by Sibelco Nordic AS and was of the Blueguard® series. The olivine was not treated in any way before use. The pine bark was a product of Nittedal Torvindrustrie A.S. and was not treated in any way before use. The charcoal was a Sigma Aldrich product named Activated Charcoal Norit®, see [104]. It had a granular form with a particle size of 1 mm. It was extract from anthracite coal and activated by steam. This was manually mixed with 50 w% quartz sand manufactured by Rådasand AB, Sweden.

3.2.2 Column preparation

The columns were made of Plexiglas, with a 10-cm diameter and length of 49 cm. A membrane was placed at the bottom of the column to prevent material leakage. Two columns were filled with each of the adsorption material (35 cm). The composition of each material can be seen in Table 8. At the top of the adsorption material another membrane was placed which was weighted down with a layer of rocks (1.5-3 cm diameter) to prevent flotation and decompression during the experiment. The hydraulic conductivity of this column setup had been measured during an earlier project, and the results can be seen in Table 8 [104].

Table 8. Adsorption material composition, and their hydraulic conductivity, used in column experiments.

Filter media	**Component 1**	**Component 2**	**Hydraulic conductivity [104] [mL/min]**
1	Activated charcoal (50 w%)	Sand (50 w%)	216
2	Olivine (100 w%)		792
3	Bottom Ash (90 w%)	Iron Oxide (10 w%)	3687
4	Pine Bark (100 w%)		8508

3.3 Pump calibration

The peristaltic pumps used in these experiments were FH100M Multichannel Pump Systems from Thermo Scientific, seen in Figure 7. Two pumps were used for the simulation columns and one for the reference columns.

Figure 7. Pumps used in this experiment

The pumps were individually calibrated using identical tubing as used in the extreme precipitation experiments, a stop watch and a graduated cylinder. The calibration used 5 measurements, at different pump speed spread over the total capacity of the pumps, and regression was used to make a calibration curve giving the relationship between revolutions per minute (rpm) and pump-flow, as seen in Figure 8.

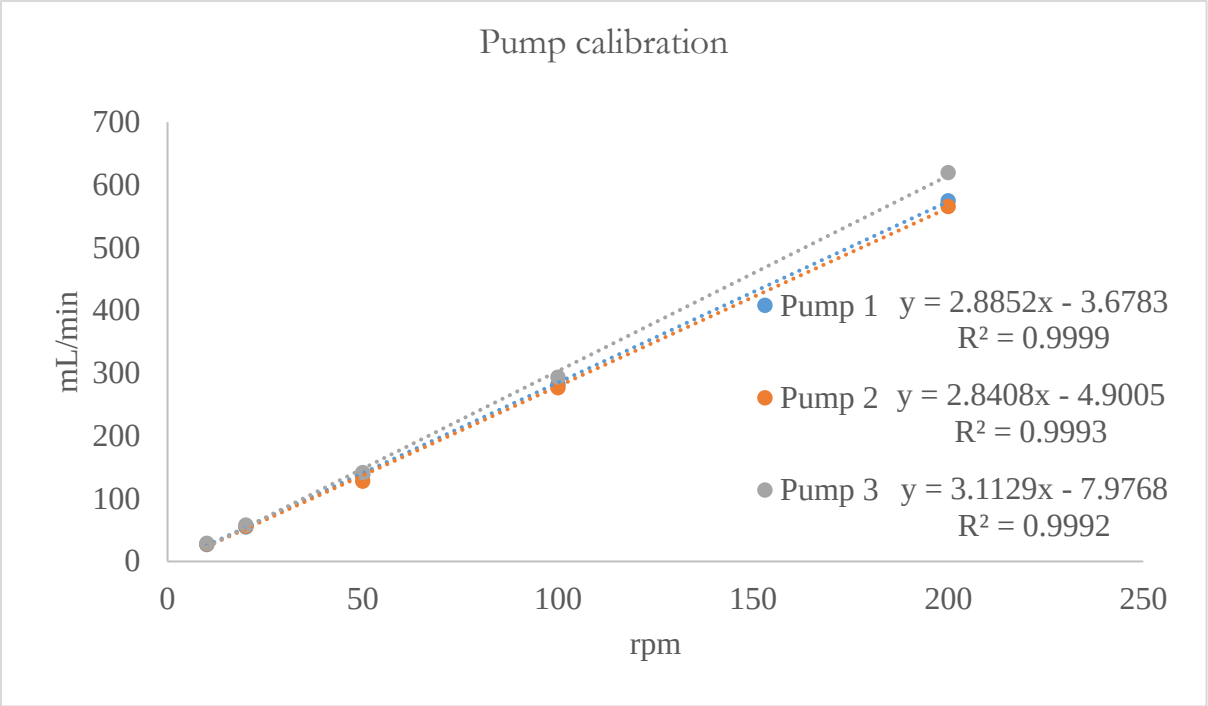

Figure 8. Calibration curve for the pump.

3.4 Hydraulic loads

Based on the research by Hailegeorgis *et al.*[102] the intensities chosen to simulate was 5 minutes, 45 minutes, and 180 minutes. To increase the number of data points four return periods (RP) was chosen: 10 years, 50 years, 100 years, and 200 years. The meteorological data for Risvollan was collected from the Norwegian Meteorological Institute [105]. The data obtained was converted to give a hydraulic load used by the pumps, and can be seen in Table 9.

Table 9. The hydraulic loads, converted from meteorological data, used in the simulations.

	5 minutes		45 minutes		180 minutes	
RP	**[L/s*ha]**	**[mL/min*m²]**	**[L/s*ha]**	**[mL/min*m²]**	**[L/s*ha]**	**[mL/min*m²]**
10	193.9	1373.4	56.9	341.4	21.5	129.0
50	306.0	1836.0	75.2	451.2	25.8	154.8
100	338.6	2031.6	82.9	497.4	27.6	165.6
200	371.1	2226.6	90.6	543.6	29.5	177.0

3.5 Synthetic stormwater

A synthetic stormwater with four metals (Zn^{2+}, Ni^{2+}, Pb^{2+}, Cu^{2+}) and a concentration of 2 mg/L was used. This concentration was much higher than that of normal urban stormwater (See Chapter 2.3). This was done to better demonstrate removal rate, and because of limitations of the analytical instrument used. The metals were dissolved in a 1000 L tank, while filling it with tap water to facilitate the dissolution. The chemicals used to produce the stormwater are listed in Table 10.

Table 10. Chemicals used in production of synthetic stormwater, Me^{2+}w% - Metal cation weight percent of total molecular weight

Chemical	**Producer**	**CAS#**	**MW [g/mol]**	**Me^{2+}w% [%]**
$PbCl_2$	Alfa Aesar	7758-95-4	278.10	75
$CuCl_2$	Sigma-Aldrich	7447-39-4	134.45	47
$ZnCl_2$	Merck	7646-85-7	136.30	48
$NiCl_2$	Sigma-Aldrich	7718-54-9	129.60	47

3.6 Experimental schedule

3.6.1 Establishing a base flow.

Before simulating any extreme precipitation events all 8 columns were run with a hydraulic load of 30 mL/min for 5 days. This was done to let the removal mechanism stabilize and reach equilibrium. This was also used to condition the columns and remove any “first flush” contaminants.

3.6.2 Simulations of extreme precipitation events

The first part of the experiments was sequential simulations of hydraulic load from extreme precipitation events. A base flow of 30 mL/min was used continuously on the reference columns, and in between simulations on the simulation columns. During the simulations, the simulation columns were run with a hydraulic load equal to that of the runoff from the precipitation event, with a maximum of 219 mL/min. This maximum flow limit was based on the hydraulic conductivity results given in Table 8. For precipitation runoff exceeding maximum flow limit the total volume of the precipitation event was calculated and run through at the maximum flow limit. The operational sequence of column experiments is given in Table 11.

Table 11. Schedule of sequential extreme precipitation event simulation execution

Day	Time	Action
1	11:00	Start base flow on all columns
	12:00	Start simulation flow on simulation columns
	After end simulation	Base flow on all columns
2	12:00	Start simulation flow on simulation columns
	After end simulation	Base flow on all columns
3	12:00	If no simulation, turn of all pumps.

The base flow did not run during weekends and maintenance. The sequence the simulation was carried out can be seen in Table 12. The sequence of the simulations was chosen based on the total volume of runoff to go through the column. This was decided based on the hypothesis that

changes in removal rate made by smaller volumes may be harder to detect if a larger volume had been simulated before.

Table 12. Sequence the sequential simulation of extreme precipitation was conducted. HLR-Hydraulic loading rate, SIM-Simulation

SIM no:	Intensity [min]	RP [years]	Runoff HLR [mL/min*m^2]	Total volume [L]	Column HLR [mL/min]	Time [min]
1	5	10	1373.4	6.9	219.0	31.4
2	5	50	1836	9.2	219.0	41.9
3	5	100	2031.6	10.2	219.0	46.4
4	5	200	2226.6	11.1	219.0	50.8
5	45	10	341.4	15.4	219.0	70.2
6	45	50	451.2	20.3	219.0	92.7
7	45	100	497.4	22.4	219.0	102.2
8	45	200	543.6	24.5	219.0	111.7
9	180	10	129	23.2	129.0	180.0
10	180	50	154.8	27.9	154.8	180.0
11	180	100	165.6	29.8	165.6	180.0
12	180	200	177.0	31.9	177.0	180.0

3.6.3 Simulation of dry periods and extreme precipitation events

The second part of the experiments was done to simulate how dry period in combination with extreme precipitation events - i.e. a dry period followed by a heavy rainfall - would affect adsorbent performance. The effect on the removal capacity of the adsorption material during extreme precipitation events, and after 24 hours of base flow for the reference column was quantified. The selected precipitation events had an intensity of 45 minutes, and return periods of 10- to 200 years. This intensity was chosen because of the high hydraulic load and volume. As in the first part, the maximum hydraulic load was set to 219 mL/min. The experiments were executed as seen in Table 13:

Table 13. Schedule of extreme precipitation event with dry periods simulation execution

Day	Time	Action
1	12:00	Simulation load on simulation columns, base flow on reference columns
	End of simulation	Pumps for simulation columns shut off.
2	12:00	Pumps for reference columns shut off.

Between the simulations the tubing from the top of the columns was removed to facilitate air flow into the columns and evaporation into the atmosphere. Increasing return period and drying periods was chosen, as seen in Table 14. The last two simulations had the same return period (200 years), to investigate if different lengths of the dry periods affected the removal capability with the same hydraulic load.

Table 14. Sequence of drying simulations was conducted.

SIM no.	Drying period [days]	RP [years]	Runoff HLR [ml/min*m^2]	Column HLR [mL/min]	Time [min]
13	7	10	341.4	219	70.2
14	13	100	497.4	219	102.2
15	20	200	543.6	219	111.7
16	34	200	543.6	219	111.7

3.7 Sampling regime

For the base flow testing samples were taken from all columns on day 1, 3 and 5.

In the first groups of experiments samples from all the columns were taken before the start of a simulation. At the end of the simulations: samples were taken from the simulation columns during the last 10 minutes before the hydraulic load was reduced to base flow. If there was no simulation the day after samples were taken from all columns 24 hours after the previous

simulation was started. In addition, the samples were taken from the bottom ash and pine bark columns after simulation no. 12 for TOC analysis.

In the second group of experiments no samples were taken at the start of the simulations. The samples were taken from the simulation columns at the end of the simulation, and of the reference columns 24 hours after the previous simulation was started. Before each sampling run, the discharge flow from the columns was measured using a gradient cylinder and a stopwatch, and volume collected in one minute, or the time to fill up 100 mL, was used to calculate discharge mL/min.

3.8 Sample analysis

All samples were tests for pH and electrical conductivity right after collection. This was done using a HACH sensION+ pH31 pH-meter (see Figure 9) and a PONSEL ODEON® Advance Digital Meter with a PONSEL C4E Conductivity sensor (see Figure 10). After these analyses, the samples were stored in a freezer at -4 °C to avoid a potential degradation of dissolved organic carbon, because the tap water used for the synthetic stormwater had TOC.

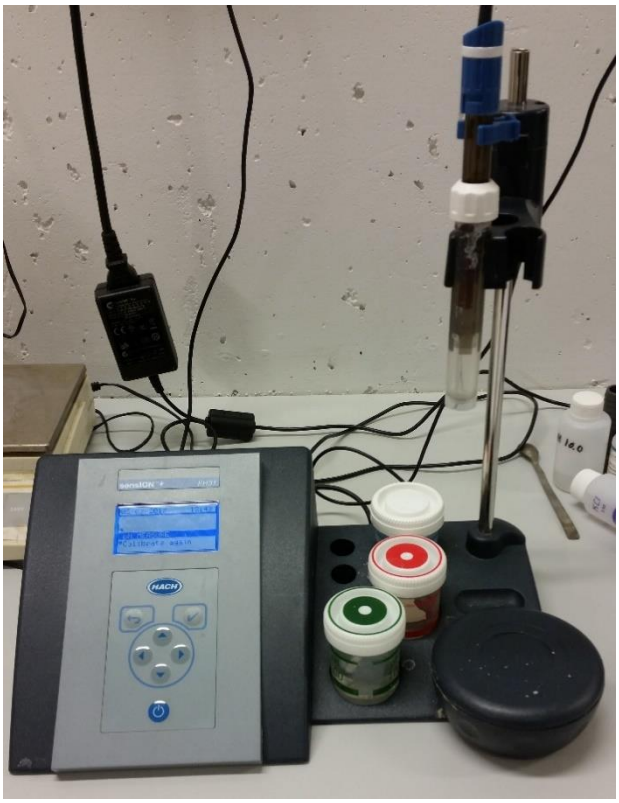

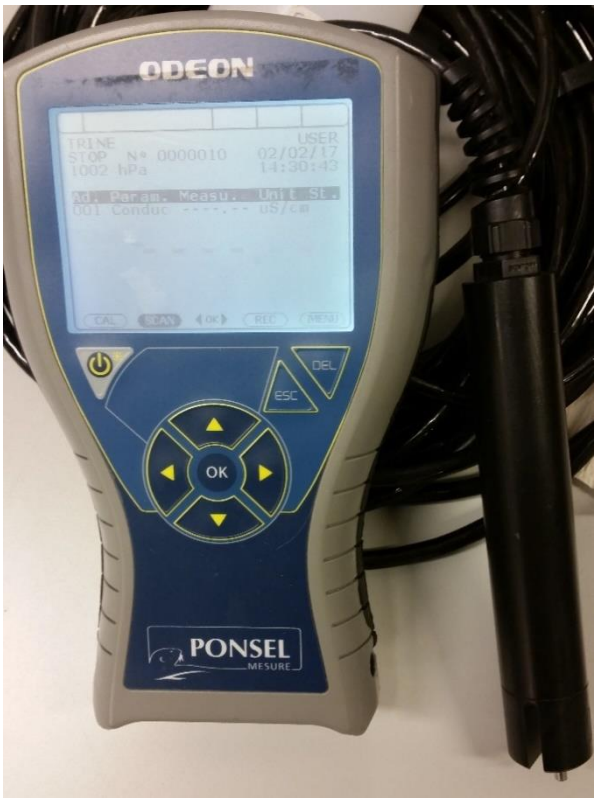

Figure 9. pH-meter used during the experiments *Figure 10. Apparatus used to measure EC*

In two batches the samples were thawed and the metal content was analyzed at an external lab using Inductively coupled plasma mass spectrometry (ICP-MS). To investigate the carbon release, discharge samples from the bottom ash, and pine bark columns was sent to an external lab for a TOC analysis after the 12th simulation (200-years RP, 180-minutes intensity storm).

4. Results and discussion

In this chapter the results of the experiments will be presented and discussed.

4.1 Removal rate 24 hours after extreme hydraulic loads

During extreme precipitation events, most of the runoff will go through an overflow to drainage or another floodway. Only a small percentage of the runoff will be treated by the filter. It is therefore important to look at how well the chosen filter materials operate after such an extreme hydraulic load, and evaluate their robustness by quantify changes in removal rate after the extreme events. This can be done by looking at the removal rate 24 hours after an extreme precipitation event simulation. These results are from the simulations done without prolonged dry periods between simulations.

Overall there were two adsorption materials which showed to be very robust: Bottom ash with iron oxide, and olivine.

4.1.1 Olivine

For Olivine, the removal rate after the simulations of storm events of three intensities and four return periods can be seen in Figure 11, Figure 12, and Figure 13.

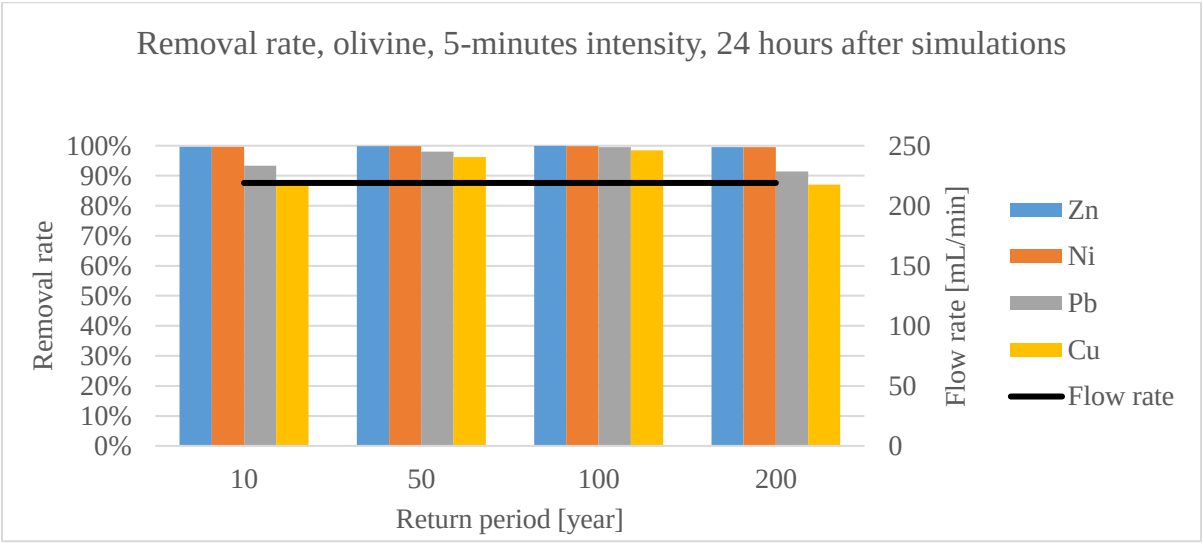

Figure 11. Removal rate of olivine 24 hours after simulations of 5-minutes intensity precipitation events. Flow rate – HLR used during simulation

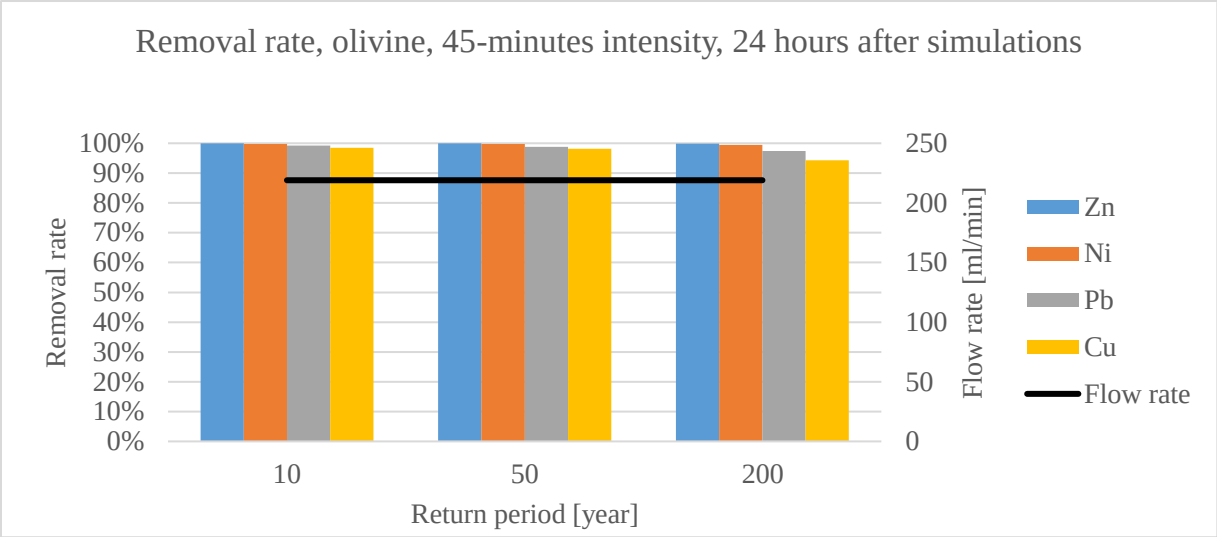

Figure 12. Removal rate of olivine 24 hours after simulations of 45-minutes intensity precipitation events. Flow rate – HLR used during simulation

The simulation of a 45-minute intensity storm with a 100-years RP was conducted, but the sample was lost during the experimental period.

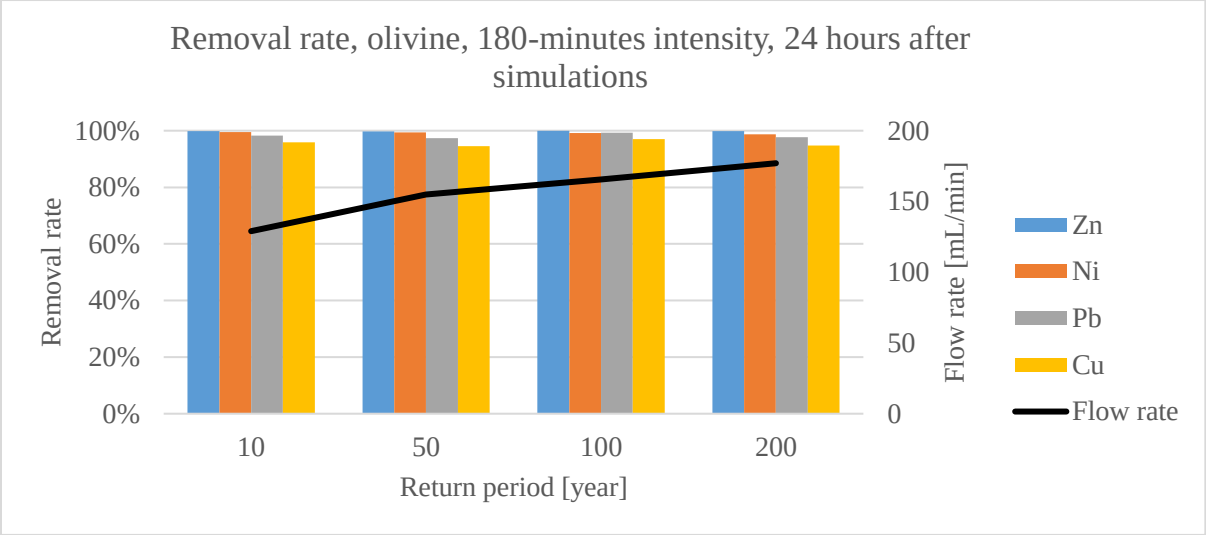

Figure 13. Removal rate of olivine 24 hours after simulations of 180-minutes intensity precipitation events. Flow rate – HLR used during simulation

The removal rate after the 180-minutes intensity simulations were lower than the removal rate after the 45-minute intensity simulations. This may be caused by accumulated metal on the material surface from the previous simulations. The lower removal rate of the 5-minutes simulations may be caused by the column going through a conditioning process where a release of Cu and Pb occured. As shown in Table 12 page 32, the 5-minutes intensity storms were the first simulation conducted in this sequence. While this theory is not supported by the base flow experiments done for a week, as seen in Figure 14, the removal rate of the reference columns,

see Figure 15, show similar behaviour. As the necessary time and volume needed for the material to reach equilibrium state of removal is unknown, the conditioning process may take place over more than 1 week, which could explain this phenomenon.

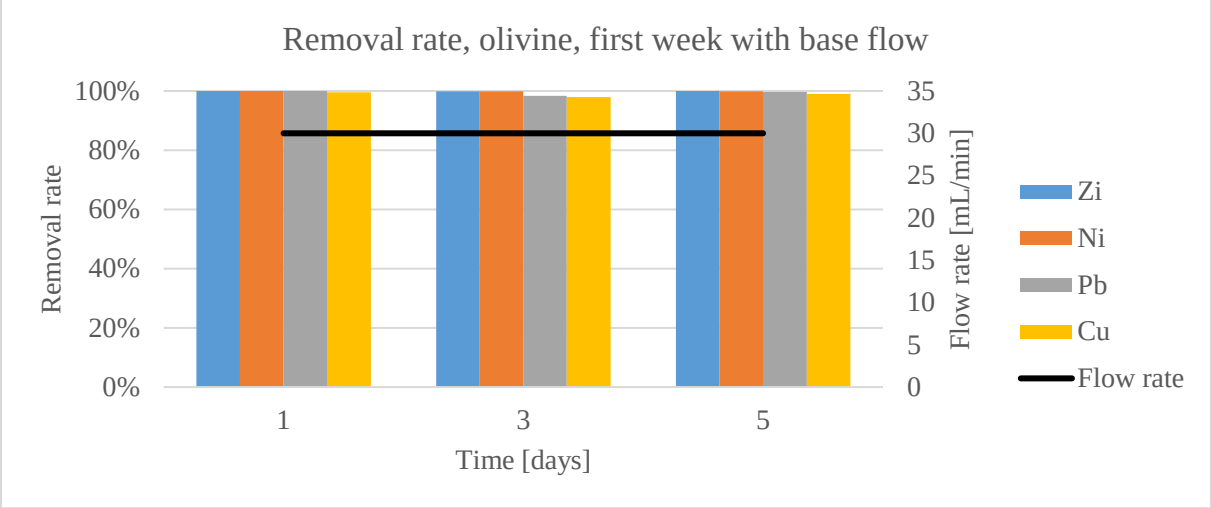

Figure 14. Removal rate of olivine during a 5 day run with base flow, before starting simulations.

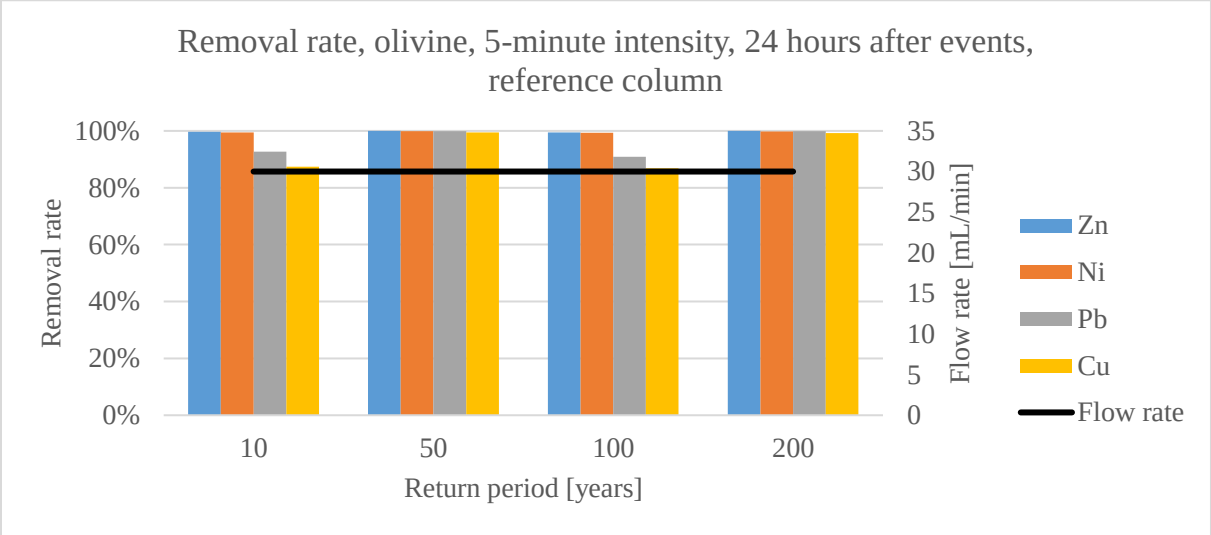

Figure 15. Removal rate of olivine reference column 24 hours after simulations of 5-minutes intensity events.

The reference column had a constant removal rate of > 95 % for the remaining sequential simulations.

Although the removal rate of the simulation column decreases somewhat after the 45-minutes simulation, Figure 12, it was still well above 90%, which is much better than the recommended 60-80 % by COWI [56].

4.1.2 Bottom ash

The bottom ash had the best removal rate throughout all the simulations. As seen in Figure 16, Figure 17, and Figure 18, the removal rate 24 hours after an extreme precipitation event was above 95 % after all the simulations. This was very consistent with the results of Ilyas *et al.*[2] which had 98 % removal rate throughout the breakthrough experiment. These results suggest that the removal rate of bottom ash with 10 w% iron oxide will not be affected by extreme precipitation events.

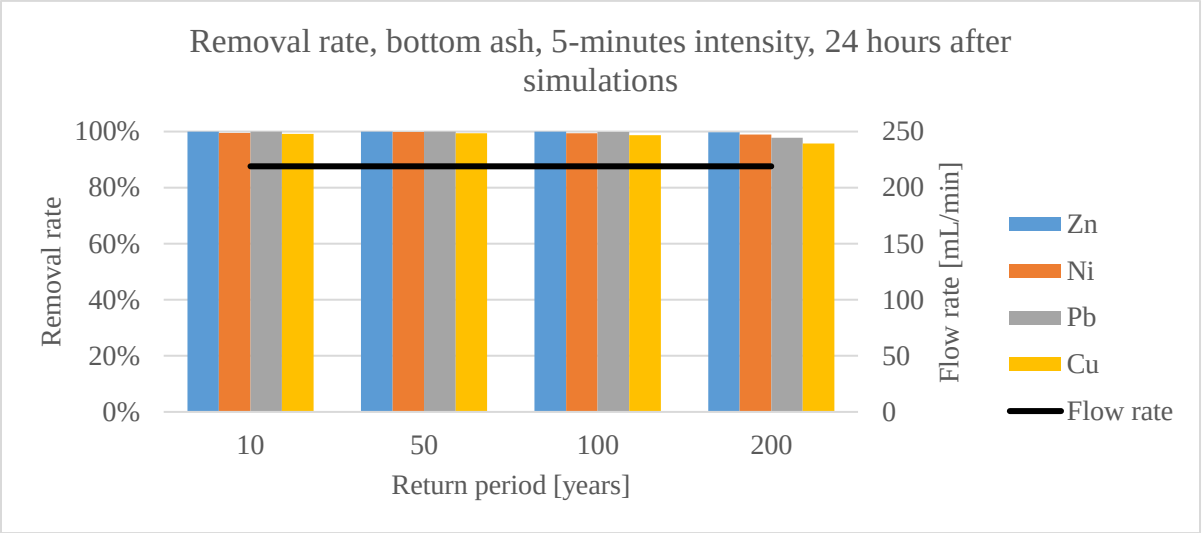

Figure 16. Removal rate of bottom ash 24 hours after simulations of 5-minutes intensity precipitation events. Flow rate – HLR used during simulation

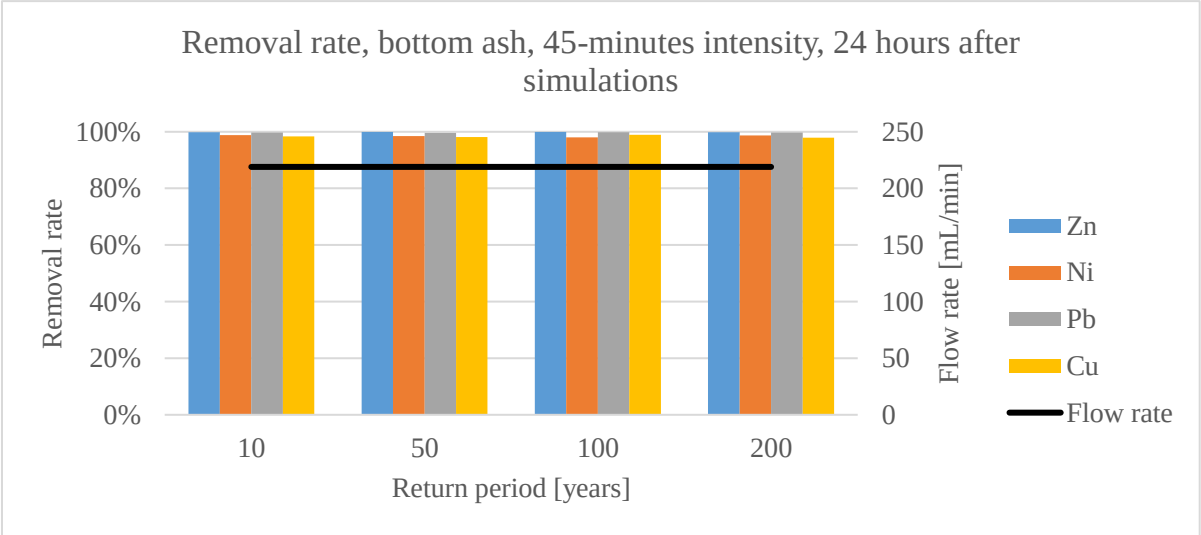

Figure 17. Removal rate of bottom ash 24 hours after simulations of 45-minutes intensity precipitation events. Flow rate – HLR used during simulation

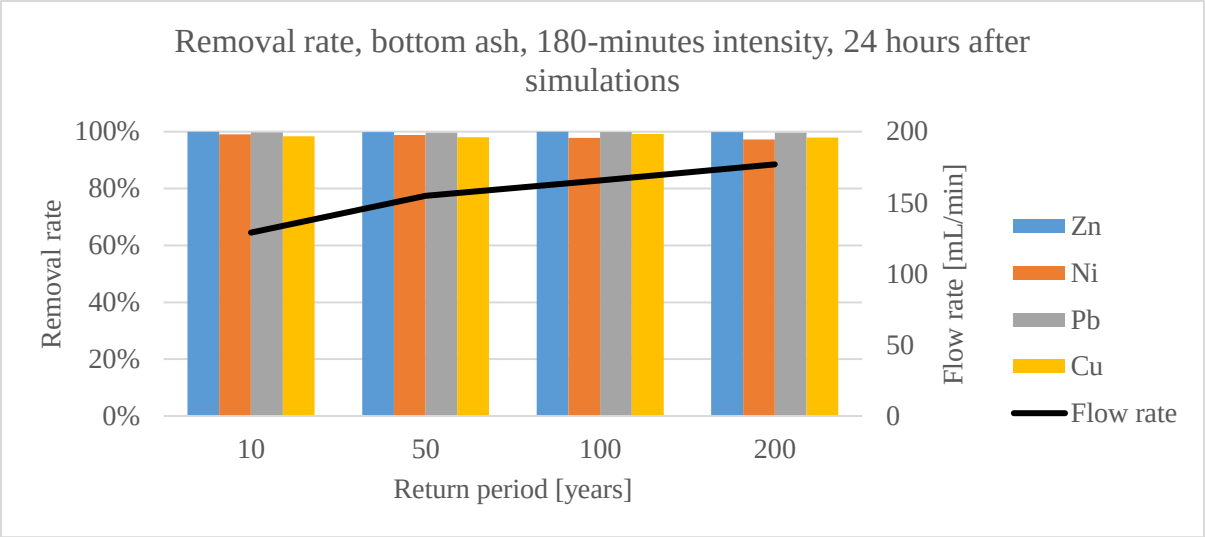

Figure 18. Removal rate of bottom ash 24 hours after simulations of 180-minutes intensity precipitation events. Flow rate – HLR used during simulation

The last two adsorption materials, pine bark and charcoal, had a much lower removal rate after the extreme precipitation simulations.

4.1.3 Pine bark

For pine bark the removal rate of Cu and Pb was > 90 % throughout the simulations. While Ni, which had the worst removal rate, had a removal rate between 40-70 %, as seen in Figure 19, and Figure 20.

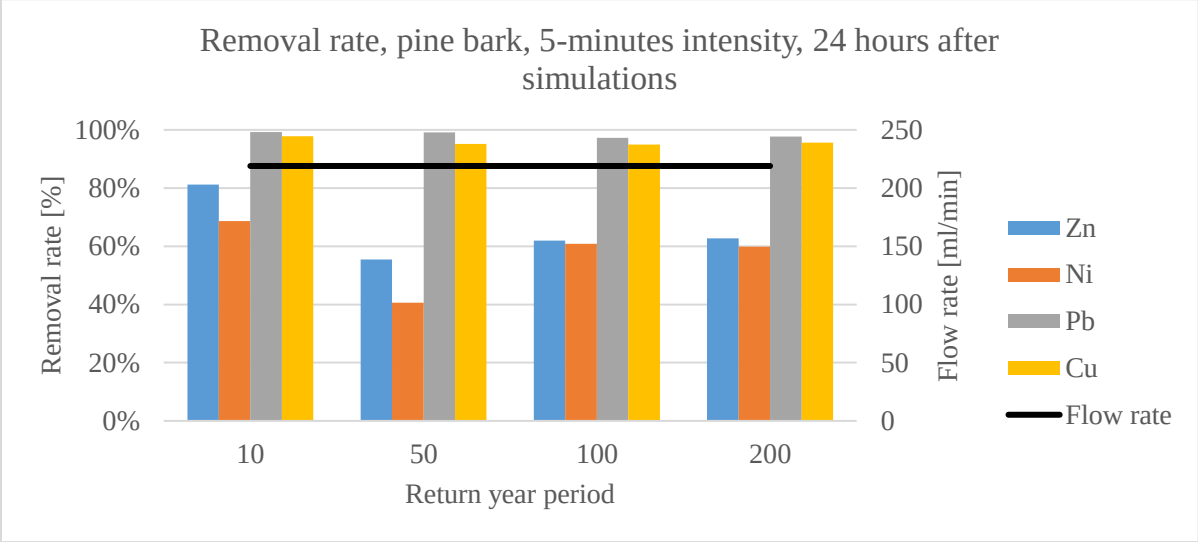

Figure 19. Removal rate of pine bark 24 hours after simulations of 5-minutes intensity precipitation events. Flow rate – HLR used during simulation

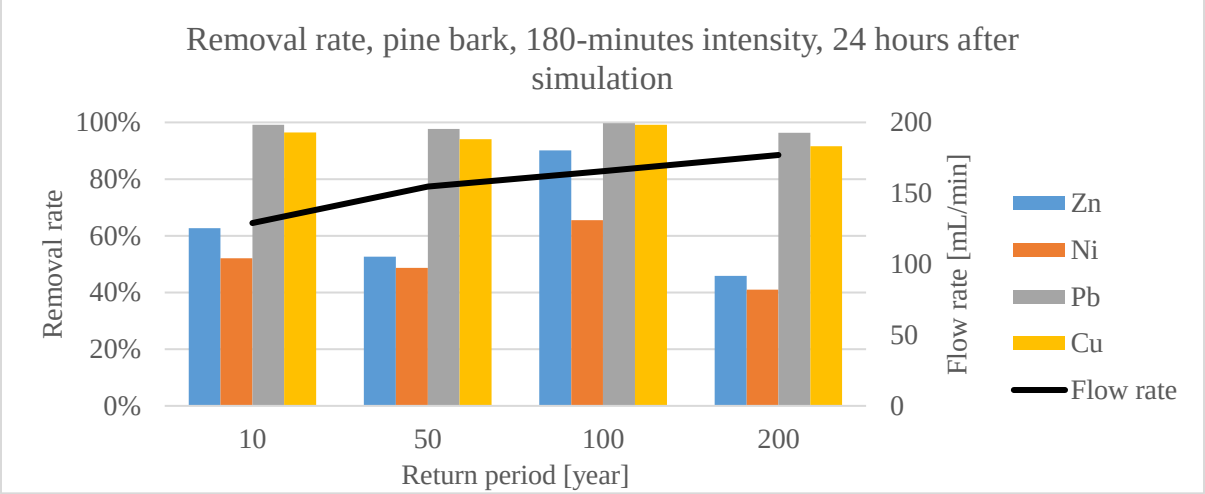

Figure 20. Removal rate of pine bark 24 hours after simulations of 180-minutes intensity precipitation events. Flow rate – HLR used during simulation

The low removal rate for the 50-years, 5-minutes intensity storm may be because this sample was not taken after 24h continuous flow, but rather 30 minutes after the pumps had been started, before the next simulation, after being shut down for 2 days. The electrical conductivity measured shows a higher content of ions in these samples than in other samples taken after 24h

of running, as seen in Figure 21. The higher ion content indicates lower removal rate due to high amount of metal ions in the runoff.

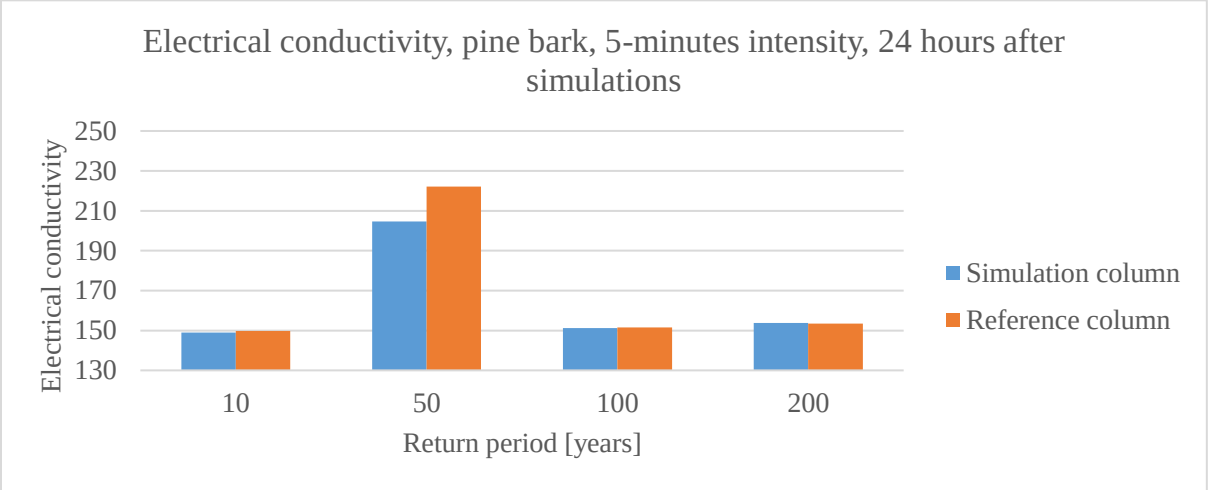

Figure 21. Electrical conductivity from samples after pine bark adsorption 24 hours after 5-minutes intensity precipitation events.

This was confirmed by the reference column which had a similar lower removal rate for the sample taken simultaneously, see Figure 22.

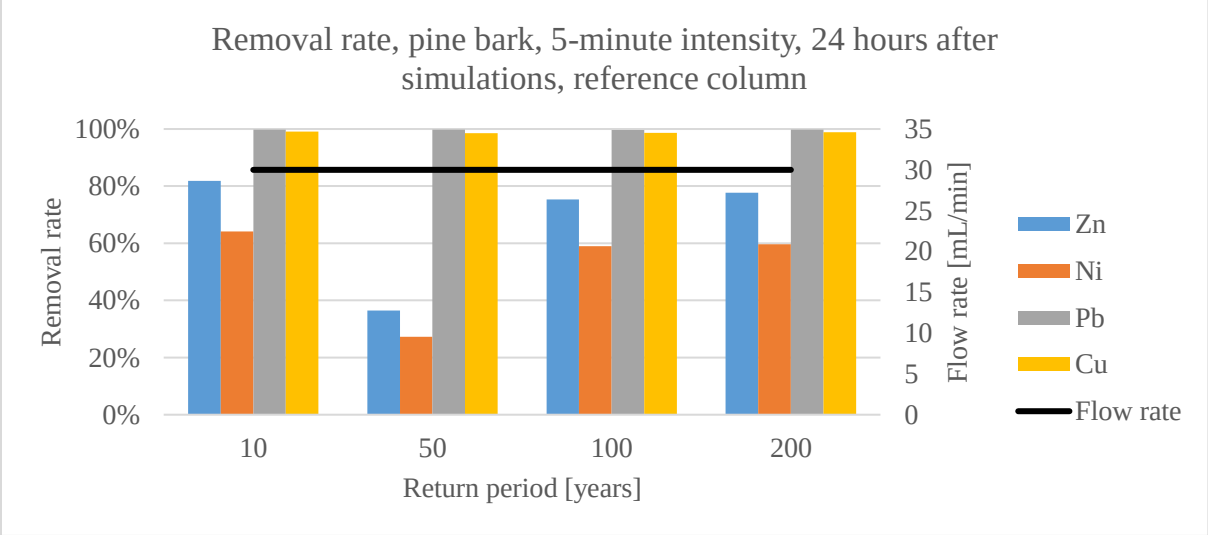

Figure 22. Removal rate of pine bark reference column 24 hours after simulations of 5-minutes intensity events. Flow rate – HLR used during simulation.

This higher ion-content may also be mostly salts, as the conductivity of samples with similar removal rate was much lower, as seen in Figure 23 and Figure 20.

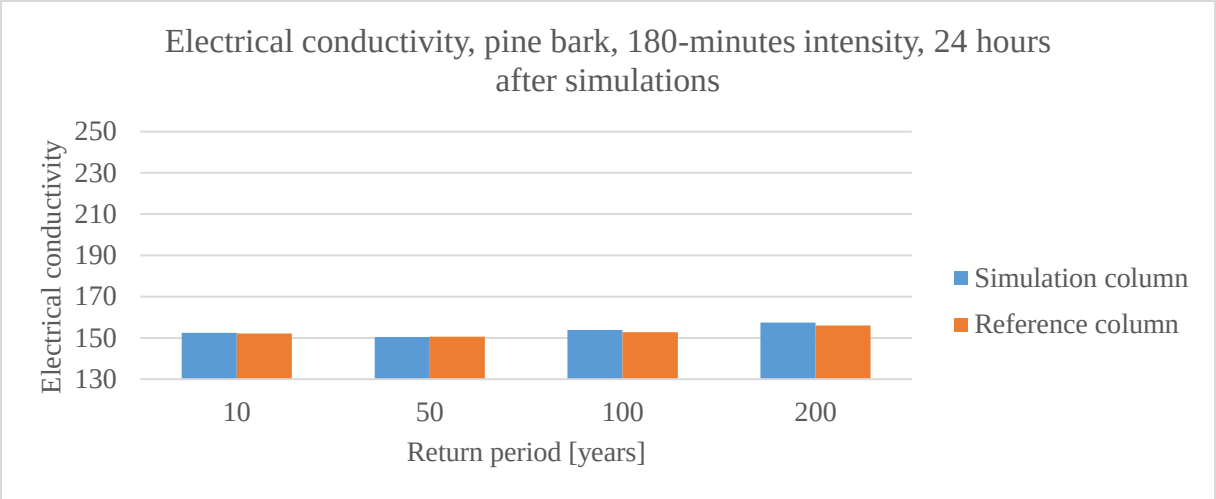

Figure 23. Electrical conductivity from samples after pine bark adsorption 24 hours after 180-minutes intensity precipitation events.

There was no relationship between the hydraulic load on the filter and the observed removal rates. This was confirmed by the removal rate for the reference column taken 24 hours after the 180-years RP simulation, see Figure 24. The removal rate of the reference column was, for some samples, lower than that of the simulation column.

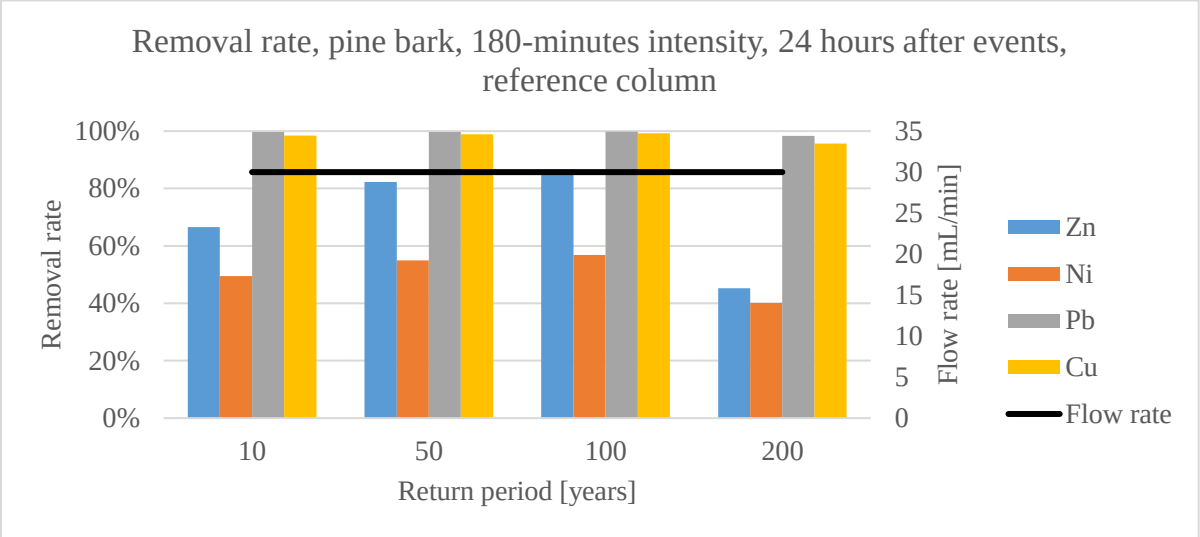

Figure 24. Removal rate of pine bark reference column 24 hours after simulations of 180-minutes intensity events. Flow rate – HLR used during simulation.

In general, the results were similar to those from the breakthrough experiments done by Ilyas *et al.*[2] which had a high removal rate of Cu and Pb, and the lowest removal rate for Ni.

4.1.4 Charcoal

Charcoal had the lowest removal rate of the four adsorption materials, see Figure 25 and Figure 26.

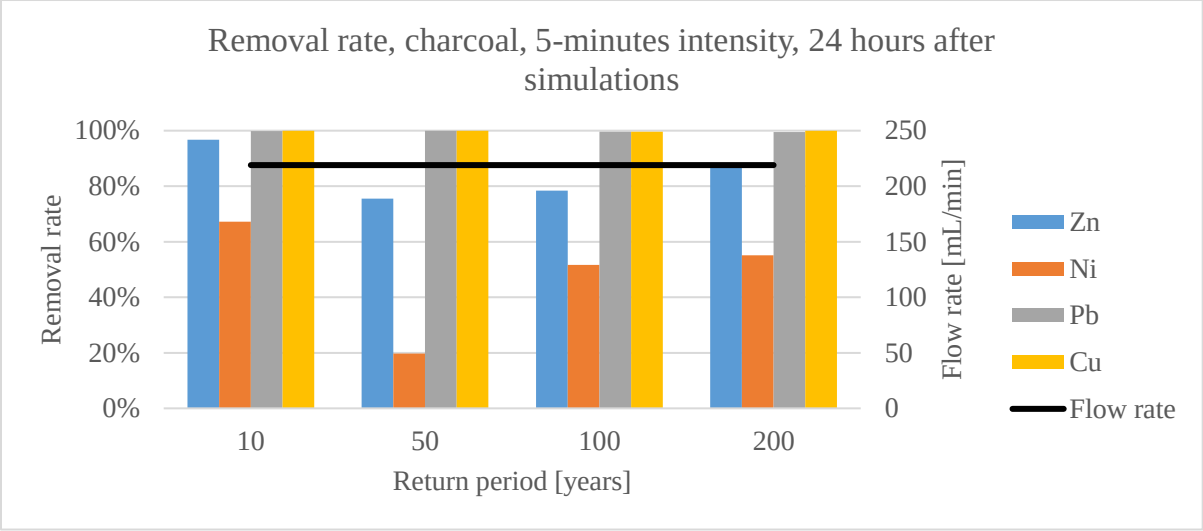

Figure 25. Removal rate of charcoal 24 hours after simulations of 5-minutes intensity precipitation events. Flow rate – HLR used during simulation.

The removal rate of Cu and Pb was steady >90 % after all the all simulation, while the removal rate of Ni fluctuated between 68 % and 1 %, and ended at 8 % after the last sequential simulation, see Figure 26 and Figure 27.

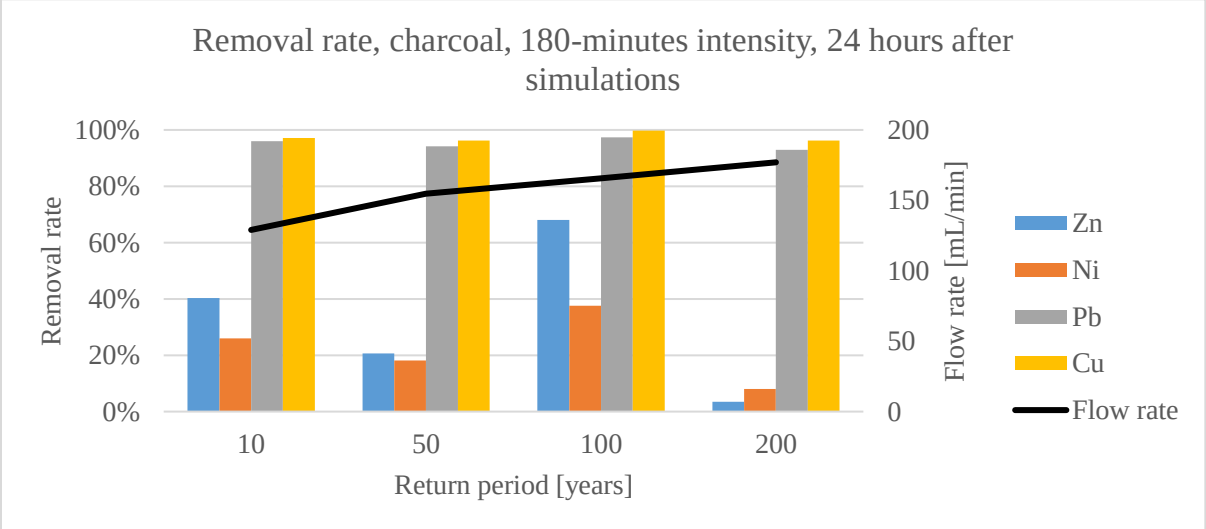

Figure 26. Removal rate of charcoal 24 hours after simulations of 180-minutes intensity precipitation events. Flow rate – HLR used during simulation.

The low removal rate of Ni can be explained by the pH of the discharge from the column. According to Shim *et al.*[84] activated carbon has several times higher adsorption affinity for

Cu than Ni at pH < 8. The pH of the discharge from the charcoal columns was steady below pH 8, as can be seen in Table 15. This may explain the overall low removal rate, but not the fluctuation as the removal rate did not seem to correlate with the pH, as seen if comparing Figure 26 and Table 15.

Table 15. pH of charcoal column discharges 24 hours after extreme precipitation event.

	Return period			
Intensity [minutes]	**10 years [pH]**	**50 years [pH]**	**100 years [pH]**	**200 years [pH]**
5	8.16	7.79	7.68	7.74
45	7.86	7.71	7.74	7.44
180	7.47	7.53	7.78	7.65

The fluctuation of Zn removal rate was even greater than that of the other metals. Between the two consecutive simulations, the removal rate went from -14 % to 80 %, as seen in Figure 27. This means that 24 hours after a 100-years, and 45-minutes intensity storm, the charcoal adsorption material had a discharge with a 14 % higher metal concentration than the initial concentration. The same sample also has the lowest removal rate of Ni (1 %).

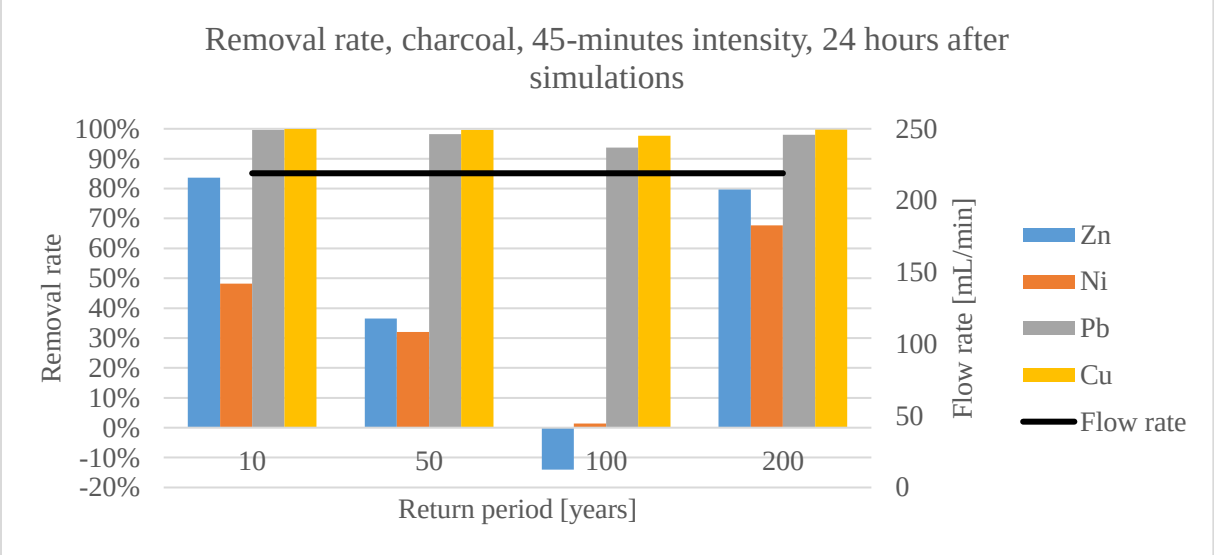

Figure 27. Removal rate of charcoal 24 hours after simulations of 45-minutes intensity precipitation events. Flow rate – HLR used during simulation.

This discharge of Zn might be driven by a sudden desorption event. A desorption mechanism may have taken place simultaneously with the adsorption. This was, however, impossible to

prove with the collected data. The desorption event may have left a large number of adsorption sites free, which may explain the large removal rate after the next simulation (200-years RP, 45-minutes intensity Figure 27).

There were no solid indications of any certain correlation between the removal rate and the magnitude of the hydraulic load, or the length of the period the load was administrated for any of these results. This was confirmed by the removal rate by the reference column which, like the simulation column, had very large fluctuations for Zn and Ni, and a little lower removal rate for Pb and Cu, see Figure 56 page 69.

4.2 Removal rate during extreme hydraulic loads

To investigate the removal capability during first flush of extreme precipitation events the quantified changes in removal rate during extreme events was measured.

4.2.1 Olivine

As for the results for the removal rate 24 hours after an event, the removal rate of olivine during extreme precipitation events was very good. Except for one sample taken during a 5-minute 10-years storm, as seen in Figure 28.

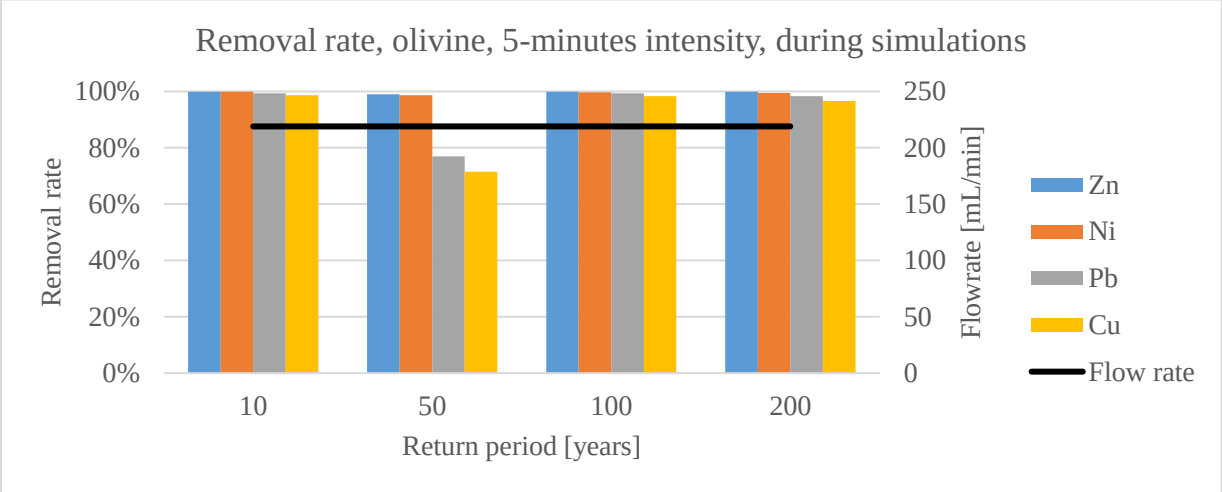

Figure 28. Removal rate of olivine during simulations of 5-minutes intensity precipitation events. Flow rate – HLR used during simulation.

This was a very different result than the others, as all other samples taken during the simulations has a removal rate of > 90 % for all four metals, as seen in Figure 29 and Figure 30 . The reason may be mechanical or human error, or a conditioning process, which was discussed in chapter 4.1.1. All other measurements taken (pH, EC, discharge) show no indication of other reason for the low removal rate.

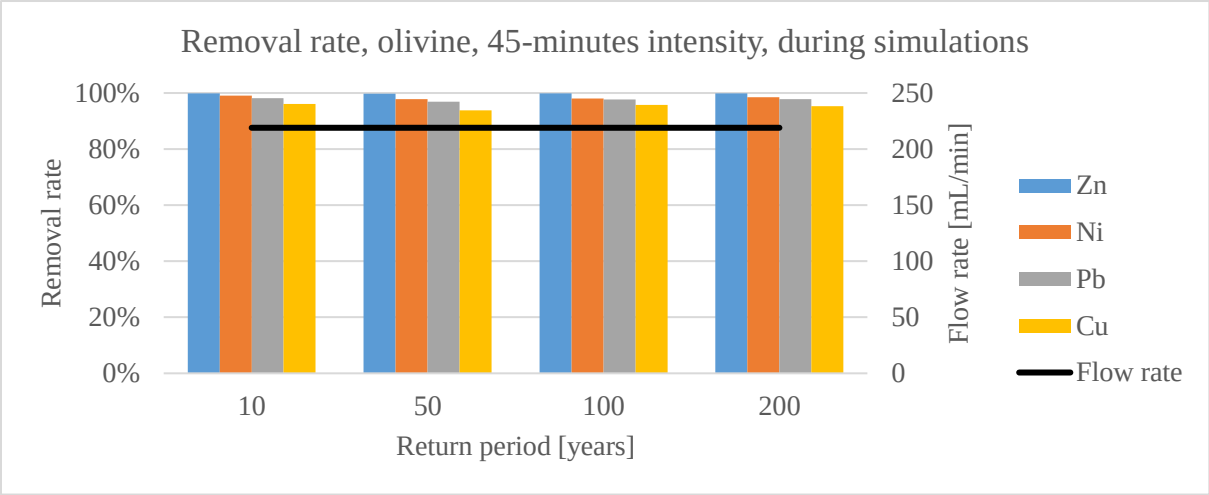

Figure 29. Removal rate of olivine during simulations of 45-minutes intensity precipitation events. Flow rate – HLR used during simulation.

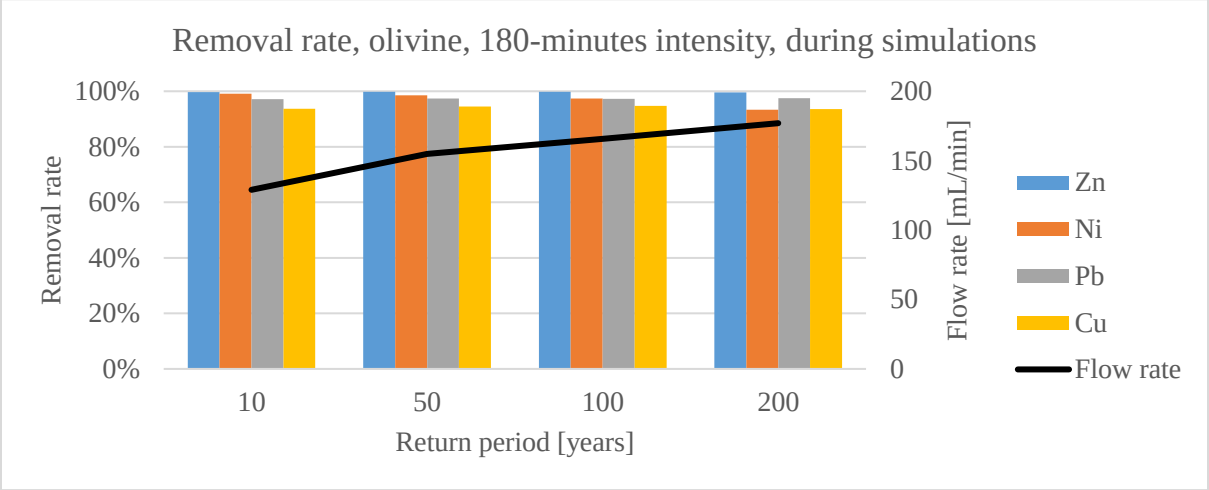

Figure 30. Removal rate of olivine during simulations of 180-minutes intensity precipitation events. Flow rate – HLR used during simulation.

From the rest of the results, overall removal rate of olivine during extreme hydraulic loads were >90 %.

The samples from both 24 hours after a simulation, and during simulations gave a solid indication that olivine's affinity towards the metals was in the order: Zn > Ni > Pb > Cu.

4.2.2 Bottom ash

For the 24 hours after simulation-samples, the bottom ash had an overall better removal rate than olivine. This was not the case for the removal rate during simulations, as seen in Figure 31.

Figure 31. Removal rate of olivine during simulations of 5-minutes intensity precipitation events. Flow rate – HLR used during simulation.

The removal rate was still greater than the removal rate suggested by COWI [56], but the hydraulic load had a larger effect on the removal rate, compared to that of olivine. The magnitude of the hydraulic load did not seem to have any large significands, as seen in Figure 32 and Figure 33. Except maybe a slight correlation between the increasing flow rate and the lower removal rate during the 180-minutes storms in Figure 33.

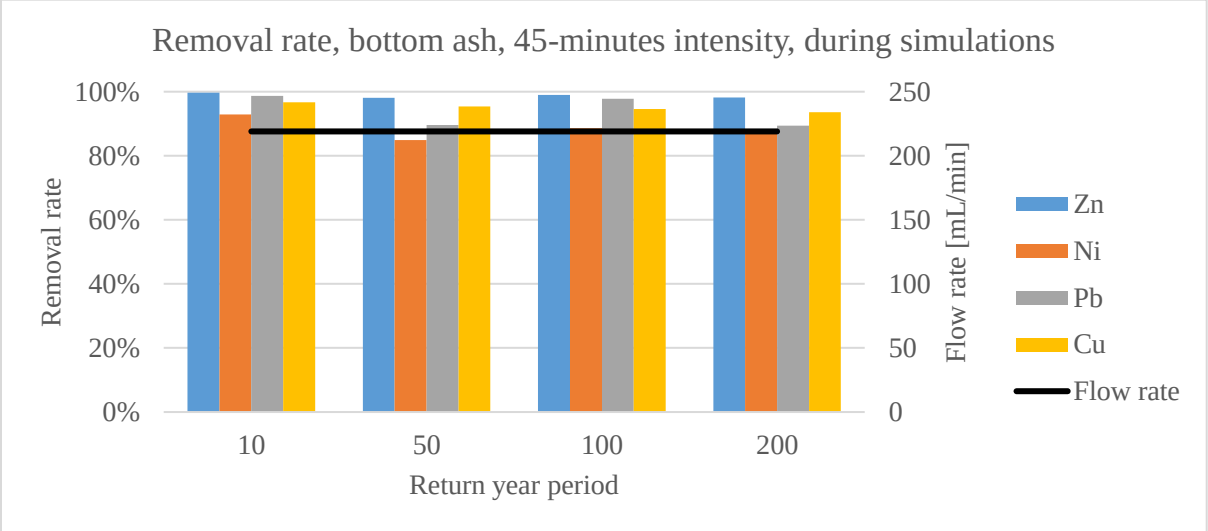

Figure 32. Removal rate of olivine during simulations of 45-minutes intensity precipitation events. Flow rate – HLR used during simulation.

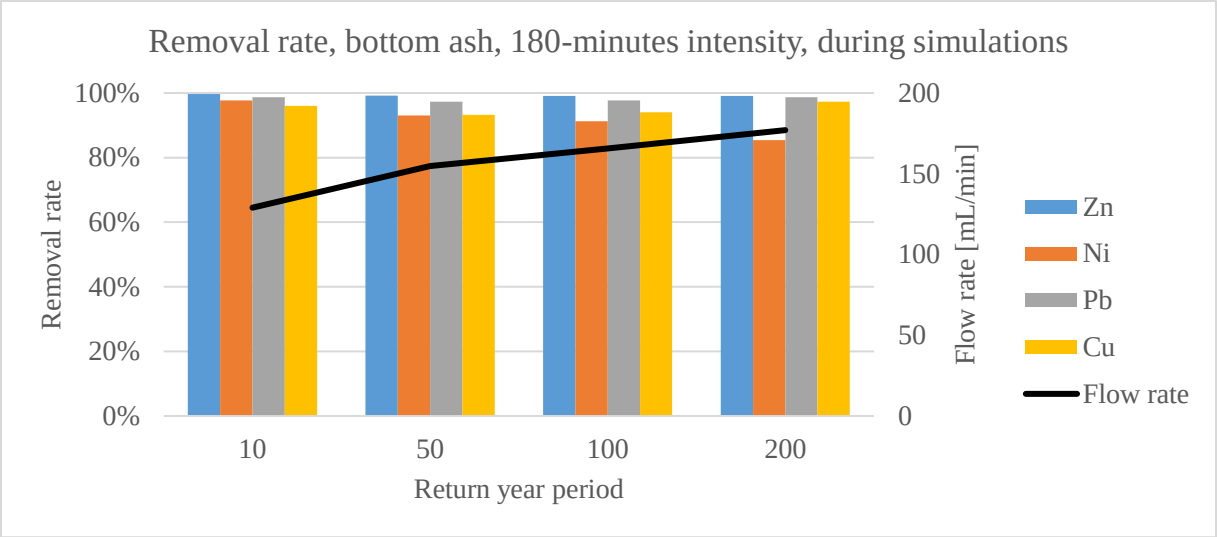

Figure 33. Removal rate of olivine during simulations of 180-minutes intensity precipitation events. Flow rate – HLR used during simulation.

If this correlation existed, the length of the period under a certain hydraulic load had less influence than the magnitude of the hydraulic load. This was based on the similarities of the removal rate during 5-minutes and 45-minute storms. These storms had similar hydraulic loads (219 mL/min), but large variations in the time under the hydraulic load (31.4 - 111.7 minutes). This was very interesting as the maximum hydraulic load on a filtration trench can be adjusted with e.g. the height of the overflow barrier, while the amount of time under the hydraulic load was dependent on the precipitation event.

As for affinity for different metals, it was clear that bottom ash has the highest affinity for Zn. The other three metals have surprisingly high variations in removal rate, relatively to each other. If looking at both the 24 hours after samples, and the samples taken during the simulation one may draw the conclusion that bottom ash has a slightly higher affinity towards Pb than towards Ni and Cu. But there were many examples where this was inconsistent as seen in Figure 32 and Figure 33.

4.2.3 Pine bark.

The pine bark column had similar results during the simulations, as after 24 hours. The removal rate of Pb and Cu was still approximately > 90 %, and the removal rate of Zn and Ni was fluctuating between 45-90 % and 45-80 %, respectively. The removal rate did not seem to be affected by the amount of time with a specific hydraulic load, as seen in Figure 34 and Figure 35.

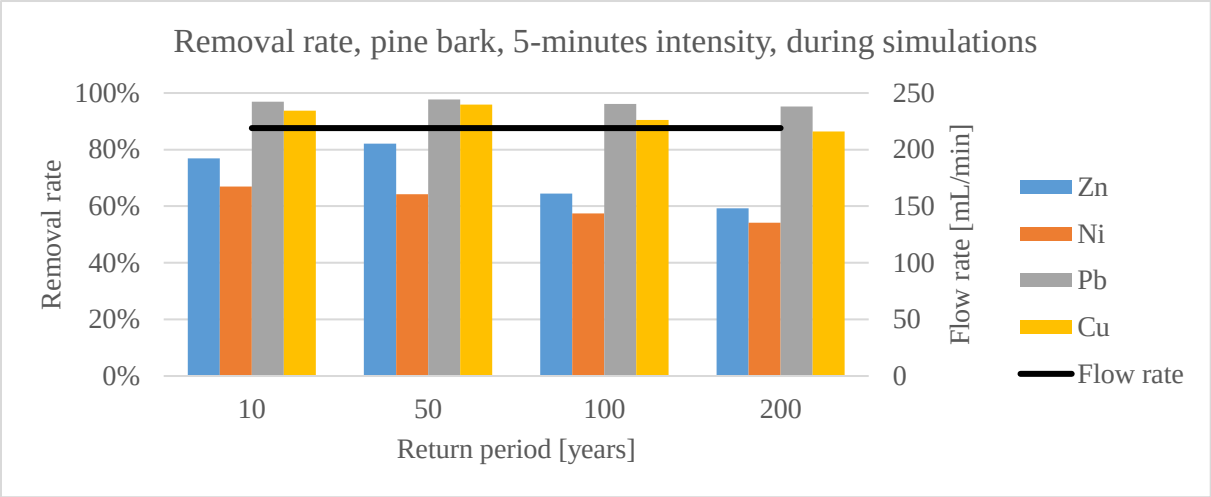

Figure 34. Removal rate of pine bark during simulations of 5-minutes intensity precipitation events. Flow rate – HLR used during simulation.

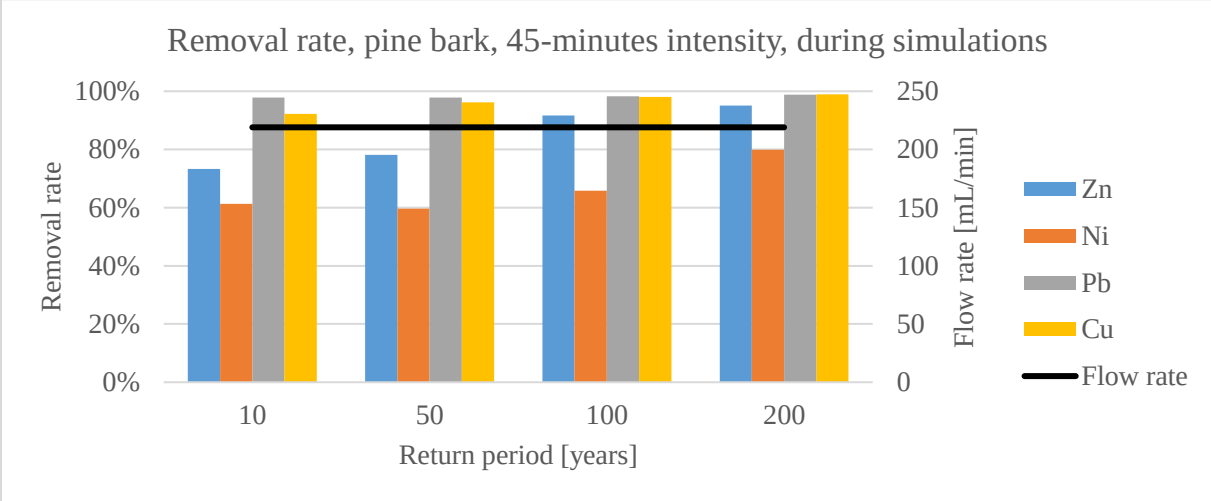

Figure 35. Removal rate of pine bark during simulations of 45-minutes intensity precipitation events. Flow rate – HLR used during simulation.

This was especially clear as the removal rate seemed to decrease as the return period increase in Figure 34, while it increased together with the return period in Figure 35. The magnitude of the hydraulic load did not seem to affect the removal rate, as seen in Figure 36.

Looking at both groups of samples; the ones taken 24 hours after simulations; and the ones taken during simulations, there were large variations in the removal of Zn and Ni. But in a whole, the hydraulic load did not seem to affect the removal rate of the different metals significant. This may be explained by very fast sorption reaction, and that the removal rate was limited by competing reaction with the other metals. This could be explored with additional simulation without Pb and Cu present. If the contact time in the column was limited, one should see a clear difference between the samples taken during extreme events, and the ones taken 24

hours after. This was confirmed by the reference column which had very similar types of removal rates, see Figure 55.

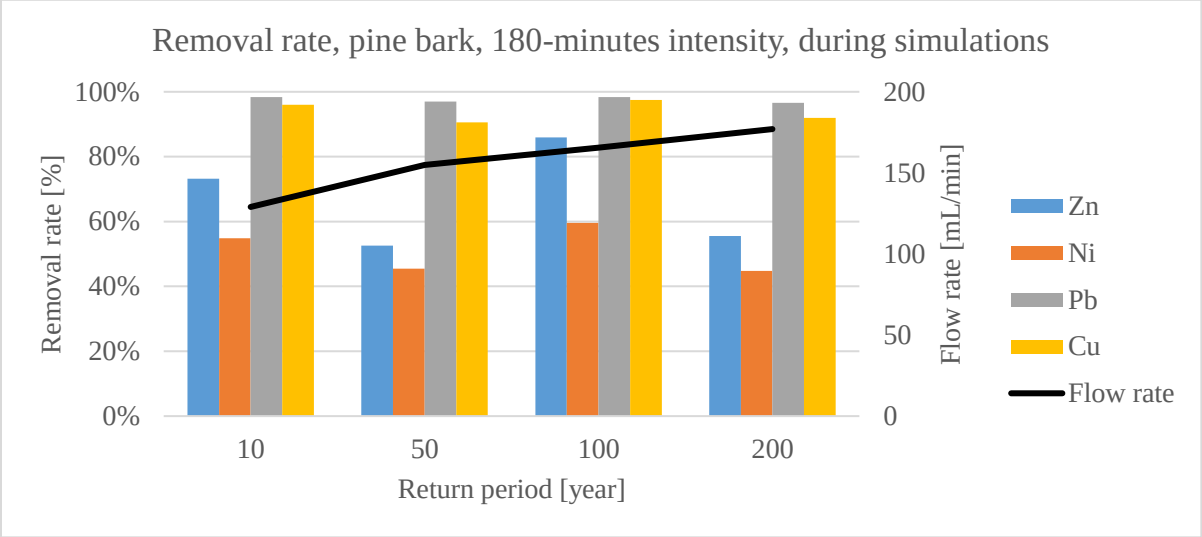

Figure 36. Removal rate of pine bark during simulations of 180-minutes intensity precipitation events. Flow rate – HLR used during simulation.

4.2.4 Charcoal

The removal rate for the charcoal column during the simulations were quite different from the ones from 24 hours after the simulation. As seen in Figure 37, the column had a very large release of Zn during the 100-years RP, 5-minutes intensity storm, which was a clear indication of a desorption. The reason for this may be the total accumulated metal, triggering the desorption. Another explanation may be a bypass situation due to low contact time, but this did not explain the desorption.

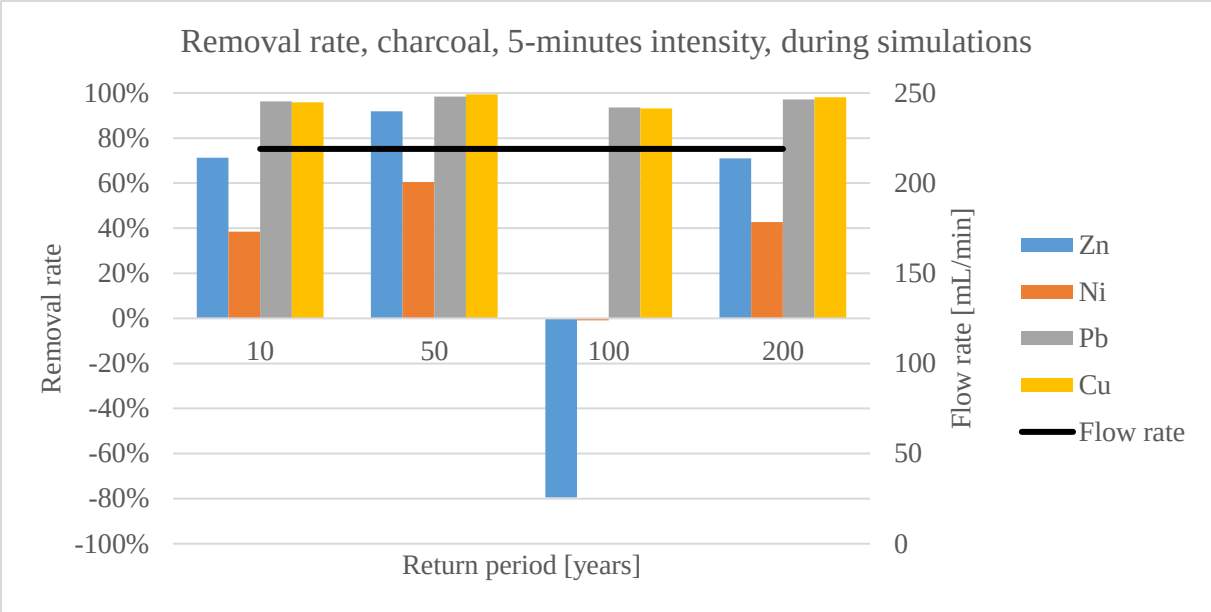

Figure 37. Removal rate of charcoal during simulations of 5-minutes intensity precipitation events. Flow rate – HLR used during simulation.

For the rest of the simulations there were indications of the removal rate stabilizing, as seen in Figure 38 and Figure 39.

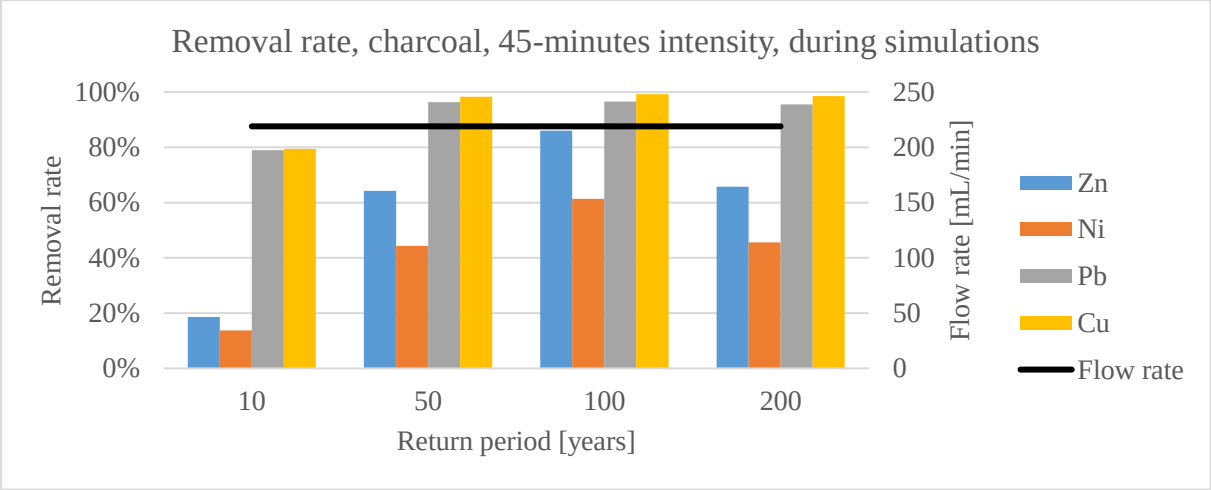

Figure 38. Removal rate of charcoal during simulations of 45-minutes intensity precipitation events. Flow rate – HLR used during simulation.

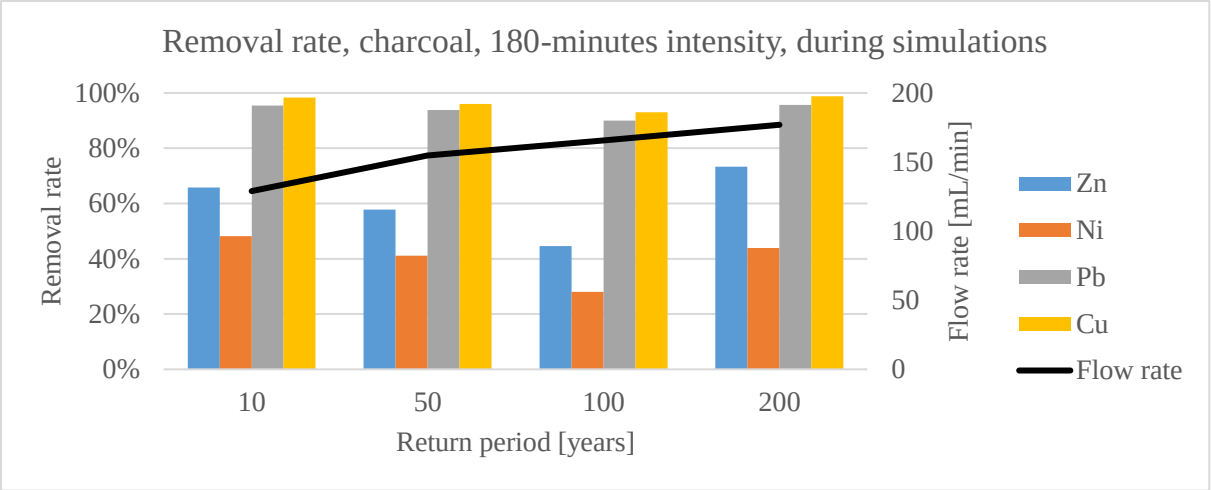

Figure 39. Removal rate of charcoal during simulations of 180-minutes intensity precipitation events. Flow rate – HLR used during simulation.

However, this stabilization was probably not consistent as Figure 27, page 46, indicates some sort of desorption event 24 hours after the 100-years RP, 45-minutes intensity storm. This desorption did not fit with the very high removal rate during the simulation, as seen in Figure 38. These results indicate that the column had a very high removal rate during the simulation, and probably underwent desorption during the 24 hours of base flow after the simulation. One would suggest the breakthrough mechanics to have a steady reduction in removal rate leading up to the breakthrough. There was no evidence of such a mechanism, so another explanation should be considered. The column seemed to go from seemingly stable removal rate, to sudden desorption, and back to seemingly steady removal rate in the matter of hours. This may indicate that the column was under conditions very close to the adsorbed-dissolved equilibrium point. This may be regulated by different parameters, but as seen in Table 16 the pH of the samples taken during the 45-minutes intensity simulations did not show anything that may explain the change.

Table 16. pH and EC of charcoal simulation column 24 hours after the 45-minute intensity simulation in sequential simulations.

	Return period			
Parameter	**10**	**50**	**100**	**200**
pH	7.86	7.71	7.74	7.44
EC	166.8	170.6	162.1	188.1

This breakthrough mechanism of steady decline in removal rate was not visibly leading up to the desorption event during the 100-years RP, 5-minutes intensity storm. Where the sample taken right before this simulation (24 hours after the 50-years RP, 5-minutes intensity storm, Figure 27) had a high Zn removal rate. These results may indicate one of two things. Either the breakthroughs were following another mechanism not explained by the results, or the breakthroughs were happening at such a high velocity that the sampling regime was not able to completely illustrate it. The latter explanation was not likely as breakthroughs does not happen so quickly.

4.3 Removal rate after dry periods

To investigate the effect of the dry periods the similar return period and intensity was investigated as was done without dry periods. The results was compared to the results of Hatt *et al.*[103] which showed that drying periods had a positive effect on the removal rate of their filter material.

4.3.1 Olivine

The dry periods had no positive affect on the olivine's removal rate during the similar hydraulic loads compared to the results without dry periods. Comparing Figure 40 with Figure 29, page 49, shows a lower removal rate during the simulations after drying. These figures, combined with Figure 30 page 49, gave no clear indication of drying having positive effect. The removal rate of Pb and Cu did however seem to increase with the drying period between the last to simulations shown in Figure 40

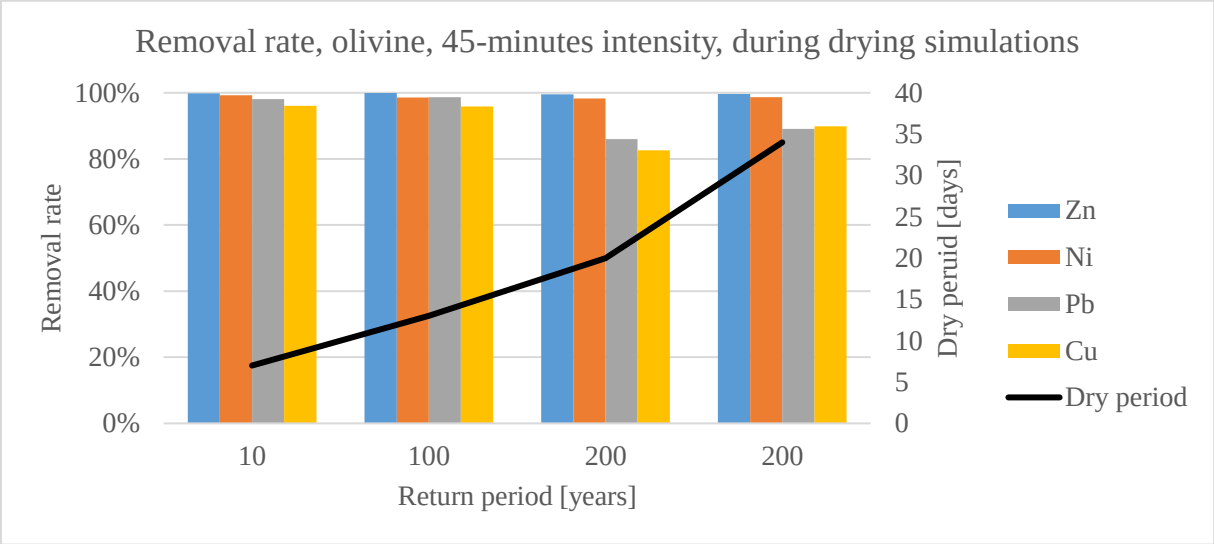

Figure 40. Removal rate of olivine during simulations of 45-minutes intensity precipitation events after drying periods

The reference column has similar results, as seen in Figure 41 which shows the last measurements for the reference column during the sequential simulations, and Figure 42. It was noteworthy that both the reference-, and the simulation column had a small increase in removal rate for the last dry period simulation (200-years RP, 45-minutes intensity). The only difference between the two 200-years RP simulations was the length of the drying period. The longer

drying period influencing the removal rate may indicate that the column did not have enough time during the shorter drying periods, under these conditions, to dry enough to make a change in the removal rate. Even though this might indicate a positive effect of drying, the sudden decrease in removal rate for the first 200-year storm cannot be explained. This decrease should not be caused by the increased hydraulic load, as it occurs for the reference column as well. This drop in removal rate made it difficult to conclude any positive effect of drying on the removal rate.

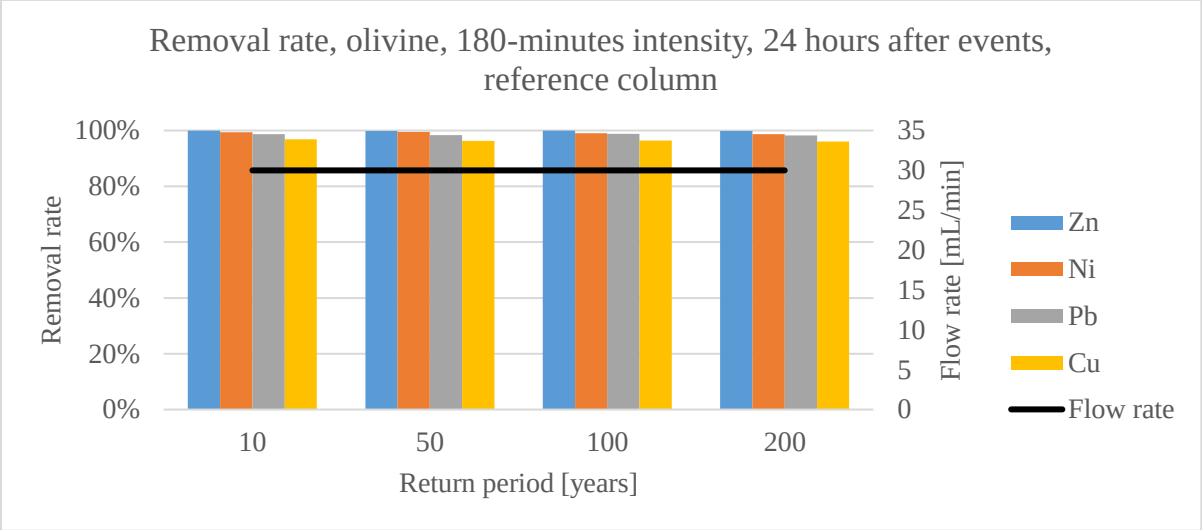

Figure 41. Removal rate of olivine reference column 24 hours after simulatiosn of 180-minutes intensity events. Flow rate – HLR used during simulation.

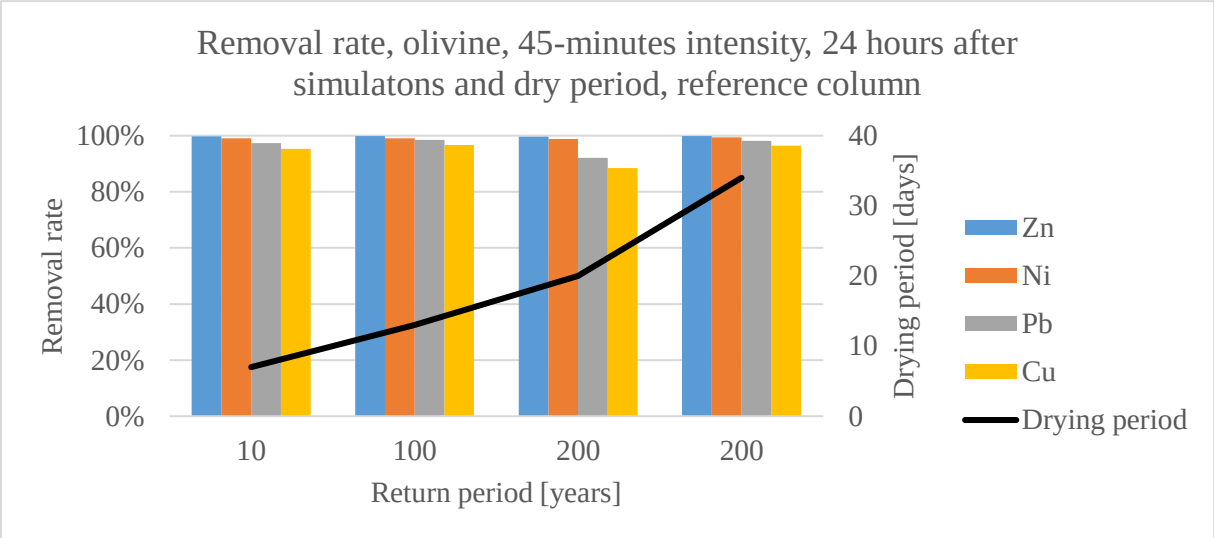

Figure 42. Removal rate of olivine reference column 24 hours after simulations of 45-minutes intensity events after drying periods

4.3.2 Bottom ash

If compared, the results from during the drying experiments (see Figure 43) and those without the drying period (see Figure 32 page 50) there may have been miniscule increase in removal rate.

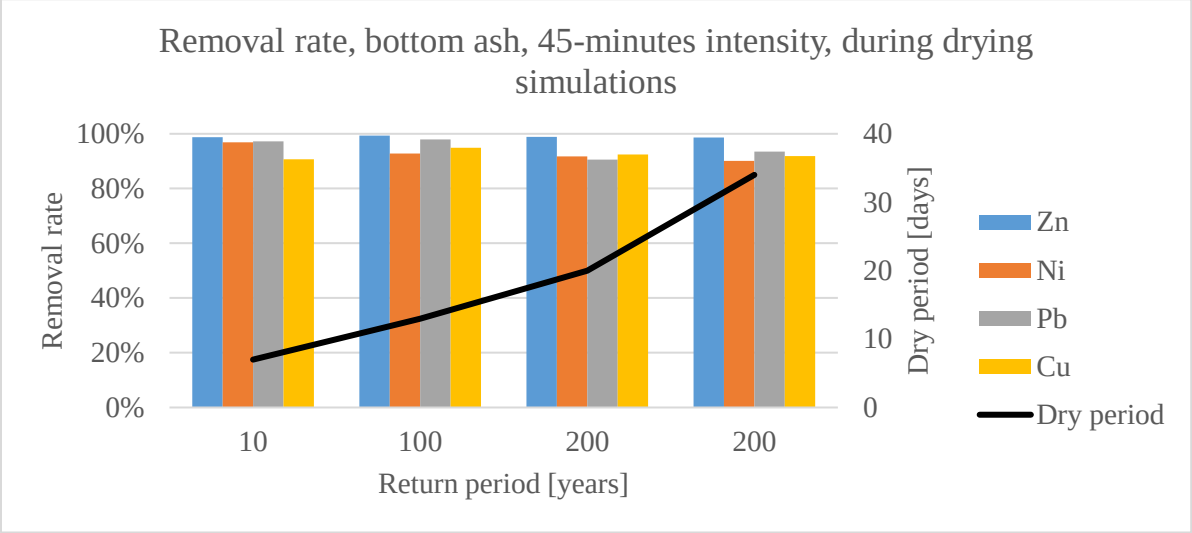

Figure 43. Removal rate of bottom ash during simulations of 45-minutes intensity precipitation events after drying periods

This increase did not occur in the reference column which had a miniscule decrease in removal rate (see Figure 45 and Figure 44).

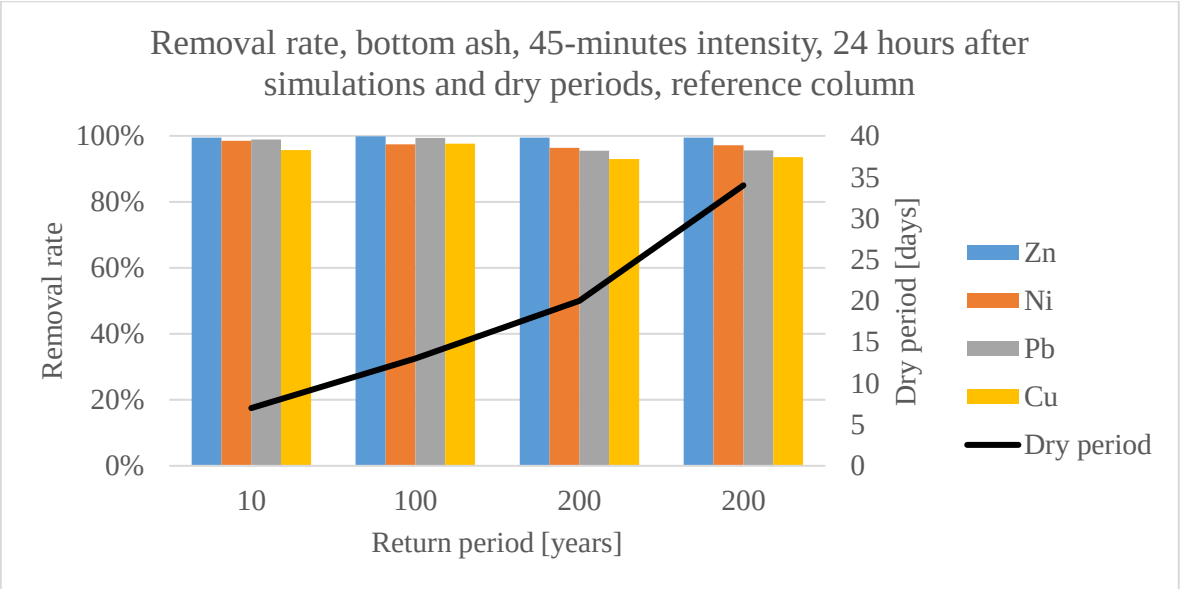

Figure 44. Removal rate of bottom ash reference column 24 hours after simulations of 45-minutes intensity events after drying periods

The sizes of these differences were on such a small scale that identifying a specific reason for the changes was not possible. The divergent effects, of the drying periods, on the simulation and the reference column did not imply any correlation between the drying and the removal rate. Because of these results one could thus conclude that the drying periods had little to no effect on the removal rate of bottom ash with iron oxide (10 w%)

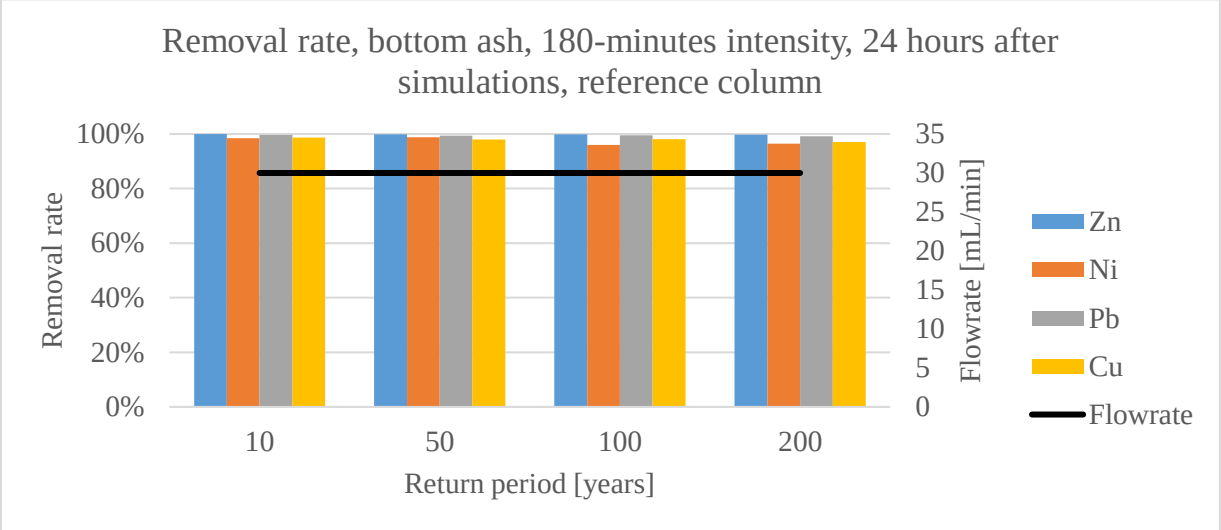

Figure 45. Removal rate of bottom ash reference column 24 hours after simulations of 180-minutes intensity events. Flow rate – HLR used during simulation.

4.3.3 Pine bark

The drying had a negative effect on the metal removal rate of pine bark (see Figure 46 and Figure 35 page 52). This was confirmed when comparing the last measurements for the reference column, 24 hours after the sequential simulations, with the ones 24 hours after the dry period simulations, Figure 24 page 44 and Figure 47 respectively. Because the pine bark is an organic material, the reduced removal rate may be caused by biodegradation in the pine bark. The contact with both water and oxygen during the intermitting wetting and drying increases the biodegradation of the pine bark, which may degrade sorption sites in the pine bark, reducing the sorption capability of the bark. As seen in Figure 46 and Figure 47, the removal rate did not decrease as the dry period increased in length. The reference column had an increase in removal rate between the last to simulations, see Figure 47. The only significant decrease in removal rate was during the initial dry period. This indicated that no degradation of sorption sites during the possible biodegradation occurred throughout the subsequent experimental period. This may be explained by the pine bark not drying properly. The reason for this may be the low drying capability of the setup, and that pine bark is harder to dry than the other material. This may

have caused the pine bark to stay wetted throughout the dry period. This would cause the dry period to not give the increased biodegradation effect caused by intermitted drying and wetting. This explanation did, however, not explain the drop in the initial dry period. Another explanation may be that the biodegradation produces sorption points as well as degrade them. Thus, the pine bark may have been biodegraded during the initial dry period down to a point where the amount of sorption site degraded and produced was equal. Causing the removal rate to stabilize for the rest of the dry period simulations. The increase in the removal rate of the reference column between the last two measurements may indicate that the drying has a positive effect on the removal rate. However, comparing the rest of the samples during the drying simulations the increase may also have other explanation not apparent by the results.

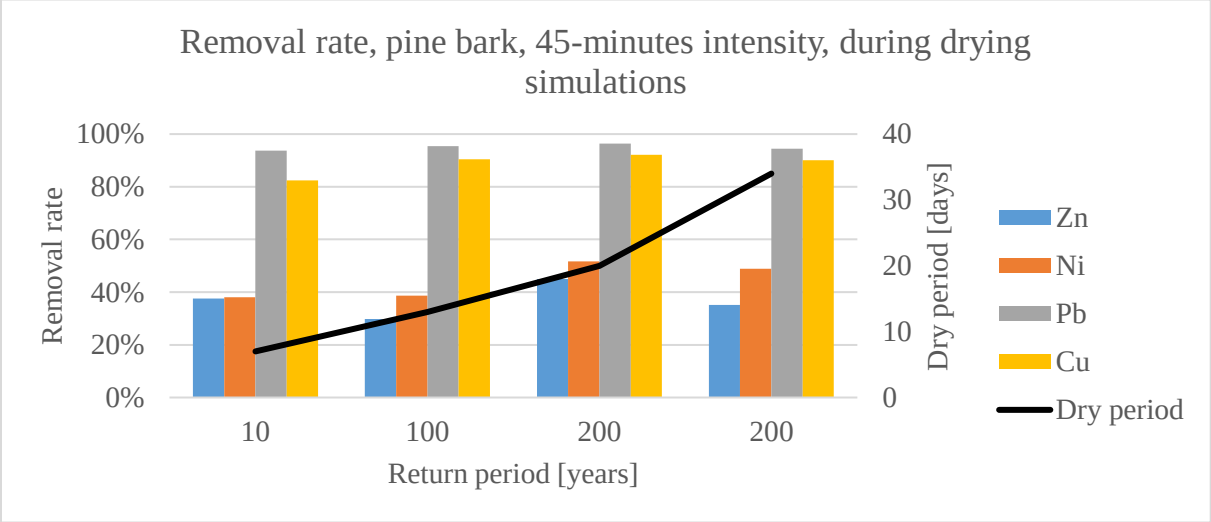

Figure 46. Removal rate of pine bark during simulations of 45-minutes intensity precipitation events after drying periods

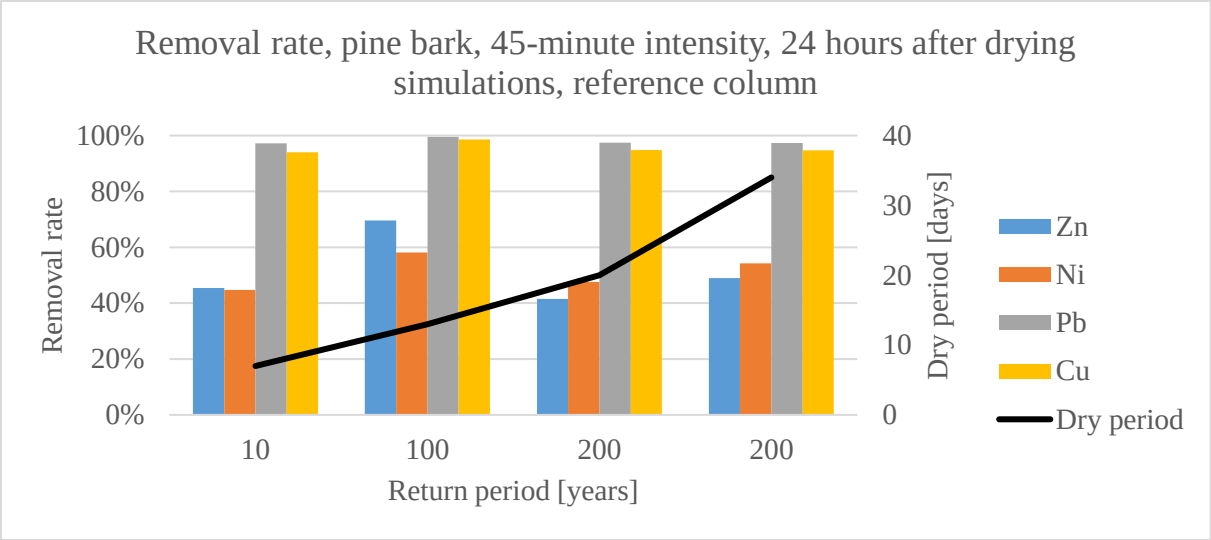

Figure 47. Removal rate of bottom ash reference column 24 hours after simulations of 45-minutes intensity events after drying periods.

4.3.4 Charcoal

Even though charcoal had the lowest removal rate, the charcoal was the only material where a clear correlation between drying period and removal rate was observed (see Figure 48). The removal rate of Zn and Ni increases 27 % and 16 %, respectively, when the drying period increased from 20 to 34 days. The increase in metal removal rate may have been caused by water evaporating from the material surface. The metal may have been competing with the water for the sorption sites on the material surface. When the water evaporated from the sorption sites the site became free to adsorb again.

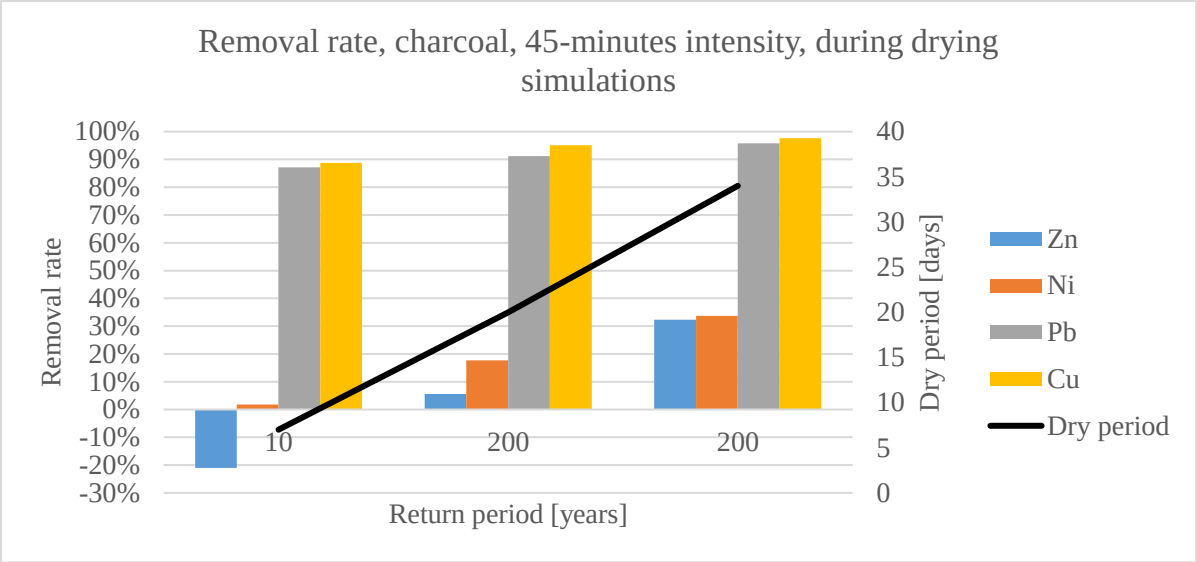

Figure 48. Removal rate of charcoal during simulations of 45-minutes intensity precipitation events after dry periods

There were no indications of such correlation in the reference column, where the removal rate was overall much lower than for the previous measurement done on the column (see Figure 49 and Figure 50). Another difference is the stable results shown for the dried measurements, while the sequential measurements had large fluctuations.

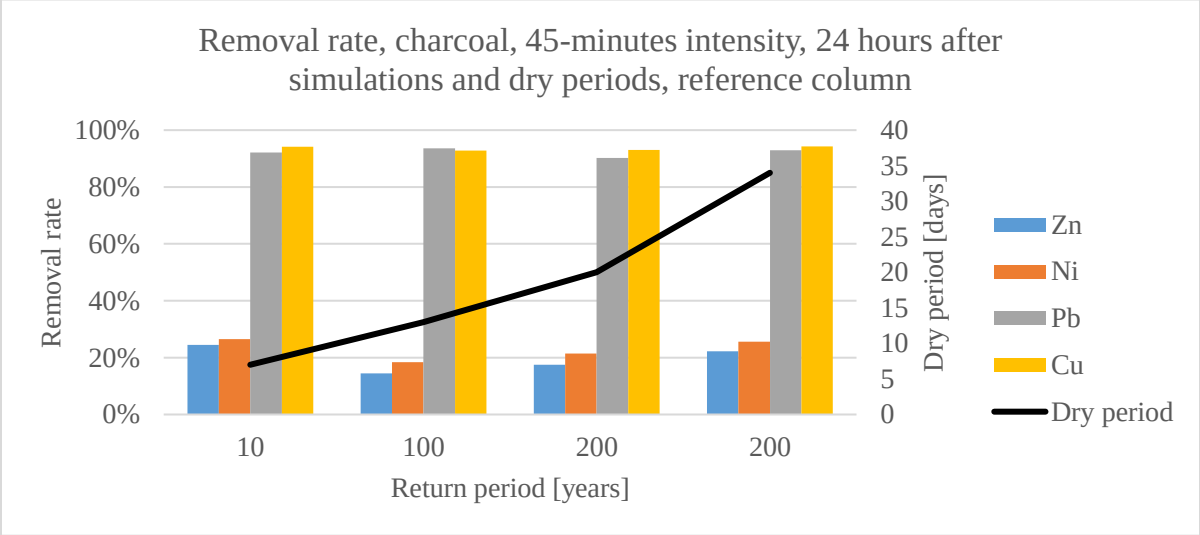

Figure 49. Removal rate of charcoal reference column 24 hours after simulations of 45-minutes intensity events after dry periods

The difference between the simulation column and the reference column may be explained by the time of sampling. The simulation column samples were taken during the simulation, while

the sorption sites freed by evaporation still might have been free. The reference column sample was taken 24 hours after the simulation was started, this may have been enough time for an equilibrium to occur, which may have caused the sample to be unaffected by the drying periods. Even though the HLR on the simulation column was much higher than on the reference column, the total volume of water passed through was much higher on the reference column.

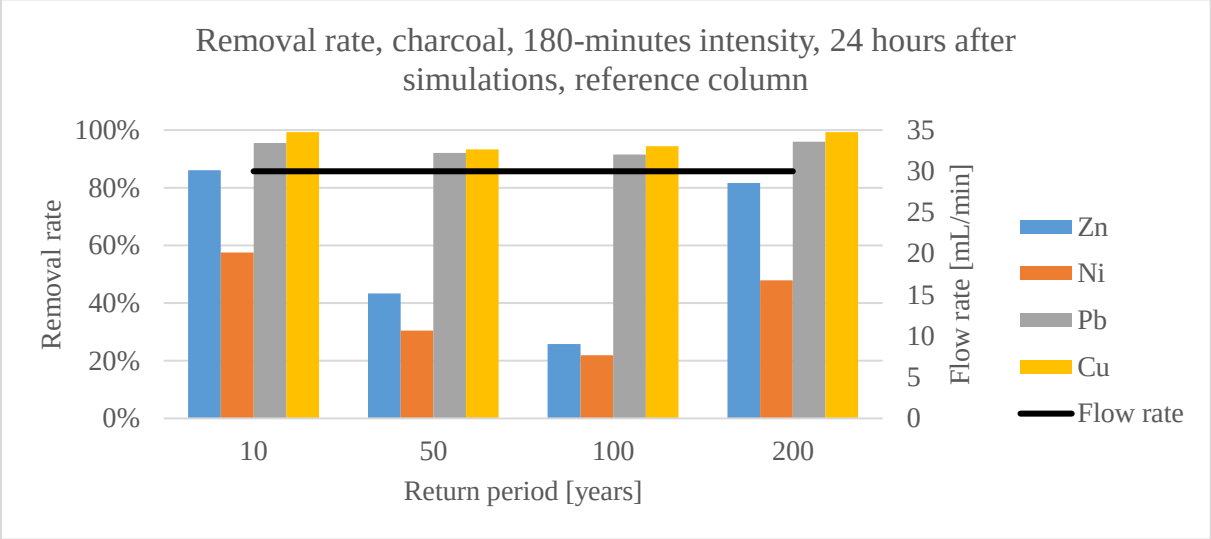

Figure 50. Removal rate of charcoal reference column 24 hours after simulations of 180-minutes intensity events. Flow rate – HLR used during simulation.

4.4 Breakthrough analysis

4.4.1 Breakthrough analysis on simulation columns

As seen in chapter 4.1, 4.2, and 4.3 multiple desorption events occurred in the charcoal simulation columns. Looking closer at the total discharge concentrations from the simulations column reveals several desorption, as seen in Figure 51. From day 0 to 5 was base flow measurements, sequential simulations happen between day 5 and day 32, and dry period simulation from there on to day 110.

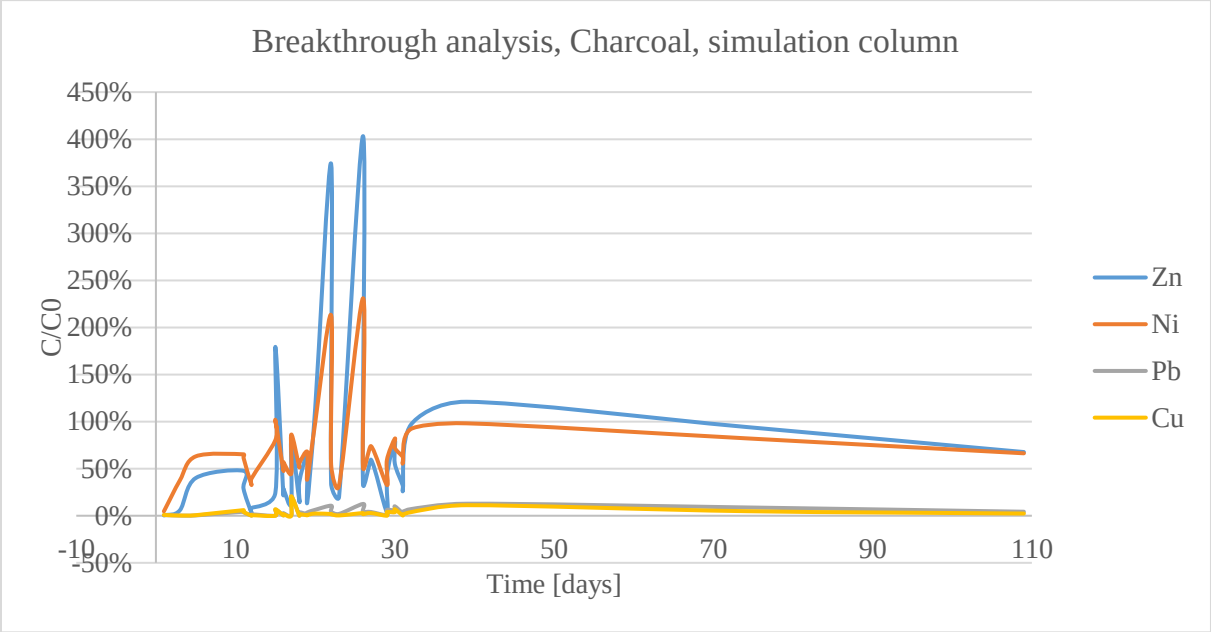

Figure 51. Breakthrough analysis of charcoal simulation column. C – outlet concentration, C_0 – inlet concentration

The first peak above the initial concentration (2000 µg/L) was measured during the 3rd simulation (100-year RP, 5-minute intensity), while the two next peaks were measured within 60 minutes of starting up the pumps after a necessary shut-down. The first peaks may be a more traditional breakthrough caused by accumulated material, which happened after two 5-minutes intensity storms (10- and 50-years) and approximately 7 days of base flow. The two other peaks were most likely caused by metals being flushed out of the column during start-up, both after 2 days without inlet flow. This metal-release was severe as the metal concentration was many times the initial concentration. If accumulated metals was released into a receiving waters at this magnitude, the fauna may suffer toxic shock due to the high concentration [29]. From Figure 51 the increased removal rate due to drying periods is also visible.

Doing the same analysis on the other columns found a desorption event in the pine bark simulation column, see Figure 52.

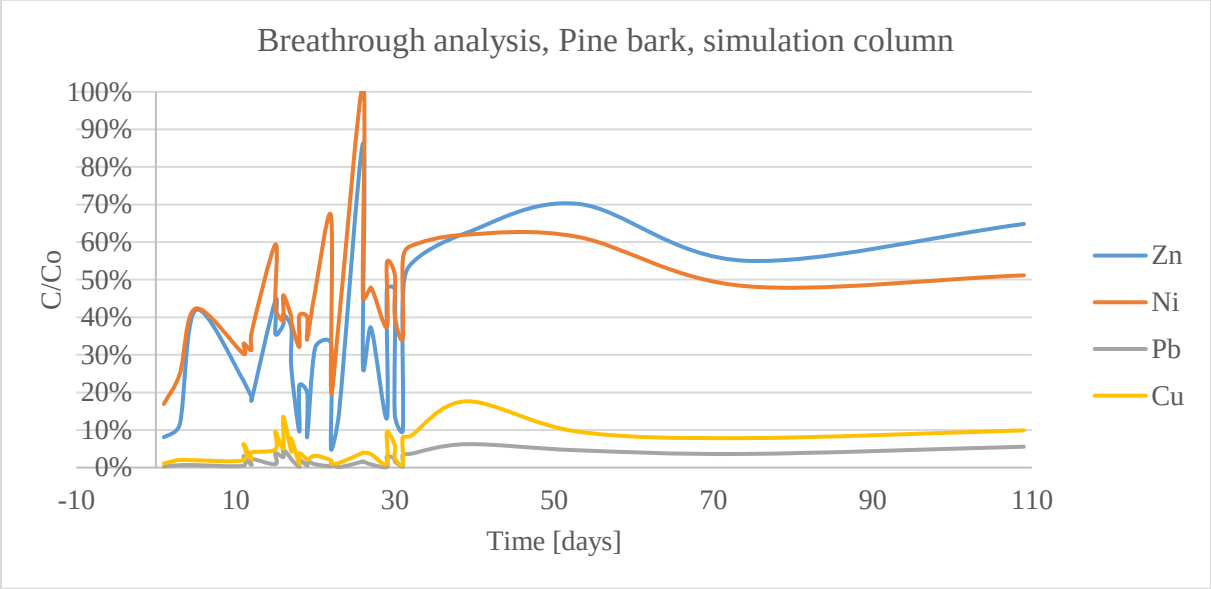

Figure 52. Breakthrough analysis of pine bark simulation column.

Similar to the two largest peaks in Figure 51, this desorption event happened after recent start-up of the pumps after a maintenance shutdown of 2 days. This desorption event had a release of metals equal to the inlet concentration. This makes it hard to identify if any accumulated metals were released, or just the initial concentration went un-adsorbed through the column. This is an important question because the release of accumulated metals may cause a discharge concentration many times higher than the inlet concentration, as seen in Figure 51. Simultaneous adsorption and desorption may also have occurred in this instance. This was, however, not possible to prove with the given data.

Figure 52 also illustrates that the removal rate was not increasing in response to increasing drying periods.

Because neither bottom ash, nor olivine had metal discharge close to the inlet concentration it was interesting to have an overview of the changes in removal rate during the experimental period. As seen in Figure 53, and from earlier figures, olivine had a very good removal rate of > 80 % during the whole experimental period. Except during the 10-year storm with 5-minute intensity, as discussed in chapter 4.2.1. An end removal rate of >= 90 % was very good after going through several simulations of very extreme precipitation events and a total volume of 1111.0 L.

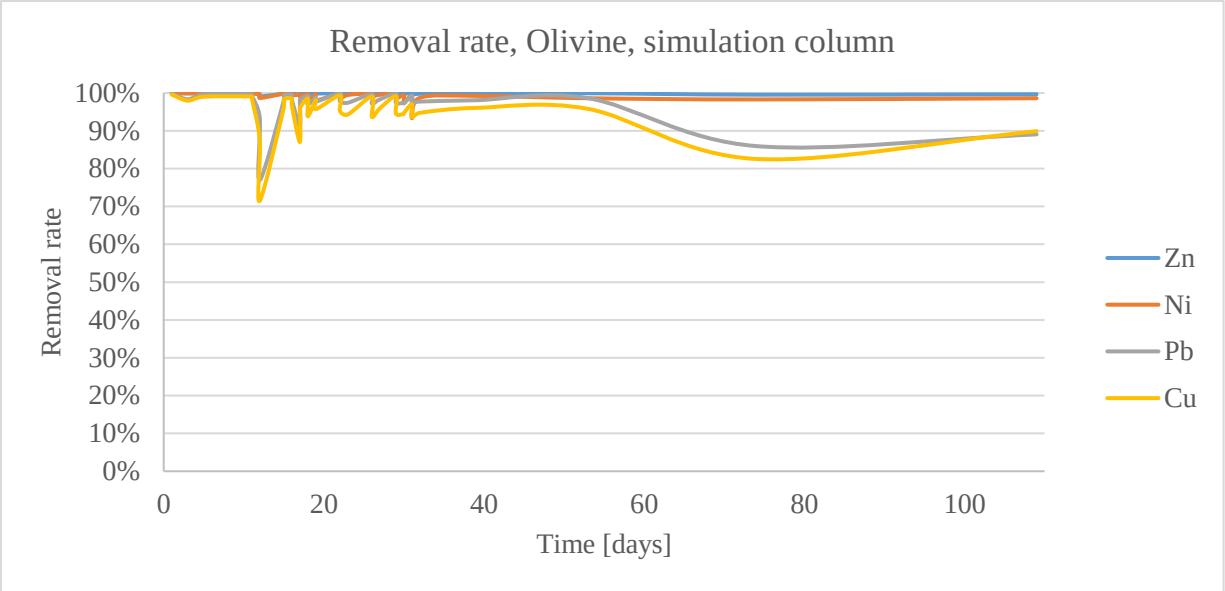

Figure 53. Removal rate of olivine, simulation column, the whole experimental period

The bottom ash had an even more stable removal rate, as seen in Figure 54. The only times the removal rate was below 90 % was during extreme hydraulic load, and then it still was > 80 %. This was overall very good results.

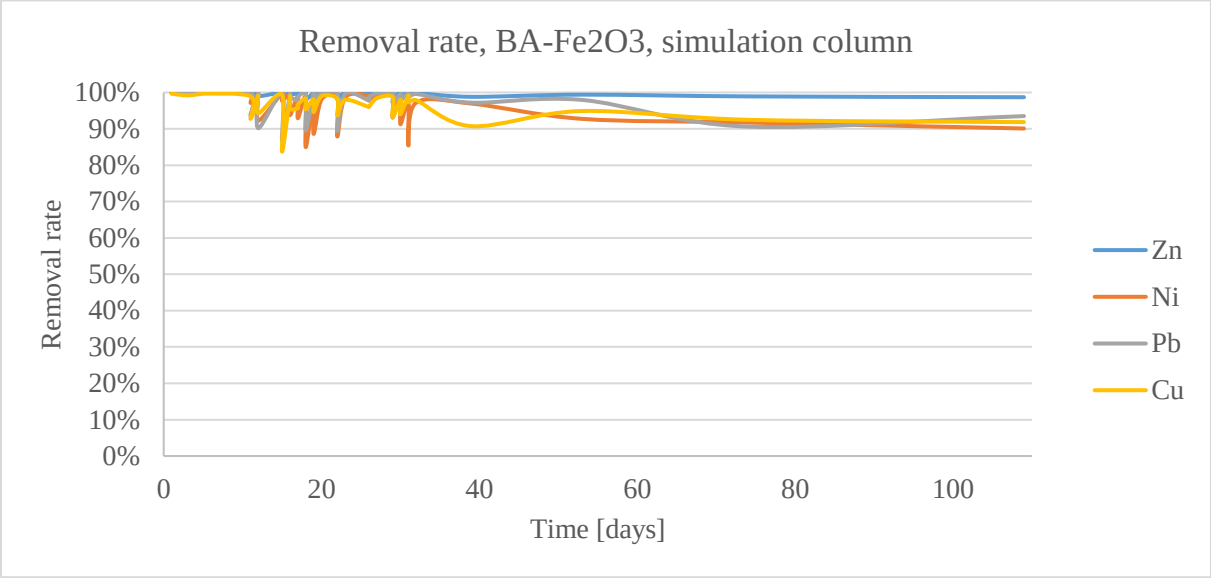

Figure 54. Removal rate of bottom ash, simulation column, the whole experimental period

4.4.2 Breakthrough analysis on reference columns

None of the reference columns experienced breakthrough or desorption events, but the pine bark was very close to, as seen in Figure 55.

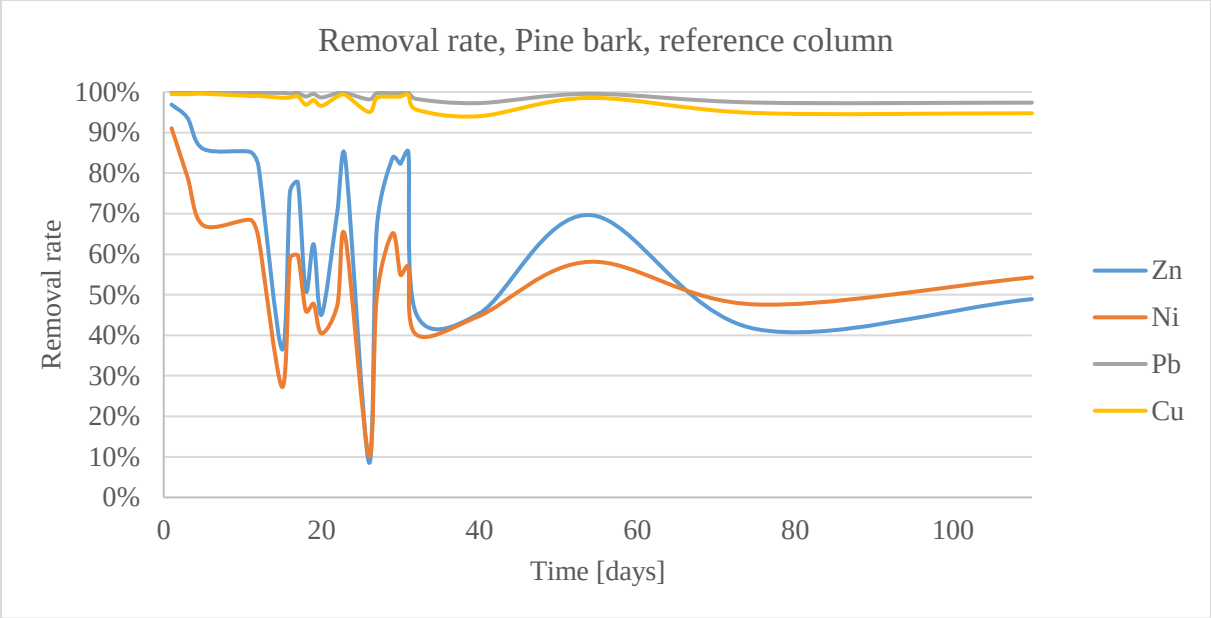

Figure 55. Removal rate of pine bark, reference column, the whole experimental period.

Even though the reference column was under a constant hydraulic load of 30 mL/min, the end removal rate of Ni and Zn was only 50-55 %. The two most prominent low-points of the Ni and Zn removal rate was caused by samples taken within 60 minutes after pump start-up after necessary shut-downs. The increase in removal rate between the last two samples, discussed in chapter 4.3.3, is more visible in Figure 55

The charcoal reference column had a lower removal rate of 20-30 % for Zn and Ni, as seen in Figure 56. This removal rate was below that of the simulation (> 30 %, see Figure 50). From this, one could conclude that the charcoal-sand mixture was highly unsuitable for removing Zn and Ni in infiltration ditches. This was confirms the previous analysis done in chapters 4.1.3, 4.2.3, and 4.3.3.

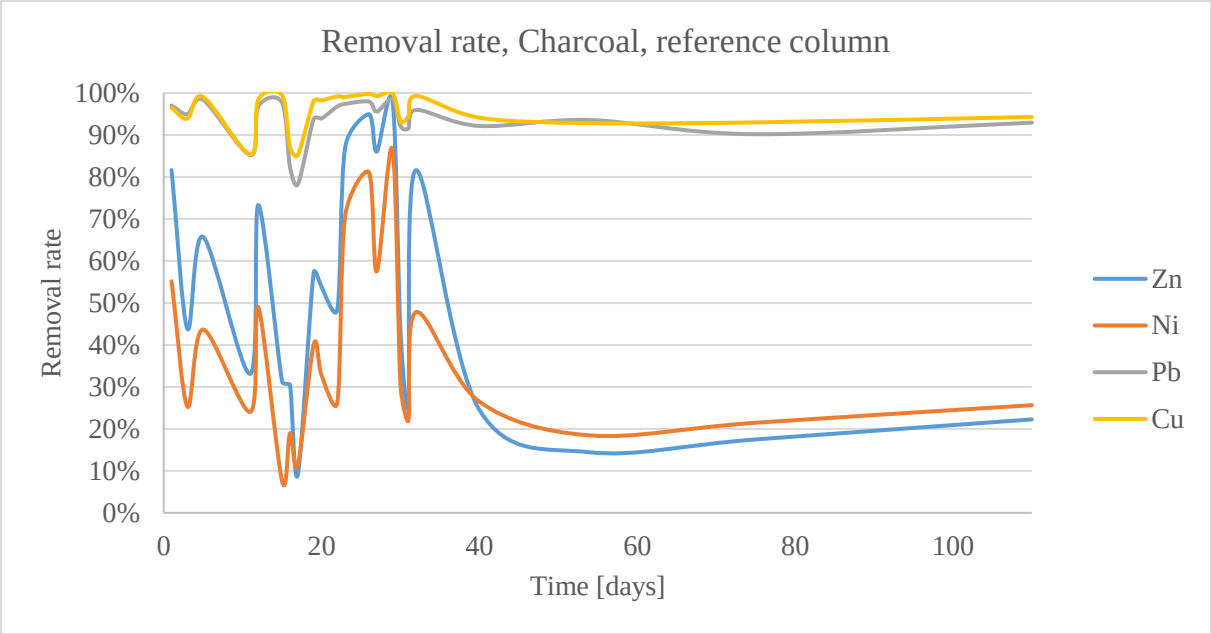

Figure 56. Removal rate of charcoal, reference column, the whole experimental period.

The removal rate of the olivine reference column was, as expected, very good, as seen in Figure 57, with an end removal rate of > 95 % for all four elements. The drying periods seems to have similar effect on the reference column, as for the simulation column, only at a smaller scale. This was noteworthy as the only effect of the extreme hydraulic loads the simulation column experienced.

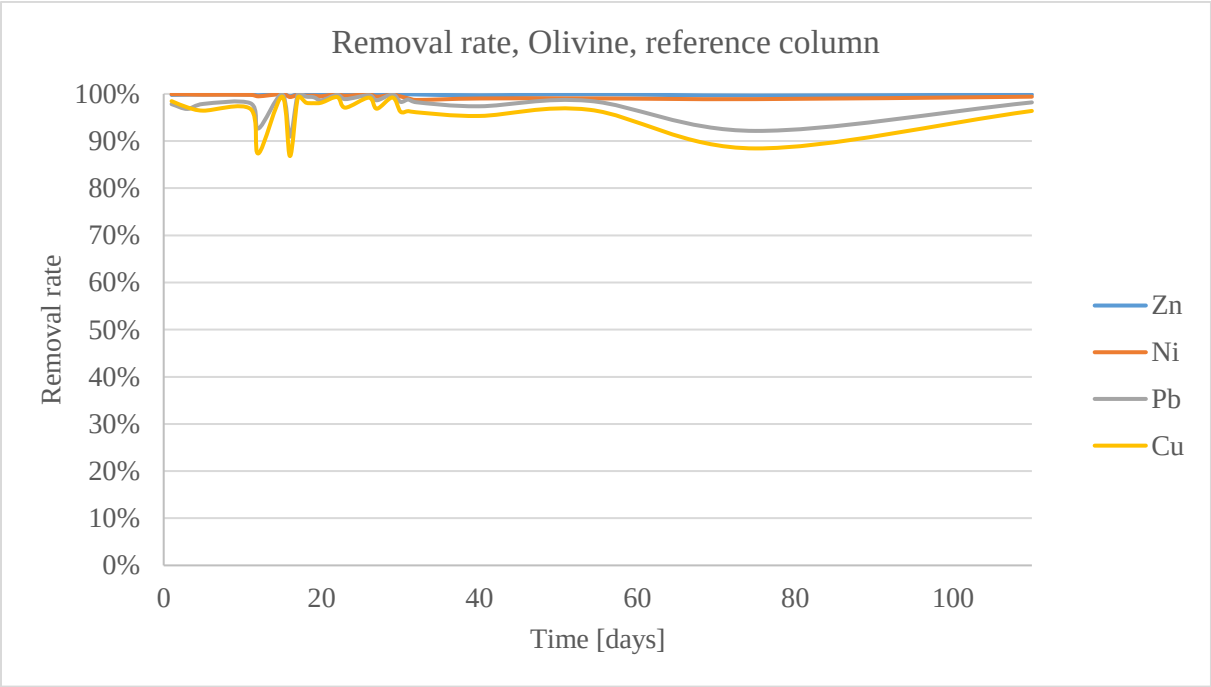

Figure 57. Removal rate of olivine, reference column, the whole experimental period.

It was interesting to notice that the 2 dips in Cu removal rate did not appear simultaneous with the similar dips in the simulation column (see Figure 53). The dips for the reference column came from samples taken 24 hours after the 10- and 100-years RP, 5-minutes intensity storm simulations, while the simulations column had dips during the 50-years RP, 5-minutes intensity storm simulation and 24 hours after the 200-years RP, 5-minutes intensity storm simulation. If this was caused by a conditioning process, it seems that a higher hydraulic load only extended the conditioning period. This may be explained in the condition process happened faster in stable hydraulic conditions of the reference column than in changing conditions in the simulation column

The bottom ash reference column had an incredible stable removal rate, as seen in Figure 58. The drying periods looks to have some effect, which stabilized during the experimental period.

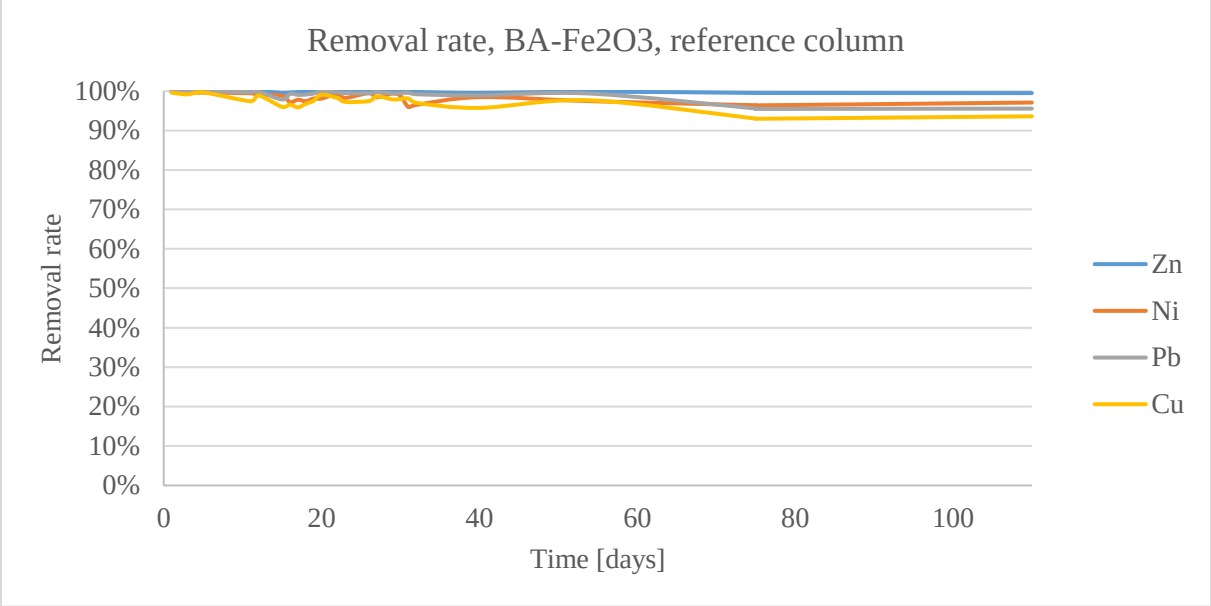

Figure 58. Removal rate of bottom ash, reference column, the whole experimental period.

One can see the effect of the increased hydraulic load easily when comparing Figure 54 and Figure 58. The increased number of dibs in the removal rate of the simulation column originates from the samples taken during the extreme precipitation event simulations.

4.5 Leaching from the adsorption materials

Some of the alternative adsorption materials used in these experiments had the potential to leach different components as it has been previously reported.

4.5.1 Elemental leaching from bottom ash.

As explained in chapter 2.7.3, the bottom ash contains many different elements. To investigate the possibility of leaching of these elements, an extensive ICP-MS analysis was done on all the samples from the bottom ash columns, for a large number of elements. Figure 59 show the concentration of the different elements investigated during the whole experimental period, on a logarithmic scale, for the simulations column.

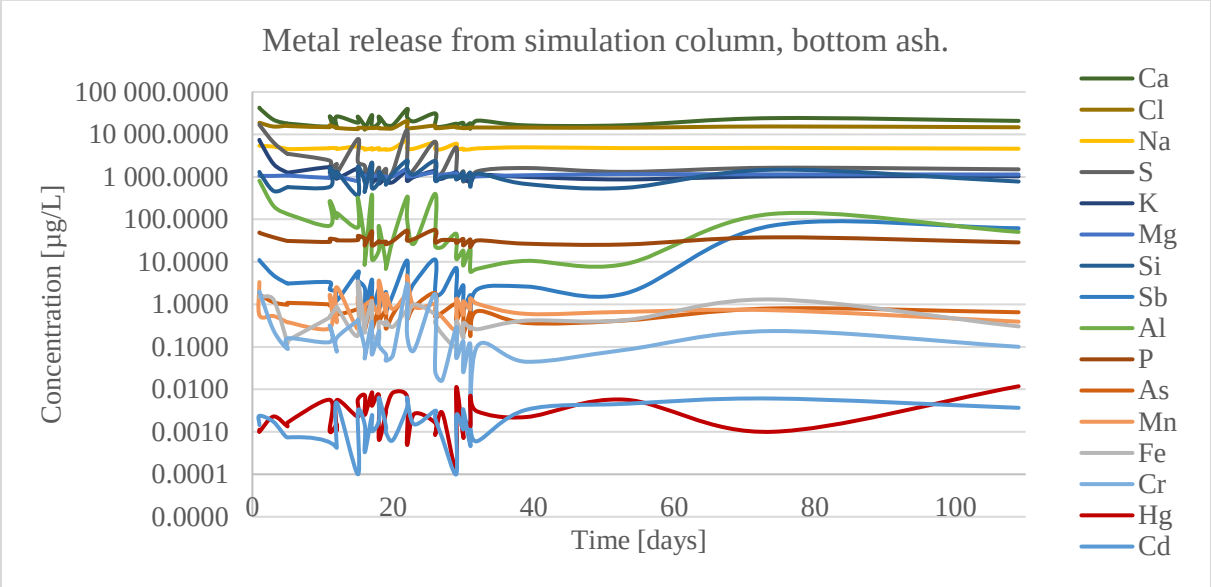

Figure 59. Concentration of elements released by bottom ash simulation column. Ca – Calcium, Na – Sodium, K – Potassium, Mg – Magnesium, Si – Silicon, Al – Aluminium, P – Phosphorus.

Based on the emission limits posted in chapter 2.3.1 the elements Cr, Hg, and Cd was released at a noticeable lower value. This is important when considering bottom ash for use in infiltration ditches.

There were high concentrations of salt-elements such as Ca, Cl, Na, K, Mg, and Si. With concentration ranging between 777 µg/L (Si) and 20 775 µg/L (Ca). The large release of salts may cause problem for the salinity of the receiving waters, if not released to the sea. An investigation on this topic should be done.

There were some clear changes during the dry periods, especially for Sb and Al. Their leaching increases significantly between and 2nd and 3rd dry period simulations, and caused a discharge concentration between 5 and 13 times higher at the end of the experimental period. This happened halfway through the dry period simulations, which made it hard to conclude a specific reason for this. It may be that a combination of drying and the hydraulic load trigged a sudden release of metals. The effect of the hydraulic load was, however, not confirmed by the reference column which had the same reaction, as seen in Figure 60. Another explanation may be that the intermitting wetting and drying caused disintegration of particles, or transformation. The accumulated effect of this during the first two dry period simulations may have caused an increased solubility of portions of these elements.

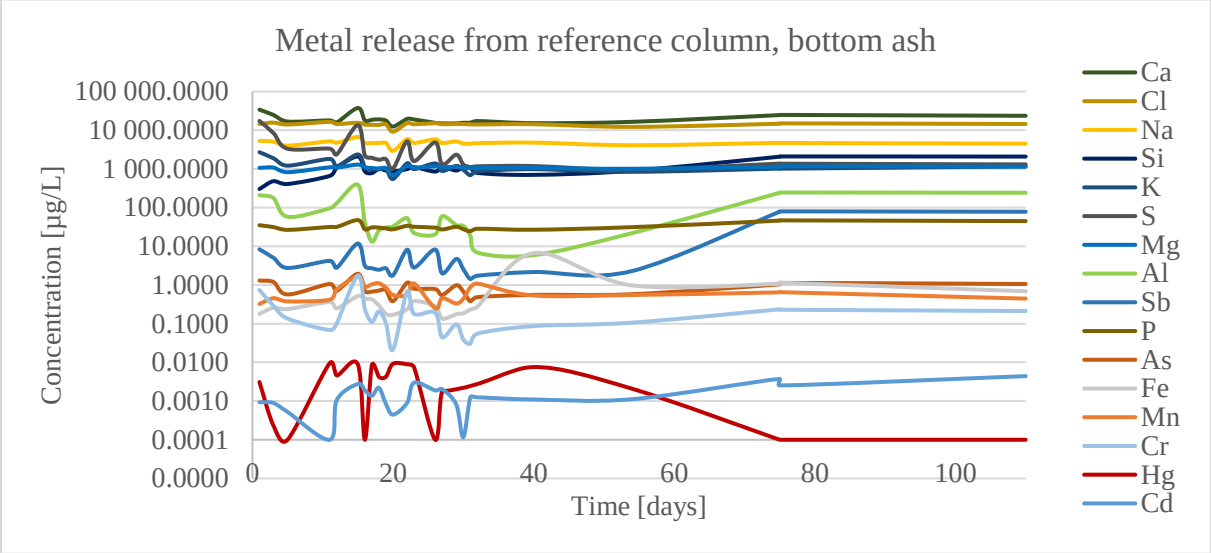

Figure 60. Concentration of elements released by bottom ash reference column.

The reference column had very similar results, except for some higher concentrations. These concentrations may be explained by the higher hydraulic load on the simulation column having washed away more of the elements already. Based on this, if one proposes a linear elemental release from the material, the elemental concentration will only decrease as more of the available elements were washed out.

4.5.2 Leaching of carbon from pine bark and bottom ash.

Pine bark is an organic material, and can thus undergo a biological decomposition. This may cause a release of carbon in the discharge. Bottom ash contains residual organic carbon (see

Table 7 page 20) which may be released in the discharge. As seen in Table 17, the carbon release was small, and should not be of concern when using the material.

Table 17. Total organic carbon analysis of samples from bottom ash, and pine bark columns after the 12th simulation.

Material	$TOC_{Sim.column}$ [µg/L]	$TOC_{Ref.column}$ [µg/L]
Bottom ash	1.44	1.62
Pine bark	2.80	2.81

4.5.3 Olivine as a nickel source

Pabst *et al.*[96] reported that weathered material containing olivine might be a source of nickel. As seen in Figure 61, the nickel concentration in the discharge from the olivine simulation column did not give any indication towards this statements. One can conclude that the Blueguard® olivine was not a source of nickel leaching.

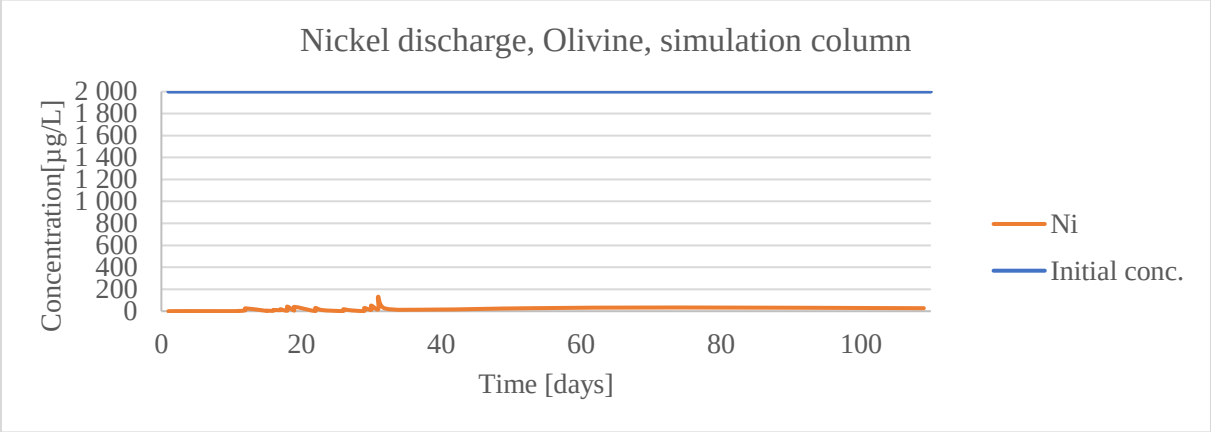

Figure 61. Nickel concentration in discharge from olivine simulation column.

4.6 Clogging and ponding

All the materials had a significant decrease in discharge rate (discharge flow as percentage of inlet flow) for the simulation column, compared to the reference column, giving evidence of the increased hydraulic load of the simulations affecting the conductivity.

4.6.1 Pine bark

The pine bark simulation column had the worst discharge rate at the end of the experiment, see Figure 62. This was in stark contrast to the hydraulic conductivity listed in Table 8, page 27.

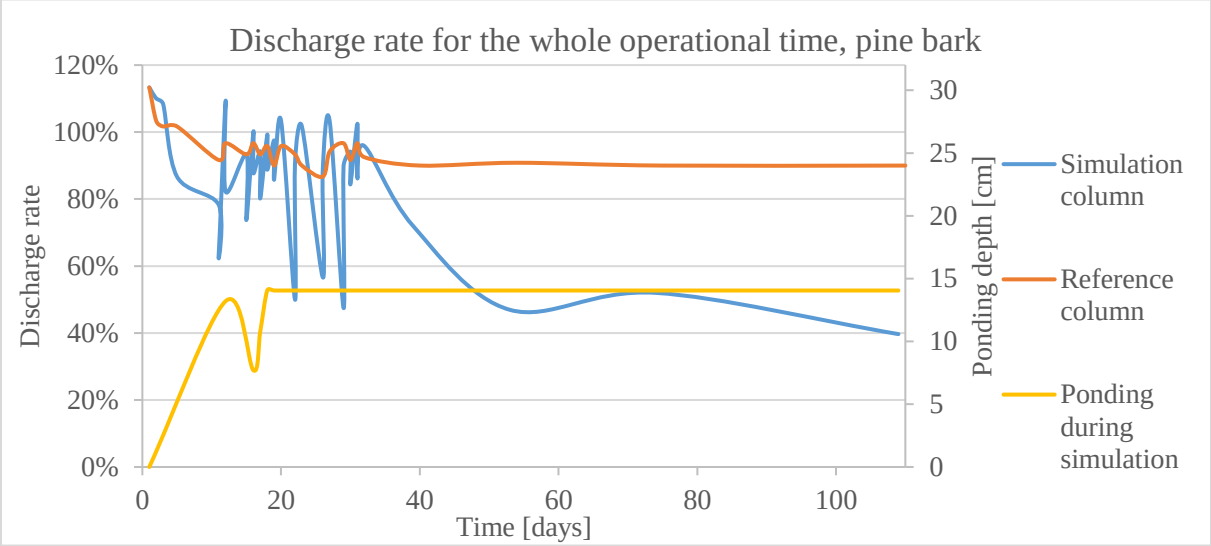

Figure 62. Pine bark discharge rate during the experimental time

The pine bark simulation column was also the only column which experienced ponding, to a large extent. The ponding depth of 14 cm, seen in Figure 62, was the maximum available ponding depth in the column. An explanation may be that the increased HLR in the simulation column compressed the material. The flat particles of pine bark would also further contribute to the decrease of the discharge rate. The dry period simulations (starting after 32 days) also had a much larger effect on the discharge rate than the sequential simulations. The largest dips in the simulations columns discharge rate before 35 days were from flow measurements within 60 minutes of start-ups.

The clogging may be caused by different mechanisms. One may be that the adsorbed metals and particles from the inflow lowered the conductivity. But this did not explain the effect of the

dry periods. Another explanation may be that the hydraulic load was compressing the material. There was no evidence of this in form of decreased material height. This may be explained by the material decompressing when the HLR was decreased again. The third reason may be biodegradation. Biodegraded pine bark have another shape and texture which may cause clogging of the column. The dry periods may increase this effect as the intermitting drying and wetting may accelerate the biodegradation process. The drying may have been sufficient for biodegradation processes contributing to clogging, while not affecting the removal rate. The difference between the reference column and simulation column during the drying simulations may be caused by the different hydraulic loads applied on the columns during the measurements. During these experiments measurements of the simulation column was only done while it was run at simulation hydraulic load, and would thus be more prone to have lower conductivity than the reference column. In conclusion, the pine bark seems prone to clogging during intermitting drying and extreme precipitation, which should be considered when deciding on alternative adsorption materials.

4.6.2 Charcoal

The discharge rate did not change significantly during the experimental period for the charcoal columns, as seen in Figure 63. The simulation column experienced ponding up to 2 cm during the first 4 simulations, no ponding after.

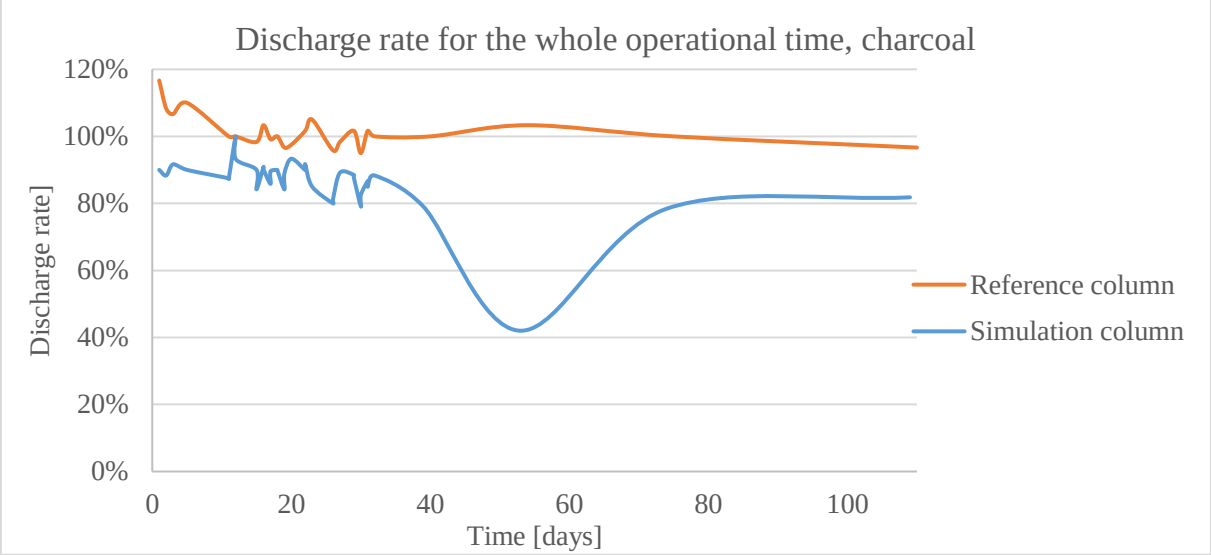

Figure 63. Charcoal discharge rate during the experimental time

The large dip of the simulation column was difficult to explain, and might have an external reason, such as human error or mechanical error during the measurement. The lower discharge rate of the simulation column may be caused by; compression of the materiel due to hydraulic load; adsorbed metal on the material and clogging of particles from the inlet solution; the hydraulic load during simulations might be higher than the hydraulic conductivity of the material. Most likely the explanation was a combination of all of the above. The compression and adsorbed metal lowered the already low hydraulic conductivity (see Table 8 page 27). None the less, the changes in hydraulic conductivity of the charcoal did not seem to be of concern during intermitting drying and extreme precipitation events.

4.6.3 Olivine

The olivine simulation column had the second to worst discharge rate at the end of the experimental period, see Figure 64. This was unexpected as the material hydraulic conductivity at the start should be more than sufficient for the hydraulic loads during the experiments (see Table 8 page 27). Olivine is a mineral, and did not undergo biodegradation, as pine bark.

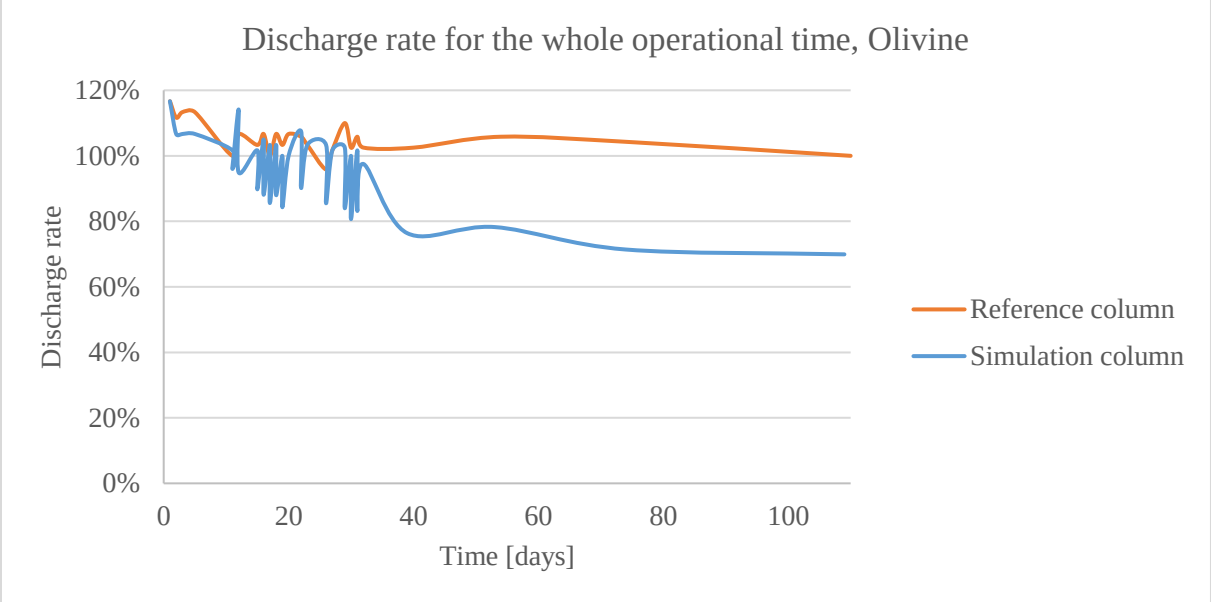

Figure 64. Olivine discharge rate during the experimental time

Like charcoal, the olivine simulation column also experienced ponding up to 2 cm, but during all the sequential simulations. And similar to charcoal the olivine may have been compressed by the hydraulic load and affected by accumulated adsorbed metal and particles from the inlet.

However, the olivine contains binding cement which may affect the conductivity. The olivine may have undergone a cementitious reaction, sticking the granulates together, and thus reduce the conductivity. Only difference was the olivine in both columns experienced algae growth, as seen in Figure 65. This, in combination with the cementitious reaction, could be the largest contributors to the lowered hydraulic conductivity, and the reasons for the downward trend shown at the end of Figure 64.

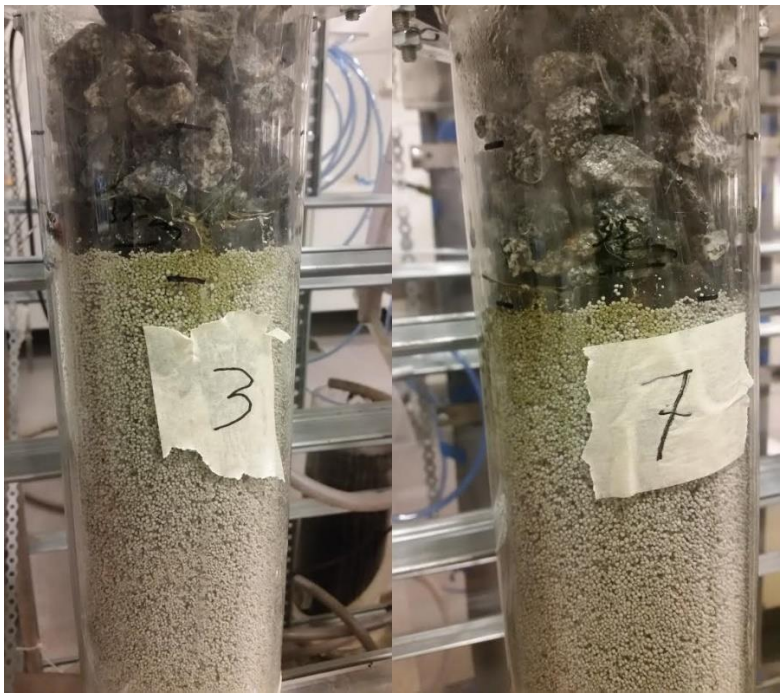

Figure 65. Green algae grown on olivine simulation column (no. 3) and reference column (no. 7)

Further research should be done to document the algae's effect on the conductivity, the origin of the algae, the possible extent of algae growth, and how to prevent the algae if need be.

4.6.4 Bottom ash

The bottom ash had the best overall discharge rate, see Figure 66. It had reduced discharge rate when the dry period simulation started, but with an increasing trend from there on. There was no apparent reason that could explain the dip. Part of it may be that the measurements taken during the dry period simulation, sampling was done during extreme hydraulic load. The lowest points before the dry period simulations all came from measurements taken during simulation. This made it evident that a higher hydraulic load caused a lower discharge rate. This may explain some of the decreased discharge rate, but not the complete reason as the dip was larger

than the ones during the sequential simulations. Another contribution to the lower discharge rate may be that the bottom ash can, like olivine, undergo a cementitious reaction. Overall the discharge rate was very good, and should not cause any problem if used in filtration trench.

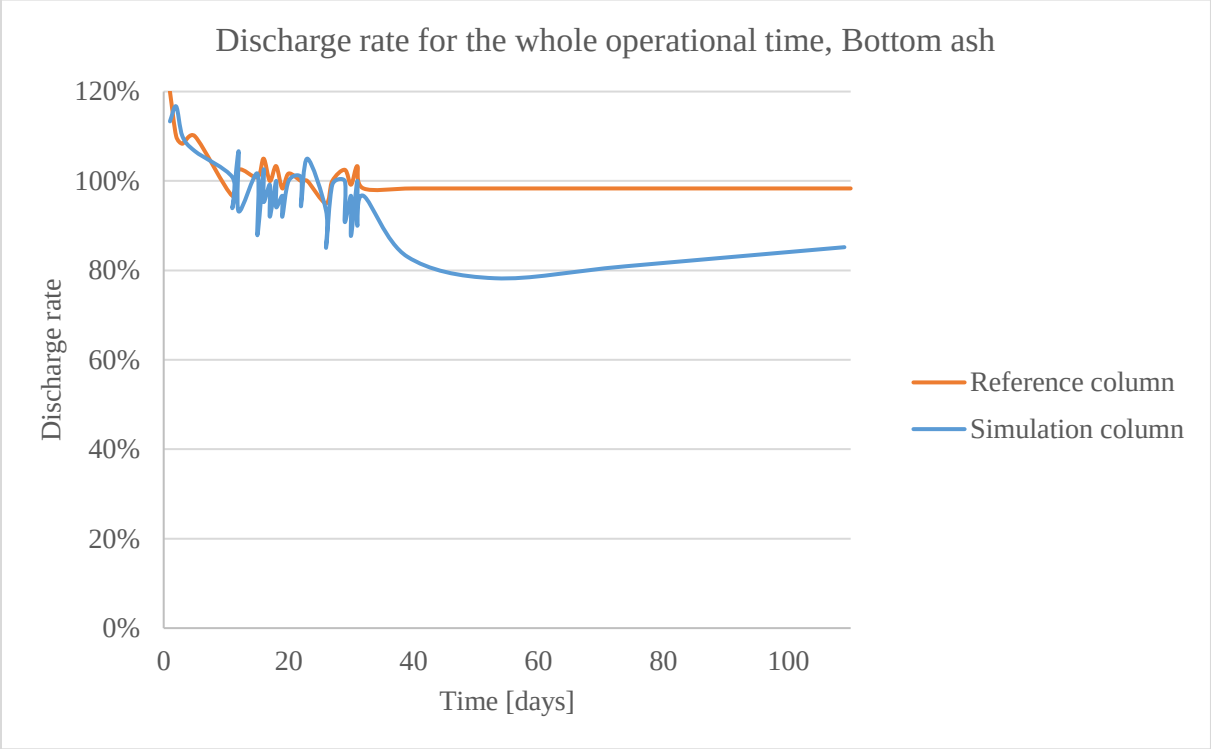

Figure 66. Bottom ash discharge rate during the experimental time

4.7 Design guidelines for use of alternative adsorption material.

For the two best adsorption materials in this research, olivine and bottom ash, one may conclude an overall removal rate of > 90 %. The filter area used in this experiment covered only 0.8 % of the total catchment contributing to the runoff. This means that a filter of 1 m^2 could treat a catchment of 127 m^2. This experiment was done using a synthetic stormwater with a 2 mg/L metal content. This was many times that of normal urban runoff. The filter depth used in these experiments was 35 cm. If assuming a linear relation between removal rate and the filter depth, the filter depth needed e.g. for treating the average runoff from an urban highway (see Table 6 page 13) would be 3.8 cm, limited by the Zn concentration. With a 90 % metal removal rate the average runoff concentration from urban highways would be reduced to much lower than the 10xAA EQS values used by the Norwegian Environment Agency as a limit for when treatment should be considered, see Table 18.

Table 18. 90 % removal rate of urban highway runoff compared with 10 x AA from EQS.

	Pb	**Cu**	**Zn**	**Ni**
Urban highway average [µg/L]	3.0	36	217	15
90 % removed [µg/L]	0.3	3.6	21.7	1.5
Urban highway max [µg/L]	7.4	151	2118	29
90 % removed [µg/L]	0.74	15.1	211.8	2.9
10 x AA from EQS [µg/L]	12	78	110	40

The maximum runoff concentration of urban highways would still have a larger Zn concentration, even after a 90 % removal. Therefore, one must decide on the target values, and the type of receiving water, that should be used to design the treatment system.

The author would suggest a design depth of 5 cm of olivine or bottom ash (with 10 w% iron oxide) for removal of dissolved toxic metals, and a filter area covering 1 % of the catchment. The 5 cm is 24 % more than the earlier calculated 3.8 cm, but extra depth is included as a safety

measure. The adsorbent filter should be used in combination with a particle removal treatment, such as a sand filter, a sedimentation basin, or as retrofit to existing detention ponds along the highways. A sedimentation basin might be best as the inlet flow to the filter could be controlled and it allows placement directly near highways

Finally, filters should be tested at field scale: to document the algae growth vs clogging (olivine); to document the leaching of salts and metals (bottom ash); to document the effect of ponding on the performance of the filter (olivine and bottom ash); and to evaluate the linearity of the adsorption capacity vs filter depth (olivine and bottom ash).

4.8 Limitations and uncertainties

4.8.1 Limitation of the experiments

One limitation of this experiments was the lack of ponding capability. To best simulate real life situations the hydraulic load should be equal to the precipitation, and the excess water should be able to pond to a designed overflow depth. This would give a more realistic results of how the removal rate would be under extreme hydraulic loads.

Another limitation was the drying conditions. During this experiment the drying was done with the column lid in place, without the inlet tube connected. The inlet was the only source of air. In real conditions the filter may be exposed to the open, which would have a significant larger drying capability. Evaporation of water from the adsorption material may have an effect on the removal rate as the metals have to compete against the water at the adsorption sites.

4.8.2 Uncertainties of the experiment

There were some important sources of uncertainties tied to the results of these experiments, in addition to human and mechanical errors.

There were two main sources of uncertainties to the concentration of the synthetic stormwater:

- The synthetic stormwater was made from hydrophilic $MeCl_2$ salts. The containers of these salts were opened in atmospheric conditions, which may have caused them to absorb water. This again would change the molecular weight used when calculating the solution and would give a lower concentration than calculated.
- There was no circulation in the tank used to store the synthetic stormwater. The synthetic stormwater was stored upwards to 3 days, and there was a visible layer of sedimentation on the bottom. These particles may have adsorbed metal and would have lowered the inlet concentration.

The result of lower inlet concentration would be an overall lower removal rate, since the removal rate was calculated using an inlet concentration of 2 mg/L. A possible uncertainty of 10 %, or 200 µg/L could be estimated. This would only change to overall removal rates with < 5%, which is within acceptable margin of error.

During the experimental period the samples were stored in a freezer before analysed with ICP-MS. The samples needed to be stored due to a lack of in-house analysis capability. The samples were stored at a frozen state because of a lack of refrigeration storage space. The samples had to be stored at a low temperature due to the presence of organic carbon which may degrade at higher temperatures and long storage time.

The freezing process of the samples may have changed the chemical composition of the solution. During freezing and thawing the equilibrium between any particle-bound metals, and dissolved metals may have shifted. This was difficult to prove with the results presented in this thesis, as there were no indications of this happening. Even though, this should, and could easily be investigated by analysing a sample with ICM-MS before and after prolonged freezing.

The ICP-MS results have an uncertainty connected it them. These uncertainties were connected to the detection limits, of which only the detection limit of Zn was a limiting factor. For concentrations lower < 5 µg/L the uncertainties could increase exponential. This detection limit did not affect the results of this thesis.

5. Conclusion

In this thesis, the effect of extreme precipitation events and drought on the performance of four alternative adsorption materials, for filtration based stormwater systems, have been investigated. The four materials were: Pine bark, charcoal, olivine, and bottom ash with 10 w% iron oxide.

Out of these four olivine and bottom ash excelled in their performance during the experiments with a removal rate of above 80 % throughout the whole experimental period. This is well above the recommended removed fractions of toxic metals. Comparingly pine bark experienced lowered hydraulic conductivity and removal rate down to 0 %, and charcoal experienced multiple desorption events where many times the inlet concentration was released.

For use in filtration based stormwater system the author would recommend an adsorption material depth of 5 cm and a filter area covering 1 % of the catchment area. The adsorption material should be used in combination with a particle removal treatment.

From the results found during this research one can conclude the following:

- Olivine, and Bottom ash with 10 w% iron oxide is not affected by extreme precipitation events, and drought to any large extent.
- Olivine and bottom ash has earlier been reported to leak minerals and metals. There was not experienced any release of minerals or metals which would have any environmental effect on receiving recipients.
- A 5 cm filter depth of olivine, or bottom ash with 10 w% iron oxide on an area covering 1 % of the catchment area will remove sufficient toxic metal pollutants.

6. References

1. FAWB, *Gudelines for Filter Media in Biofiltration Systems*, F.f.A.W. Biofiltration, Editor. 2009: Melboure, Australia.
2. Ilyas, A. and T.M. Muthanna, *Assessment of upscaling potential of alternative adsorbent materials for highway stormwater treatment in cold climates.* Environmental Technology, 2016: p. 1-13.
3. Monrabal-Martinez, C., A. Ilyas, and T.M. Muthanna, *Pilot Scale Testing of Adsorbent Amended Filters under High Hydraulic Loads for Highway Runoff in Cold Climates.* Water, 2017. **9**(3): p. 14.
4. Larsen, A.N., et al., *Potential future increase in extreme one-hour precipitation events over Europe due to climate change.* Water Science and Technology, 2009. **60**(9): p. 2205-2216.
5. United Nations, D.o.E.a.S.A., Population Division, *World Urbanization Prospects: The 2014 Revision, Highlights (ST/ESA/SER.A/352).* 2014.
6. Fletcher, T.D., H. Andrieu, and P. Hamel, *Understanding, management and modelling of urban hydrology and its consequences for receiving waters: A state of the art.* Advances in Water Resources, 2013. **51**: p. 261-279.
7. Kaushal, S.S. and K.T. Belt, *The urban watershed continuum: evolving spatial and temporal dimensions.* Urban Ecosystems, 2012. **15**(2): p. 409-435.
8. Meierdiercks, K.L., et al., *Analyses of urban drainage network structure and its impact on hydrologic response.* Journal of the American Water Resources Association, 2010. **46**(5): p. 932-943.
9. Hatt, B.E., T.D. Fletcher, and A. Deletic, *Hydraulic and pollutant removal performance of fine media stormwater filtration systems.* Environmental Science & Technology, 2008. **42**(7): p. 2535-2541.
10. Li, H. and A.P. Davis, *Heavy metal capture and accumulation in bioretention media.* Environmental Science & Technology, 2008. **42**(14): p. 5247-5253.
11. Carey, R.O., et al., *Evaluating nutrient impacts in urban watersheds: Challenges and research opportunities.* Environmental Pollution, 2013. **173**: p. 138-149.
12. Hatt, B.E., et al., *Retention of heavy metals by stormwater filtration systems: breakthrough analysis.* Water Science and Technology, 2011. **64**(9): p. 1913-1919.
13. O'Driscoll, M.A., J.R. Soban, and S.A. Lecce, *Stream channel enlargement response to urban land cover in small coastal plain watersheds, North Narolina.* Physical Geography, 2009. **30**(6): p. 528-555.
14. Devereux, O.H., et al., *Suspended-sediment sources in an urban watershed, Northeast Branch Anacostia River, Maryland.* Hydrological Processes, 2010. **24**(11): p. 1391-1403.
15. Konrad, C.P., D.B. Booth, and S.J. Burges, *Effects of urban development in the Puget Lowland, Washington, on interannual streamflow patterns: Consequences for channel form and streambed disturbance.* Water Resources Research, 2005. **41**(7).
16. Alberti, M., et al., *The impact of urban patterns on aquatic ecosystems: An empirical analysis in Puget lowland sub-basins.* Landscape and Urban Planning, 2007. **80**(4): p. 345-361.
17. *Low-Impact Development Hydrologic Analysis*, D.o.E. Resources, Editor. 1999, Program and Planning Division: Prince George's County, Maryland, USA.
18. Bledsoe, B.P., *Stream erosion potential and stormwater management strategies.* Journal of Water Resources Planning and Management-Asce, 2002. **128**(6): p. 451-455.
19. Gurnell, A., Lee, M., Souch, C., *Urban Rivers: Hydrology, Geomorphology, Ecology and Opportunities for Change.* Geograpy Compass, 2007. **1**(5): p. 1118-1137.

20. Poff, N.L., et al., *The ecological limits of hydrologic alteration (ELOHA): a new framework for developing regional environmental flow standards.* Freshwater Biology, 2010. **55**(1): p. 147-170.
21. Gift, D.M., et al., *Denitrification Potential, Root Biomass, and Organic Matter in Degraded and Restored Urban Riparian Zones.* Restoration Ecology, 2010. **18**(1): p. 113-120.
22. Groffman, P.M. and M.K. Crawford, *Denitrification potential in urban riparian zones.* Journal of Environmental Quality, 2003. **32**(3): p. 1144-1149.
23. Walsh, C.J., et al., *The urban stream syndrome: current knowledge and the search for a cure.* Journal of the North American Benthological Society, 2005. **24**(3): p. 706-723.
24. Beach, D., *Coastal Sprawl. The effects of urban design on aquatic ecosystems in the United States.*, P.O. Commision, Editor. 2001: Arlington, Virginia p. 8.
25. King, R.S., et al., *How novel is too novel? Stream community thresholds at exceptionally low levels of catchment urbanization.* Ecological Applications, 2011. **21**(5): p. 1659-1678.
26. Paul, M.J. and J.L. Meyer, *Streams in the urban landscape.* Annual Review of Ecology and Systematics, 2001. **32**: p. 333-365.
27. Passeport, E. and W.F. Hunt, *Asphalt Parking Lot Runoff Nutrient Characterization for Eight Sites in North Carolina, USA.* Journal of Hydrologic Engineering, 2009. **14**(4): p. 352-361.
28. Hatt, B.E., et al., *The influence of urban density and drainage infrastructure on the concentrations and loads of pollutants in small streams.* Environmental Management, 2004. **34**(1): p. 112-124.
29. Traas, T.P. and C.J. van Leeuwen, *Exotoxicologica Effects*, in *Risk Assessment of Chemicals - An Introduction*, C.J. van Leeuwen and T.G. Vermeire, Editors. 2007, Springer: Dordrecht, The Netherlands. p. 281-356.
30. Ellis, J.B., et al., *The Contribution of Highway Surfaces to Urban Stormwater Sediments and Metal Loadings.* Science of the Total Environment, 1987. **59**: p. 339-349.
31. Bergbäck, B., K. Johansson, and U. Mohlander, *Urban Metal Flows - a case study of Stockholm.* Water, Air, and Soil Pollution: Focus, 2001. **1**(3): p. 3-24.
32. Muthanna, T.M., *Stormwater Quality*, in *TVM4141*, D.o.H.a.E.E. NTNU, Editor. 2016: Trondheim, Norway.
33. Davis, A.P., M. Shokouhian, and S.B. Ni, *Loading estimates of lead, copper, cadmium, and zinc in urban runoff from specific sources.* Chemosphere, 2001. **44**(5): p. 997-1009.
34. Sorme, L. and R. Lagerkvist, *Sources of heavy metals in urban wastewater in Stockholm.* Science of the Total Environment, 2002. **298**(1-3): p. 131-145.
35. Weckwerth, G., *Verification of traffic emitted aerosol components in the ambient air of Cologne (Germany).* Atmospheric Environment, 2001. **35**(32): p. 5525-5536.
36. Thorpe, A. and R.M. Harrison, *Sources and properties of non-exhaust particulate matter from road traffic: A review.* Science of the Total Environment, 2008. **400**(1-3): p. 270-282.
37. Kemp, K., *Trends and sources for heavy metals in urban atmosphere.* Nuclear Instruments and Methods in Physics Research B, 2002. **189**: p. 227-232.
38. Ekvall, J., et al., *Klassificering av dagvatten och recipienter samt riktlinjer för reningskrav- del 2*, Stockholm, Editor. 2001: [Online] Available: http://www.stockholmvatten.se/globalassets/pdf1/rapporter/dagvatten/dagvattenklassificeringdel2.pdf [Accessed 13.01.2016].
39. Ozaki, H., I. Watanabe, and K. Kuno, *As, Sb and Hg distribution and pollution sources in the roadside soil and dust around Kamikochi, Chubu Sangaku National Park, Japan.* Geochemical Journal, 2004. **38**(5): p. 473-484.
40. Cadle, S.H., et al., *Composition of light-duty motor vehicle exhaust particulate matter in the Denver, Colorado area.* Environmental Science & Technology, 1999. **33**(14): p. 2328-2339.
41. Saint'Pierre, T.D., et al., *Determination of Cd, Cu, Fe, Pb and Tl in gasoline as emulsion by electrothermal vaporization inductively coupled plasma mass spectrometry with analyte addition and isotope dilution calibration techniques.* Spectrochimica Acta Part B-Atomic Spectroscopy, 2004. **59**(4): p. 551-558.

42. Li, X., C. Poon, and P.S. Liu, *Heavy metal contamination of urban soils and street dusts in Hong Kong.* Applied Geochemistry, 2001. **16**: p. 1361-1368.
43. Legret, M. and C. Pagotto, *Evaluation of pollutant loadings in the runoff waters from a major rural highway.* Science of the Total Environment, 1999. **235**(1-3): p. 143-150.
44. Monaci, F., et al., *Biomonitoring of airborne metals in urban environments: new tracers of vehicle emission, in place of lead.* Environmental Pollution, 2000. **107**(3): p. 321-327.
45. San Miguel, G., G.D. Fowler, and C. Sollars, *The leaching of inorganic species from activated carbons produced from waste tyre rubber.* Water Research, 2002. **36**(8): p. 1939-1946.
46. Lindgren, A., *Asphalt wear and pollution transport.* Science of the Total Environment, 1996. **189**: p. 281-286.
47. Gustafsson, M., *Icke-avgasrelaterade partiklar i vägmiljön*, in *VTI meddelande 910*. 2001, Swedish National Road Administration: Lindköping, Sweden.
48. Bäckström, M., S. Karlsson, and B. Allard, *Metal leachability and anthropogenic signal in roadside soils estimated from sequential extraction and stable lead isotopes.* Environmental Monitoring and Assessment, 2004. **90**(1-3): p. 135-160.
49. Glenn, D.W. and J.J. Sansalone, *Accretion and partitioning of heavy metals associated with snow exposed to urban traffic and winter storm maintenance activities. II.* Journal of Environmental Engineering-Asce, 2002. **128**(2): p. 167-185.
50. Lindholm, O.G., *Forurensinger i urbant overvann.* VANN, 2003. **4**.
51. Amundsen, C.E. and R. Roseth, *Utslippsfaktorer fra veg til vann og jord i Norge* in *UTB 2004/08*. 2004, Statens Vegvesen: Norway.
52. Maniquiz-Redillas, M. and L.H. Kim, *Fractionation of heavy metals in runoff and discharge of a stormwater management system and its implications for treatment.* Journal of Environmental Sciences, 2014. **26**(6): p. 1214-1222.
53. Riktvärdesgruppen, *Förslag til riktvärden för dagvattenutsläpp.*, R.-o. trafikkontoret, Editor. 2009: Stockholms läns landsting.
54. Meland, S., S.B. Ranneklev, and T. Hertel-Aas, *Forslag til nye retningslinjer for rensing av veiavrenning og tunnelvaskevann.* VANN, 2016. **03**: p. 263-273.
55. Huber, M., A. Welker, and B. Helmreich, *Critical review of heavy metal pollution of traffic area runoff: Occurrence, influencing factors, and partitioning.* Science of the Total Environment, 2016. **541**: p. 895-919.
56. Åstebøl, S.O., et al., *På lag med regnet - Veileder for Lokal Overvannshåndtering*, COWI, Editor. 2013, Rogaland fylkeskommune/Jæren vannområde: [Online] http://www.miljodirektoratet.no/Global/klimatilpasning/COWI_Veileder%20overvann%20overvannsh%C3%A5ndtering%20J%C3%A6ren_2013.pdf (Accessed: 18.01.2017).
57. Skaaraas, H., et al., *Overvann i byer og tettsteder*, in *Norges offentlige utredninger*. 2015, Norwegian Government Security and Service Organisation: Ministry of Climate and Environment.
58. Commision, E., *Proposal for a DIRECTIVE OF THE EUROPEAN PARLIAMENT AND OF THE COUNCIL amending Directives 2000/60/EC and 2008/105/EC as regards priority substances in the field of water policy*, W.F. Directive, Editor. 2001.
59. Bertrand-Krajewski, J.L., G. Chebbo, and A. Saget, *Distribution of pollutant mass vs volume in stormwater discharges and the first flush phenomenon.* Water Research, 1998. **32**(8): p. 2341-2356.
60. Deletic, A., *The first flush load of urban surface runoff.* Water Research, 1998. **32**(8): p. 2462-2470.
61. Sansalone, J.J. and S.G. Buchberger, *Partitioning and first flush of metals in urban roadway storm water.* Journal of Environmental Engineering-Asce, 1997. **123**(2): p. 134-143.
62. Lee, J.H., et al., *First flush analysis of urban storm runoff.* Science of the Total Environment, 2002. **293**(1-3): p. 163-175.
63. Han, Y.H., et al., *Characteristics of highway stormwater runoff.* Water Environment Research, 2006. **78**(12): p. 2377-2388.

64. Soller, J., et al., *Evaluation of seasonal scale first flush pollutant loading and implications for urban runoff management.* Journal of Environmental Management, 2005. **76**(4): p. 309-318.
65. Gnecco, I., et al., *Storm water pollution in the urban environment of Genoa, Italy.* Atmospheric Research, 2005. **77**(1-4): p. 60-73.
66. Lind, B.B., M. Backstrom, and E. Geisler, *First flush effect of metals and anions in stormwater runoff from roads in mid-Sweden.* Urban Transport Vii: Urban Transport and the Environment in the 21st Century, 2001. **8**: p. 497-507.
67. Group, N.S.W., *Interim Code of Practice for Sustainable Drainage Systems*, O.o.t.D.P. Minister, Editor. 2004.
68. Wong, T.H.F., *Water sensitive urban design - the journey thus far.* Australian Journal of Water Resources, 2007. **10**(3): p. 213-222.
69. *Water Sensitive Urban Design*, M.V.C. Council, Editor. 2014: Moonee Valley, Australia.
70. Burns, M.J., et al., *Hydrologic shortcomings of conventional urban stormwater management and opportunities for reform.* Landscape and Urban Planning, 2012. **105**(3): p. 230-240.
71. Roy-Poirier, A., P. Champagne, and Y. Filion, *Review of Bioretention System Research and Design: Past, Present, and Future.* Journal of Environmental Engineering-Asce, 2010. **136**(9): p. 878-889.
72. Dietz, M.E., *Low impact development practices: A review of current research and recommendations for future directions.* Water Air and Soil Pollution, 2007. **186**(1-4): p. 351-363.
73. Davis, A.P., et al., *Bioretention Technology: Overview of Current Practice and Future Needs.* Journal of Environmental Engineering-Asce, 2009. **135**(3): p. 109-117.
74. Lucas, W.C., *Design of Integrated Bioinfiltration-Detention Urban Retrofits with Design Storm and Continuous Simulation Methods.* Journal of Hydrologic Engineering, 2010. **15**(6): p. 486-498.
75. Davis, A.P.T., R. G.; Hunt, W. F., *Improving Urban Stormwater Quality: Applying Fundamental Principles.* Journal of Contemporary Water Research & Education, 2010. **146**(1): p. 3-10.
76. Bratieres, K., et al., *Nutrient and sediment removal by stormwater biofilters: A large-scale design optimisation study.* Water Research, 2008. **42**(14): p. 3930-3940.
77. DeBusk, K.M. and T.M. Wynn, *Storm-Water Bioretention for Runoff Quality and Quantity Mitigation.* Journal of Environmental Engineering-Asce, 2011. **137**(9): p. 800-808.
78. Barrett, M.E., M. Limouzin, and D.F. Lawler, *Effects of Media and Plant Selection on Biofiltration Performance.* Journal of Environmental Engineering-Asce, 2013. **139**(4): p. 462-470.
79. Li, H., et al., *Mitigation of Impervious Surface Hydrology Using Bioretention in North Carolina and Maryland.* Journal of Hydrologic Engineering, 2009. **14**(4): p. 407-415.
80. Ilyas, A., C.M. Martinex, and T.M. Muthanna, *Alternative Adsorbents for Infiltration Based Highway Stormwater Treatment in Norway*. 2016, Department of Civil and Environmental Engineering: Norwegian University of Science and Technology.
81. Crittenden, J.C., et al., *Water Treatment. Principles and Design*. 3rd ed. 2012, Hoboken, New Jersey: John Wiley & Sons, Inc.
82. Benjamin, M.M., *Water Chemisry*. 2002, Long Grove, Illinois: Waveland Press, Inc.
83. Chen, J.P. and M.S. Lin, *Equilibrium and kinetics of metal ion adsorption onto a commercial H-type granular activated carbon: Experimental and modeling studies.* Water Research, 2001. **35**(10): p. 2385-2394.
84. Shim, J.W., S.J. Park, and S.K. Ryu, *Effect of modification with HNO3 and NaOH on metal adsorption by pitch-based activated carbon fibers.* Carbon, 2001. **39**(11): p. 1635-1642.
85. Lam, C.H.K., et al., *Use of Incineration MSW Ash: A Review.* Sustainability, 2010. **2**: p. 1943-1968.
86. Gorme, J.B., M.C. Maniquiz-Redillas, and L.H. Kim, *Development of a stormwater treatment system using bottom ash as filter media.* Desalination and Water Treatment, 2015. **53**(11): p. 3118-3125.
87. Hsu, T.C., C.C. Yu, and C.M. Yeh, *Adsorption of Cu2+ from water using raw and modified coal fly ashes.* Fuel, 2008. **87**(7): p. 1355-1359.

88. Babel, S. and T.A. Kurniawan, *Low-cost adsorbents for heavy metals uptake from contaminated water: a review*. Journal of Hazardous Materials, 2003. **97**(1-3): p. 219-243.
89. Heie, A., et al., *Basiskarakterisering av bunnaske fra forbrenning av avfall i Norge*, in *Avfall Norge-rapport*. 2015, COWI: Avfall Norge.
90. Gaballah, I., et al., *Recovery of copper through decontamination of synthetic solutions using modified barks*. Metallurgical and Materials Transactions B-Process Metallurgy and Materials Processing Science, 1997. **28**(1): p. 13-23.
91. Vazquez, G., et al., *Removal of cadmium and mercury ions from aqueous solution by sorption on treated Pinus pinaster bark: kinetics and isotherms*. Bioresource Technology, 2002. **82**(3): p. 247-251.
92. AlAsheh, S. and Z. Duvnjak, *Sorption of cadmium and other heavy metals by pine bark*. Journal of Hazardous Materials, 1997. **56**(1-2): p. 35-51.
93. Kleiv, R.A. and K.L. Sandvik, *Modelling copper adsorption on olivine process dust using a simple linear multivariable regression model*. Minerals Engineering, 2002. **15**(10): p. 737-744.
94. Wium-Andersen, T., et al., *Sorption Media for Stormwater Treatment-A Laboratory Evaluation of Five Low-Cost Media for Their Ability to Remove Metals and Phosphorus from Artificial Stormwater*. Water Environment Research, 2012. **84**(7): p. 605-616.
95. Luz, M.G., *Removal of Dissolved Pollutants from Highway Stormwater with Low-cost Adsorbents*, in *Department of Hydraulic and Environmental Engineering*. 2014, Norwegian University of Science and Technology: NTNU.
96. Pabst, T., et al., *The potential impact of various rock types on the aquatic environment during building and construction projects*, T. Pabst, Editor. 2015, Traffic Safety, Environment and Technology Department: [Online] http://www.vegvesen.no/en/professional/Research+and+development/NORWAT/Publications (Accessed 31.01.2017).
97. Trenberth, K.E., et al., *The changing character of precipitation*. Bulletin of the American Meteorological Society, 2003. **84**(9): p. 1205-1217.
98. Kjellstrom, E., et al., *21st century changes in the European climate: uncertainties derived from an ensemble of regional climate model simulations*. Tellus Series a-Dynamic Meteorology and Oceanography, 2011. **63**(1): p. 24-40.
99. Nikulin, G., et al., *Evaluation and future projections of temperature, precipitation and wind extremes over Europe in an ensemble of regional climate simulations*. Tellus Series a-Dynamic Meteorology and Oceanography, 2011. **63**(1): p. 41-55.
100. Olsson, J. and K. Foster, *Short-term precipitation extremes in regional climate simulations for Sweden*. Hydrology Research, 2014. **45**(3): p. 479-489.
101. Thorolfsson, S.T., et al. *Extreme rainfalls and damages on August 13 2007 in the City of Trondheim, Norway*. in *The XXV Nordic Hydrological Conference Northern Hydrology and its Global role*. 2008. Reykjavik, Iceland.
102. Hailegeorgis, T.T., S.T. Thorolfsson, and K. Alfredsen, *Regional frequency analysis of extreme precipitation with consideration of uncertainties to update IDF curves for the city of Trondheim*. Journal of Hydrology, 2013. **498**: p. 305-318.
103. Hatt, E., D. Fletcher, and A. Deletic, *Hydraulic and pollutant removal performance of stormwater filters under variable wetting and drying regimes*. Water Science and Technology, 2007. **56**(12): p. 11-19.
104. Solemslie, H.W., *An investigation of hydraulic conductivity of novel filter medias for infiltration units*, in *Department of Hydraulic and Environmental engineering*. 2016, Norwegian University of Science and Technology: (Unpublished student thesis).
105. Institute, N.M. *eKlima - Free access to weather- and climate date from Norwegian Meteorological Institute from historical data to real time observation*. 2016 02.08.2016]; Available from: www.eklima.met.no.

Appendixes

Appendix A: Base flow removal rate

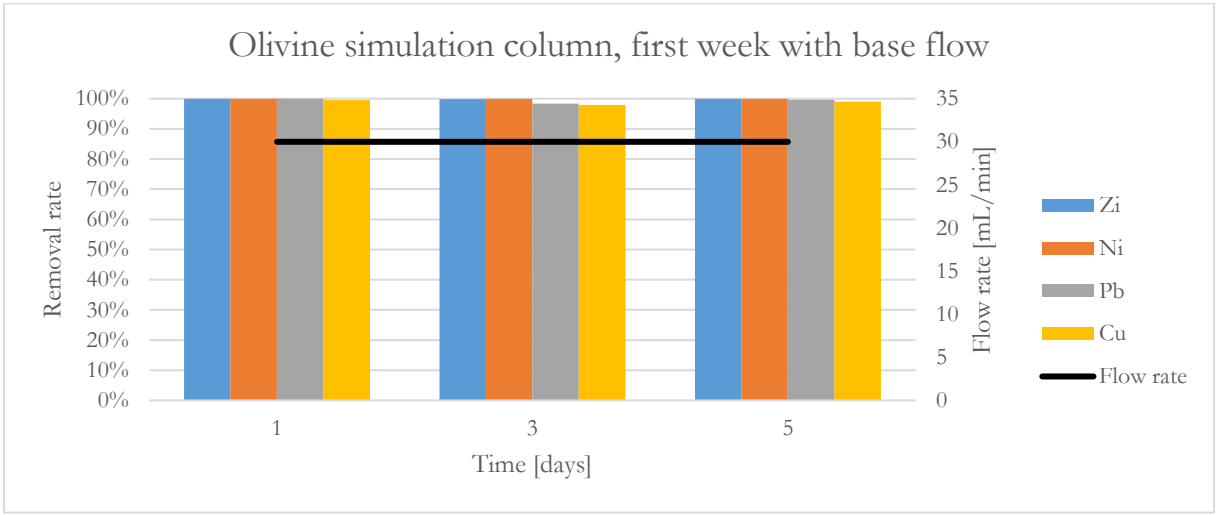

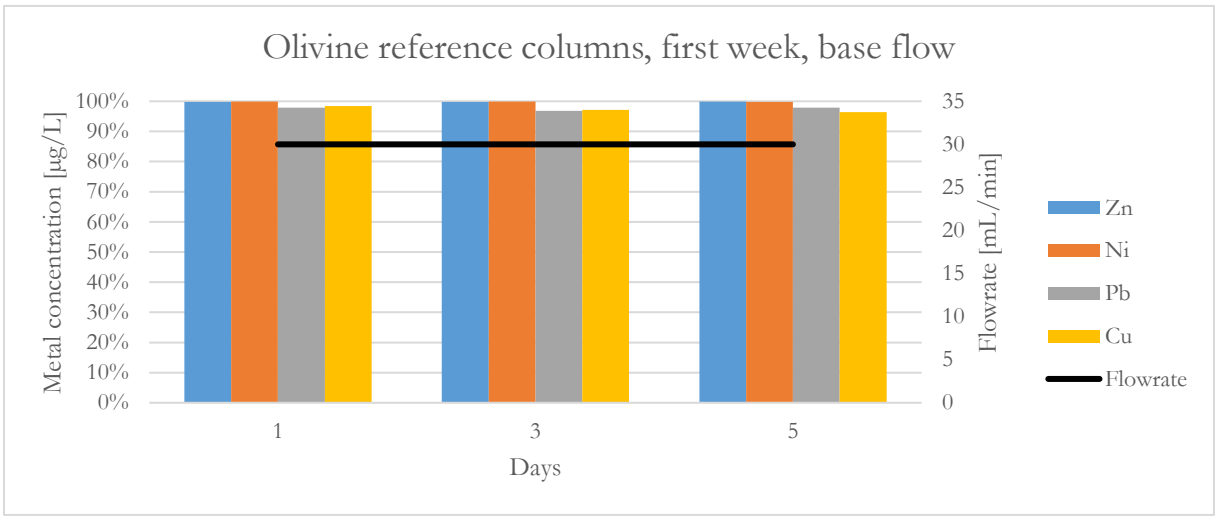

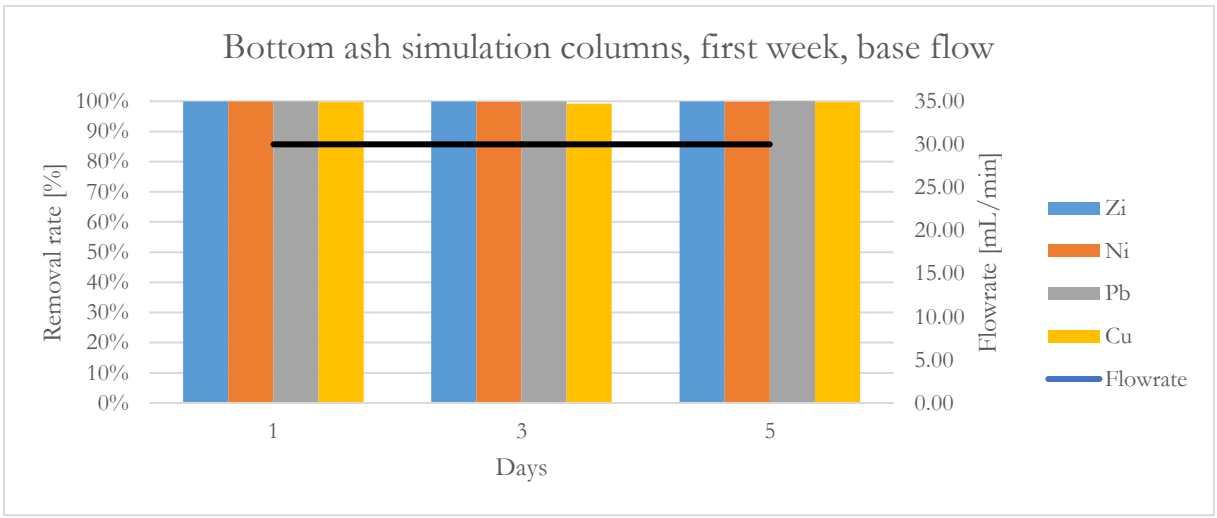

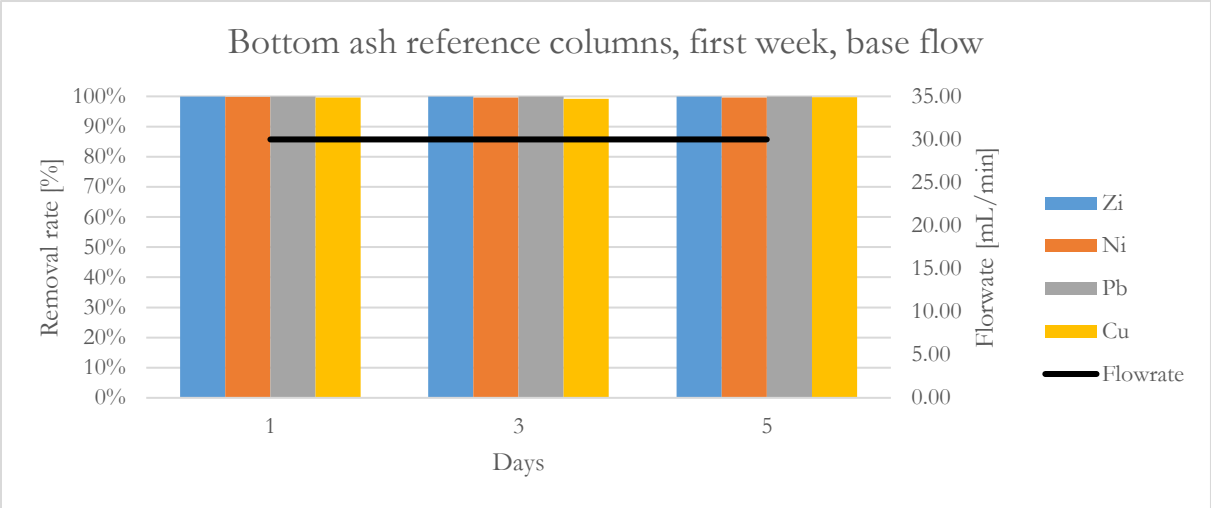
Bottom ash reference columns, first week, base flow
Removal rate [%]
100%
90%
80%
70%
60%
50%
40%
30%
20%
10%
0%
35.00
30.00
25.00
20.00
15.00
10.00
5.00
0.00
Florwate [mL/min]
1
3
5
Days
Zi
Ni
Pb
Cu
Flowrate

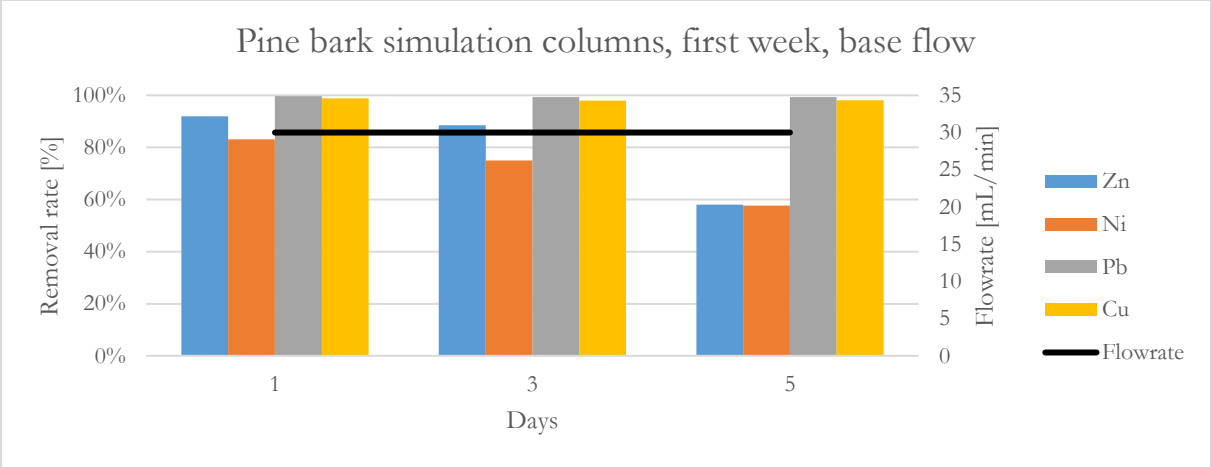
Pine bark simulation columns, first week, base flow
Removal rate [%]
100%
80%
60%
40%
20%
0%
35
30
25
20
15
10
5
0
Flowrate [mL/min]
1
3
5
Days
Zn
Ni
Pb
Cu
Flowrate

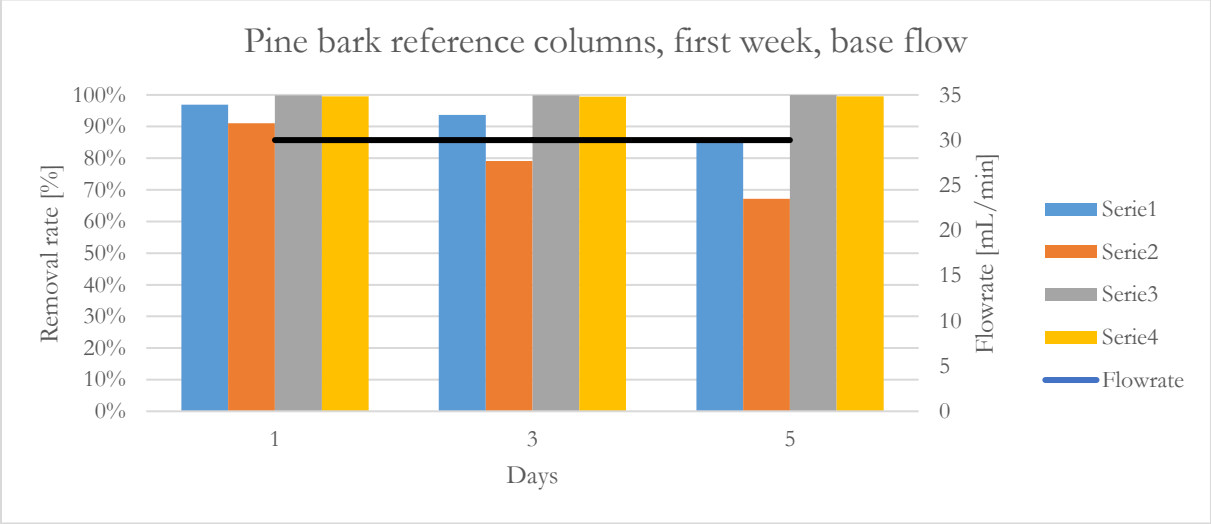
Pine bark reference columns, first week, base flow
Removal rate [%]
100%
90%
80%
70%
60%
50%
40%
30%
20%
10%
0%
35
30
25
20
15
10
5
0
Flowrate [mL/min]
1
3
5
Days
Serie1
Serie2
Serie3
Serie4
Flowrate

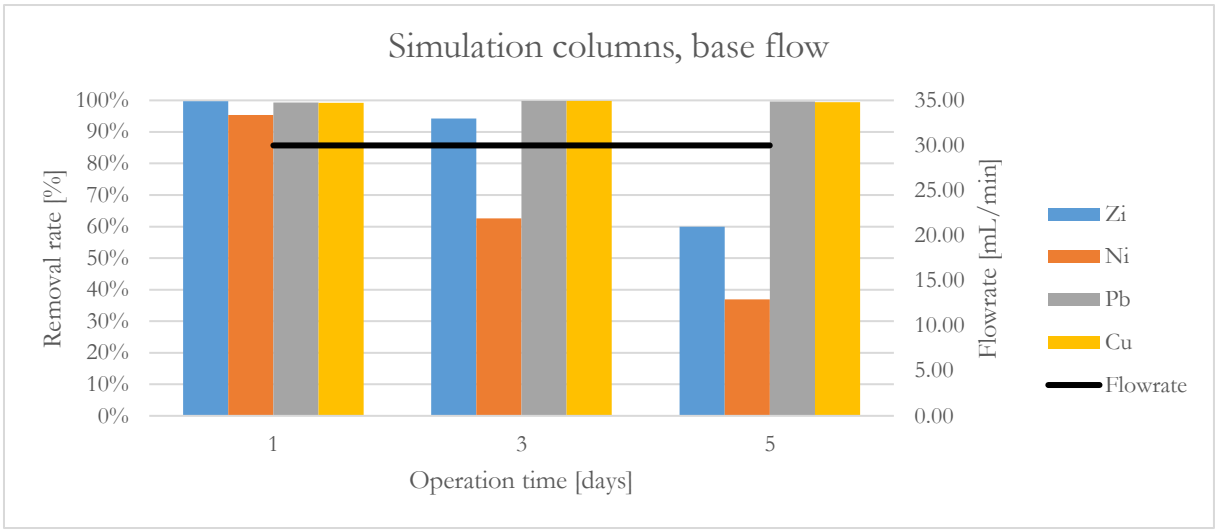
Simulation columns, base flow
Removal rate [%]
100%
90%
80%
70%
60%
50%
40%
30%
20%
10%
0%
35.00
30.00
25.00
20.00
15.00
10.00
5.00
0.00
Flowrate [mL/min]
1
3
5
Operation time [days]
Zi
Ni
Pb
Cu
Flowrate

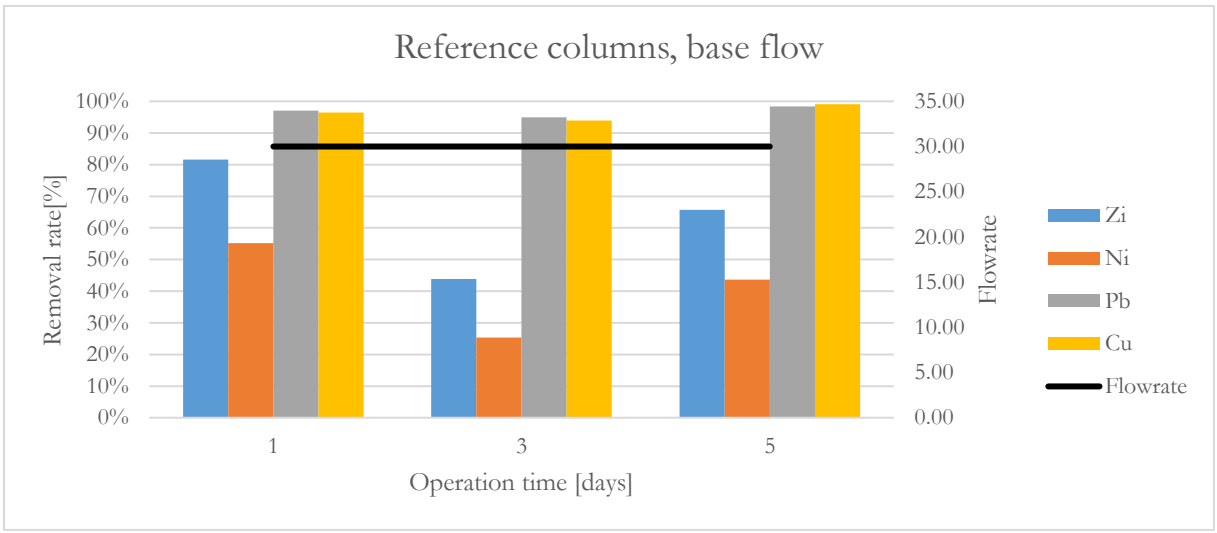
Reference columns, base flow
Removal rate[%]
100%
90%
80%
70%
60%
50%
40%
30%
20%
10%
0%
35.00
30.00
25.00
20.00
15.00
10.00
5.00
0.00
Flowrate
1
3
5
Operation time [days]
Zi
Ni
Pb
Cu
Flowrate

Appendix B: pH throughout the experiments

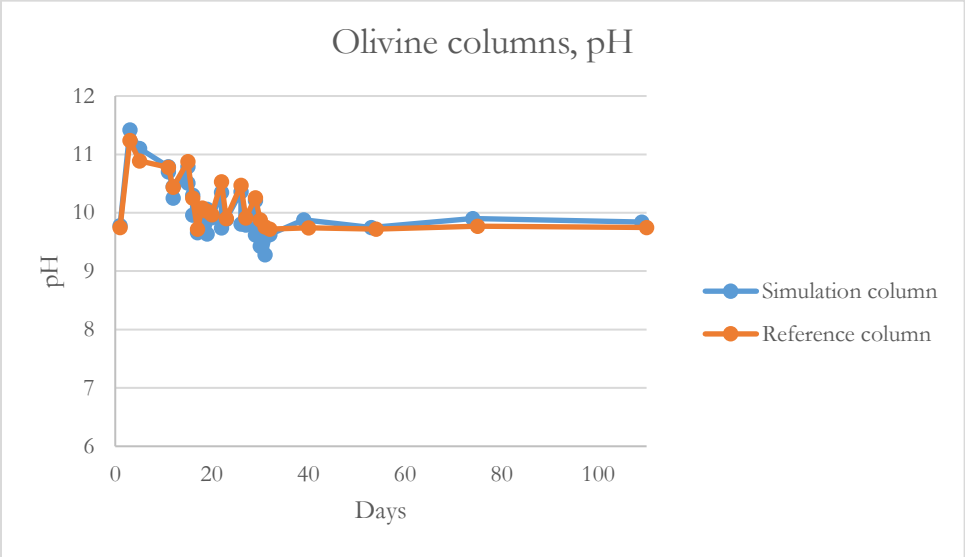

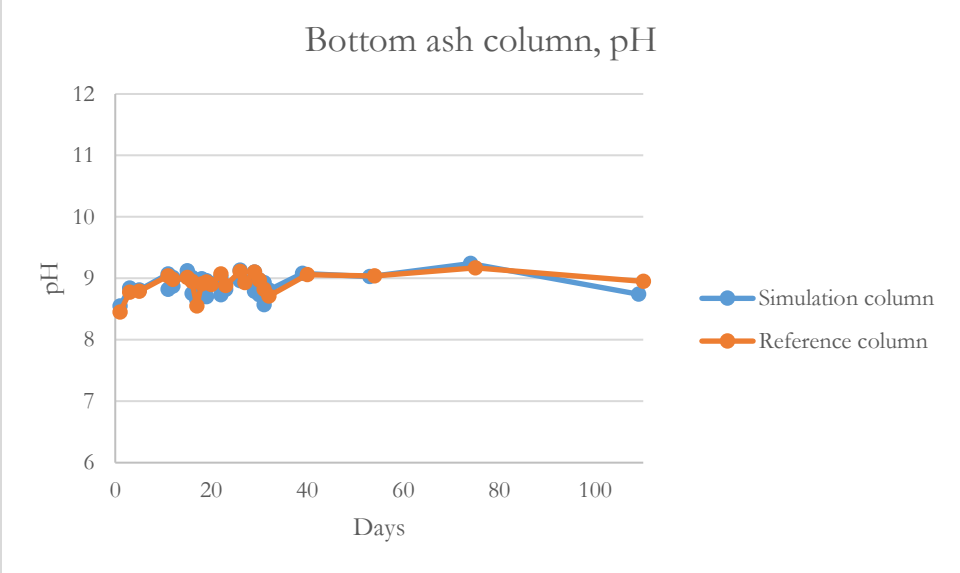

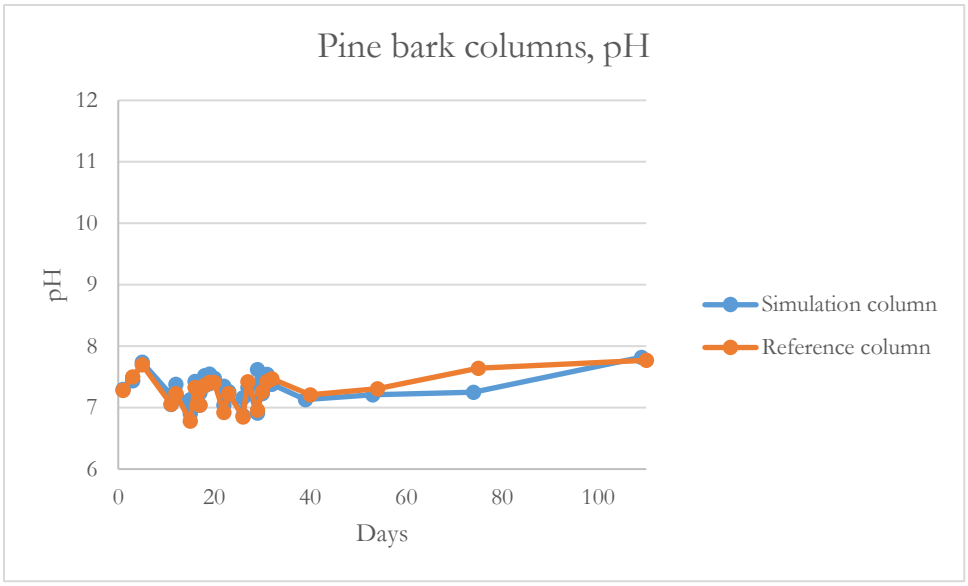
Pine bark columns, pH
12
11
10
9
8
7
6
pH
0
20
40
60
80
100
Days
Simulation column
Reference column

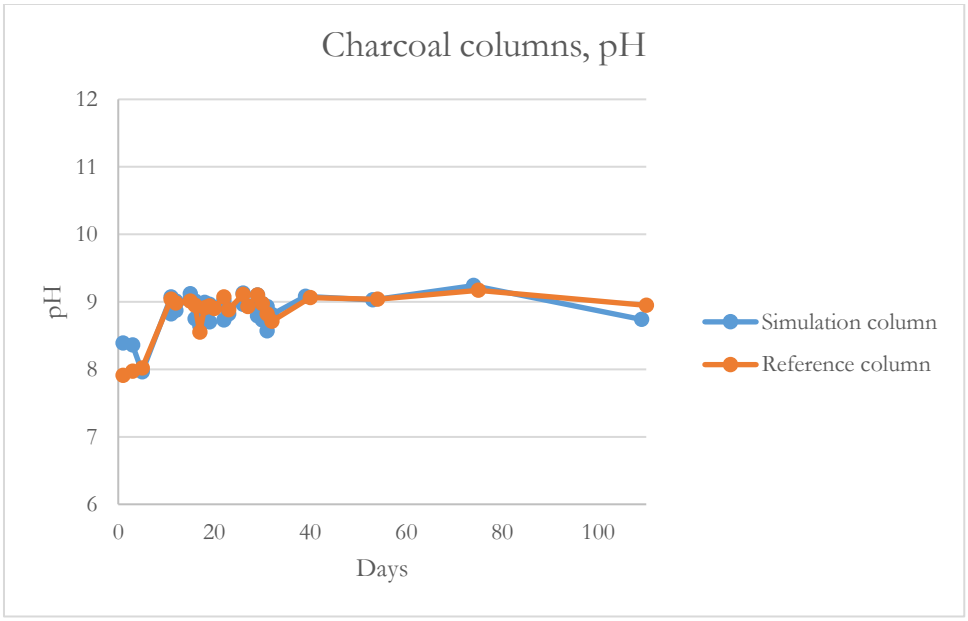
Charcoal columns, pH
12
11
10
9
8
7
6
pH
0
20
40
60
80
100
Days
Simulation column
Reference column

Appendix C: Electrical conductivity throughout the experiments

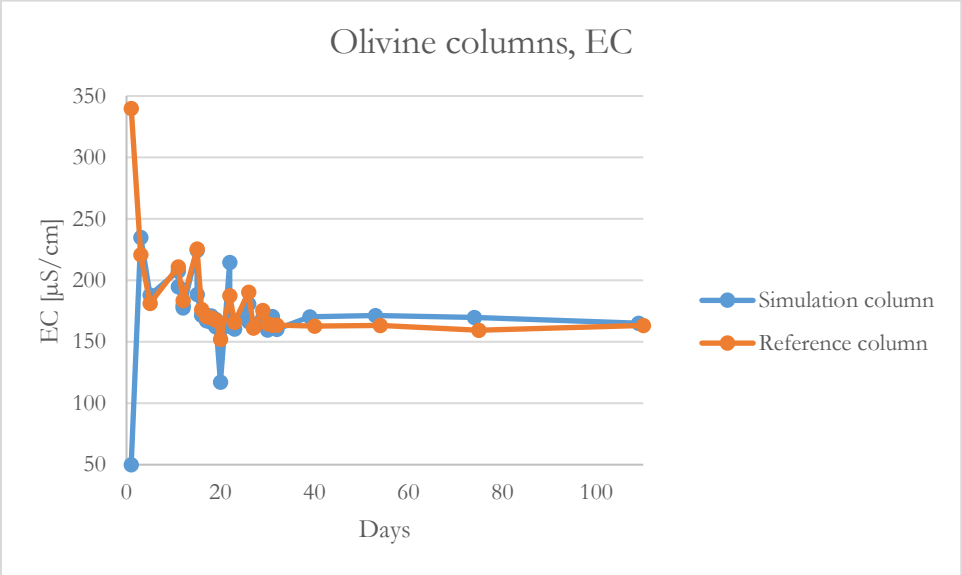

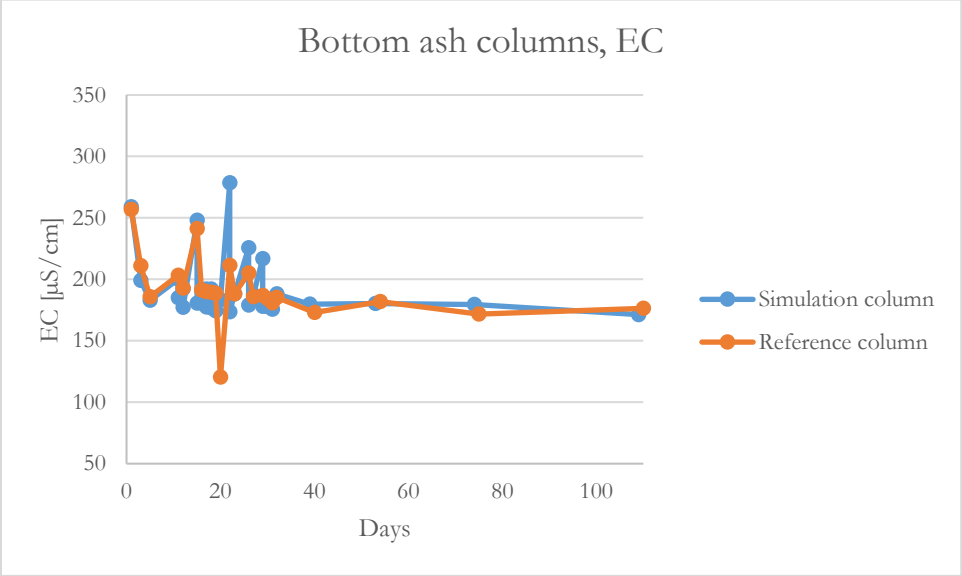

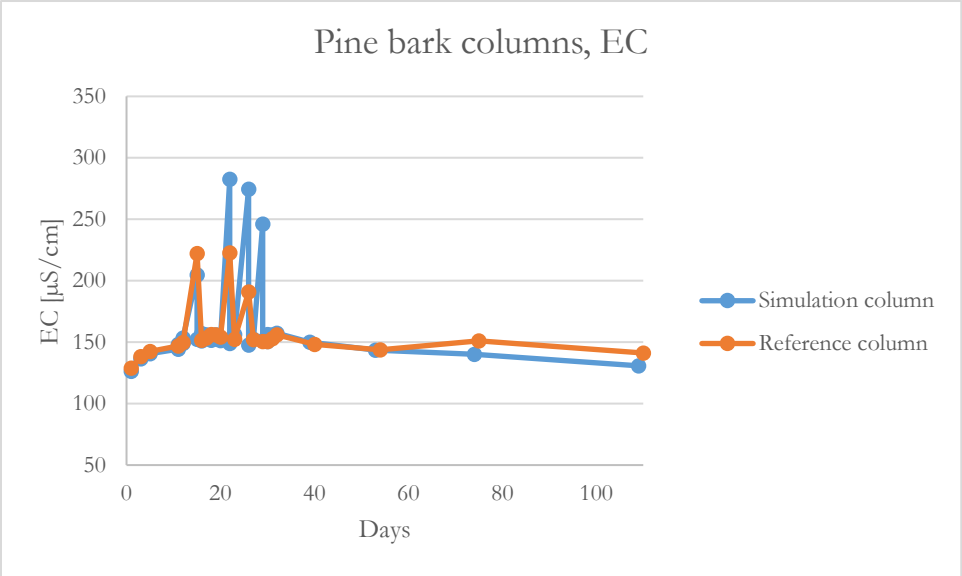
Pine bark columns, EC
350
300
250
200
150
100
50
EC [µS/cm]
0
20
40
60
80
100
Days
Simulation column
Reference column

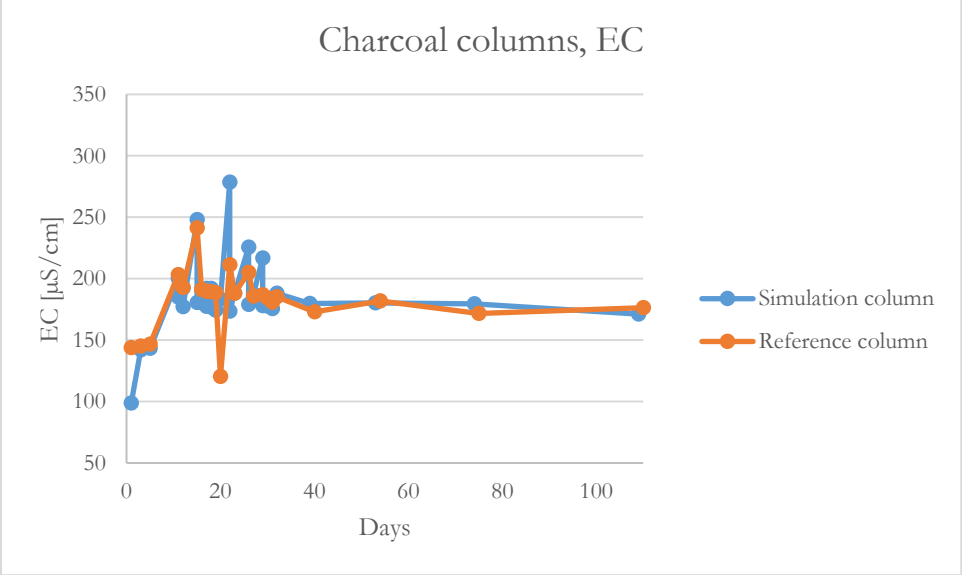
Charcoal columns, EC
350
300
250
200
150
100
50
EC [µS/cm]
0
20
40
60
80
100
Days
Simulation column
Reference column

Appendix D: Metal content olivine columns

Metal concentration

Sample name	Type	Media	SIM#	Date SIM	Pb208(LR) Conc. µg/L	Pb208(LR) RSD, %	Ni60(MR) Conc. µg/L	Ni60(MR) RSD, %	Cu63(MR) Conc. µg/L	Cu63(MR) RSD, %	Zn66(MR) Conc. µg/L	Zn66(MR) RSD, %
B1.3	SIM	Olivine	B1	25.07.2016	1.15	0.2	0.35	16.1	8.23	5.0	0.68	21.4
B2.3	SIM	Olivine	B2	27.07.2016	33.49	0.9	1.37	13.5	40.28	0.2	2.09	19.1
B3.3	SIM	Olivine	B3	29.07.2016	7.23	2.0	1.18	4.4	19.48	6.4	0.89	9.7
SIM 1.1.3	SIM	Olivine	SIM 1	04.08.2016	6.05	3.1	1.15	16.7	18.23	2.2	0.39	24.3
SIM 1.2.3	SIM	Olivine	SIM 1	04.08.2016	12.62	2.8	2.46	11.3	26.74	1.3	1.02	10.3
SIM 2.1.3	SIM	Olivine	SIM 2	05.08.2016	132.83	1.5	7.68	1.4	249.53	3.2	6.56	7.6
SIM 2.2.3	SIM	Olivine	SIM 2	05.08.2016	461.04	2.4	26.72	1.4	570.11	1.8	18.85	2.3
SIM 3.1.3	SIM	Olivine	SIM 3	08.08.2016	39.42	1.1	3.27	8.2	75.80	1.2	2.60	13.8
SIM 3.2.3	SIM	Olivine	SIM 3	08.08.2016	12.19	3.4	5.36	4.4	33.33	3.8	1.03	21.2
SIM 4.1.3	SIM	Olivine	SIM 4	09.08.2016	9.27	3.9	3.23	4.0	29.91	1.4	0.69	29.6
SIM 4.2.3	SIM	Olivine	SIM 4	09.08.2016	34.15	1.7	11.5	3.6	66.4	1.4	2.0	2.1
SIM 5.1.3	SIM	Olivine	SIM 5	10.08.2016	172.53	1.0	9.7	2.2	259.7	2.9	8.6	2.4
SIM 5.2.3	SIM	Olivine	SIM 5	10.08.2016	35.42	1.0	18.7	0.8	74.2	3.9	3.5	7.0
SIM 5.2.3	SIM	Olivine	SIM 5	10.08.2016	36.33	1.5	19.3	0.5	77.5	1.3	3.5	6.3
SIM 6.1.3	SIM	Olivine	SIM 6	11.08.2016	14.43	2.8	4.5	1.2	29.5	1.8	0.5	14.9
SIM 6.2.3	SIM	Olivine	SIM 6	11.08.2016	61.89	1.5	42.7	1.0	123.5	0.3	5.4	5.2
SIM 7.1.3	SIM	Olivine	SIM 7	12.08.2016	22.85	2.4	5.4	2.1	37.3	3.0	0.9	6.2
SIM 7.2.3	SIM	Olivine	SIM 7	12.08.2016	45.41	1.4	39.8	3.9	85.2	0.8	2.8	1.8
SIM 8.1.3	SIM	Olivine	SIM 8	15.08.2016	1.49	2.8	1.4	11.0	12.8	1.1	0.7	18.0
SIM 8.2.3	SIM	Olivine	SIM 8	15.08.2016	43.58	0.9	30.4	1.9	93.6	1.3	2.0	1.1
SIM 8.3.3	SIM	Olivine	SIM 8	16.08.2016	51.41	0.5	10.3	2.0	113.3	2.3	2.9	3.3
SIM 9.1.3	SIM	Olivine	SIM 9	19.08.2016	6.42	3.2	2.0	6.4	19.2	2.0	2.5	125.1
SIM 9.2.3	SIM	Olivine	SIM 9	19.08.2016	56.33	2.6	18.2	2.6	126.4	2.3	5.9	6.8
SIM 9.3.3	SIM	Olivine	SIM 9	20.08.2016	33.53	1.2	8.8	2.3	81.2	3.4	2.4	3.4
SIM 10.1.3	SIM	Olivine	SIM 10	22.08.2016	2.77	2.7	2.2	2.1	16.6	3.5	0.3	3.1
SIM 10.2.3	SIM	Olivine	SIM 10	22.08.2016	51.54	1.6	29.7	1.7	109.3	0.3	3.9	2.5
SIM 11.1.3	SIM	Olivine	SIM 11	23.08.2016	52.74	0.9	11.8	2.8	110.3	0.7	4.1	2.6
SIM 11.2.3	SIM	Olivine	SIM 11	23.08.2016	55.10	1.2	52.1	2.7	105.8	2.1	4.5	3.2
SIM 12.1.3	SIM	Olivine	SIM 12	24.08.2016	13.86	3.3	16.9	1.3	59.1	0.5	0.8	11.9
SIM 12.2.3	SIM	Olivine	SIM 12	24.08.2016	50.89	1.5	133.0	1.7	128.4	0.4	8.3	3.5

SIM 12.3.3	SIM	Olivine	SIM 12	25.08.2016	45.14	2.5	25.2	0.6	104.8	3.2	3.5	5.0
SIM 13.2.3	SIM	Olivine	SIM 13	01.09.2016	38.18	1.0	15.0	1.1	78.8	2.8	3.7	5.9
SIM 14.2.3	SIM	Olivine	SIM 14	15.09.2016	27.33	1.6	27.7	0.9	83.8	0.9	1.5	1.2
SIM 15.2.3	SIM	Olivine	SIM 15	06.10.2016	280.72	1.5	34.0	1.7	348.7	0.7	8.9	4.5
SIM 16.2.3	SIM	Olivine	SIM 16	10.11.2016	218.66	1.8	27.5	1.6	202.0	1.4	6.8	1.4
B1.7	REF	Olivine	B1	25.07.2016	43.21	2.6	1.03	2.8	30.52	1.1	4.03	13.4
B2.7	REF	Olivine	B2	27.07.2016	63.67	1.7	2.06	20.8	56.99	1.6	3.03	10.2
B3.7	REF	Olivine	B3	29.07.2016	42.44	1.4	3.36	11.9	70.94	1.6	2.45	5.6
SIM 1.1.7	REF	Olivine	SIM 1	04.08.2016	39.71	0.4	3.95	4.9	63.71	0.4	2.55	10.4
SIM 2.1.7	REF	Olivine	SIM 2	05.08.2016	146.57	0.5	10.15	1.8	252.39	1.7	5.63	3.7
SIM 3.1.7	REF	Olivine	SIM 3	08.08.2016	2.20	1.4	0.74	17.7	11.35	0.2	0.35	4.9
SIM 4.1.7	REF	Olivine	SIM 4	09.08.2016	181.25	1.1	13.00	4.5	263.89	0.8	9.88	3.8
SIM 5.1.7	REF	Olivine	SIM 5	10.08.2016	1.61	2.4	4.3	2.2	16.2	1.9	0.3	14.5
SIM 6.1.7	REF	Olivine	SIM 6	11.08.2016	11.31	1.0	7.9	5.3	36.9	1.2	0.5	4.7
SIM 7.1.7	REF	Olivine	SIM 7	12.08.2016	13.97	1.9	7.5	1.3	39.3	1.7	0.5	2.2
SIM 7.3.7	REF	Olivine	SIM 7	13.08.2016	26.99	1.9	9.8	5.2	36.9	1.4	0.6	29.1
SIM 8.1.7	REF	Olivine	SIM 8	15.08.2016	3.74	1.7	1.0	0.8	13.5	1.3	0.4	8.2
SIM 8.3.7	REF	Olivine	SIM 8	16.08.2016	22.12	2.1	8.1	3.4	58.3	1.9	1.1	7.4
SIM 9.1.7	REF	Olivine	SIM 9	19.08.2016	5.60	0.2	1.7	4.5	15.9	2.0	0.4	16.2
SIM 9.3.7	REF	Olivine	SIM 9	20.08.2016	27.02	0.9	11.9	2.7	62.7	1.3	1.5	6.2
SIM 10.1.7	REF	Olivine	SIM 10	22.08.2016	1.97	1.4	3.3	5.0	15.1	0.8	0.3	15.6
SIM 11.1.7	REF	Olivine	SIM 11	23.08.2016	33.60	1.4	10.6	1.2	75.2	1.4	2.4	0.8
SIM 12.1.7	REF	Olivine	SIM 12	24.08.2016	23.64	2.4	18.8	3.6	72.9	2.2	1.6	2.3
SIM 12.3.7	REF	Olivine	SIM 12	25.08.2016	35.30	0.8	25.7	3.2	77.9	0.8	2.4	4.7
SIM 13.3.7	REF	Olivine	SIM 13	02.09.2016	52.43	2.4	19.3	3.8	93.4	1.5	5.6	7.3
SIM 14.3.7	REF	Olivine	SIM 14	16.09.2016	29.81	0.6	19.1	3.9	67.5	0.5	1.8	2.1
SIM 15.3.7	REF	Olivine	SIM 15	07.10.2016	156.85	0.7	22.0	1.8	231.2	2.5	6.9	2.9
SIM 16.3.7	REF	Olivine	SIM 16	11.11.2016	35.93	0.4	11.7	1.8	72.1	0.7	2.7	1.4

Appendix E: Metal content pine bark columns

Sample name	Type	Media	SIM#	Date SIM	Pb208(LR) Conc. µg/L	Pb208(LR) RSD, %	Ni60(MR) Conc. µg/L	Ni60(MR) RSD, %	Cu63(MR) Conc. µg/L	Cu63(MR) RSD, %	Zn66(MR) Conc. µg/L	Zn66(MR) RSD, %
B 1.4	SIM	Pine Bark	B1	25.07.2016	6.17	1.7	338.95	2.0	22.43	1.9	161.88	1.0
B 2.4	SIM	Pine Bark	B2	27.07.2016	12.91	4.5	499.72	1.6	40.86	2.1	230.84	2.2
B 3.4	SIM	Pine Bark	B3	29.07.2016	13.30	2.5	846.68	1.8	39.00	2.7	838.31	1.3
SIM 1.1.4	SIM	Pine Bark	SIM 1	04.08.2016	10.02	1.1	605.42	0.7	40.35	2.6	463.44	1.3
SIM 1.2.4	SIM	Pine Bark	SIM 1	04.08.2016	61.60	1.6	660.68	2.9	125.46	3.4	462.06	3.4
SIM 2.1.4	SIM	Pine Bark	SIM 2	05.08.2016	13.97	1.1	625.62	1.4	44.63	4.1	375.96	0.3
SIM 2.2.4	SIM	Pine Bark	SIM 2	05.08.2016	46.02	2.4	716.40	3.3	80.80	0.8	356.73	1.1
SIM 3.1.4	SIM	Pine Bark	SIM 3	08.08.2016	18.12	2.1	1 186.68	1.8	96.81	1.4	889.95	1.1
SIM 3.2.4	SIM	Pine Bark	SIM 3	08.08.2016	76.21	2.0	851.95	1.9	190.88	1.7	711.30	1.4
SIM 4.1.4	SIM	Pine Bark	SIM 4	09.08.2016	55.53	0.9	782.18	1.8	101.37	2.4	761.46	1.0
SIM 4.2.4	SIM	Pine Bark	SIM 4	09.08.2016	95.72	2.2	917.3	0.8	271.4	0.6	814.2	0.6
SIM 5.1.4	SIM	Pine Bark	SIM 5	10.08.2016	46.10	1.3	803.2	0.5	86.5	1.8	745.1	0.8
SIM 5.2.4	SIM	Pine Bark	SIM 5	10.08.2016	43.97	2.7	774.3	2.0	155.6	1.2	533.2	3.9
SIM 6.1.4	SIM	Pine Bark	SIM 6	11.08.2016	4.06	2.9	642.2	1.2	20.0	0.3	192.4	2.7
SIM 6.2.4	SIM	Pine Bark	SIM 6	11.08.2016	43.64	2.5	807.8	4.7	76.7	1.6	437.0	3.7
SIM 7.1.4	SIM	Pine Bark	SIM 7	12.08.2016	10.19	0.6	802.3	0.8	41.7	2.3	396.6	1.5
SIM 7.2.4	SIM	Pine Bark	SIM 7	12.08.2016	34.96	1.9	683.1	0.6	38.6	1.5	165.5	0.5
SIM 7.3.4	SIM	Pine Bark	SIM 7	13.08.2016	17.72	1.2	939.7	3.7	63.0	0.7	638.0	1.7
SIM 8.1.4	SIM	Pine Bark	SIM 8	15.08.2016	7.57	3.0	1 338.2	1.6	38.9	0.6	658.0	0.7
SIM 8.2.4	SIM	Pine Bark	SIM 8	15.08.2016	24.21	0.6	402.9	0.6	21.1	1.1	97.6	1.2
SIM 8.3.4	SIM	Pine Bark	SIM 8	16.08.2016	2.75	3.7	790.7	2.8	24.8	3.2	294.5	4.0

SIM 9.1.4	SIM	Pine Bark	SIM 9	19.08.2016	32.80	2.3	2 038.9	3.2	79.2	1.6	1 725.7	3.3
SIM 9.2.4	SIM	Pine Bark	SIM 9	19.08.2016	33.29	2.2	903.3	1.9	80.4	2.3	535.5	0.6
SIM 9.3.4	SIM	Pine Bark	SIM 9	20.08.2016	17.25	1.9	958.4	1.4	71.6	2.5	745.3	0.4
SIM 10.1.4	SIM	Pine Bark	SIM 10	22.08.2016	2.89	1.5	747.3	1.7	20.1	0.2	261.7	0.8
SIM 10.2.4	SIM	Pine Bark	SIM 10	22.08.2016	59.54	1.1	1 090.6	1.0	188.2	1.2	948.9	0.8
SIM 11.1.4	SIM	Pine Bark	SIM 11	23.08.2016	47.11	0.7	1 027.4	0.3	118.3	1.0	947.6	1.3
SIM 11.2.4	SIM	Pine Bark	SIM 11	23.08.2016	32.85	1.5	807.8	2.8	50.2	2.6	281.1	1.0
SIM 12.1.4	SIM	Pine Bark	SIM 12	24.08.2016	5.62	0.3	690.0	1.8	17.4	2.9	198.3	1.2
SIM 12.2.4	SIM	Pine Bark	SIM 12	24.08.2016	68.97	1.8	1 103.7	1.6	161.3	2.4	889.2	1.6
SIM 12.3.4	SIM	Pine Bark	SIM 12	25.08.2016	73.70	1.9	1 179.3	3.7	168.6	1.8	1 081.8	0.2
SIM 13.2.4	SIM	Pine Bark	SIM 13	01.09.2016	124.71	1.2	1 239.8	1.5	352.6	1.6	1 249.3	1.6
SIM 14.2.4	SIM	Pine Bark	SIM 14	15.09.2016	92.23	2.2	1 227.6	1.2	191.1	2.2	1 403.6	0.6
SIM 15.2.4	SIM	Pine Bark	SIM 15	06.10.2016	72.77	1.6	965.8	1.9	156.9	1.5	1 100.9	0.6
SIM 16.2.4	SIM	Pine Bark	SIM 16	10.11.2016	111.18	0.5	1 023.3	1.0	198.0	0.2	1 296.7	1.9
B 1.8	REF	Pine Bark	B1	25.07.2016	2.08	3.4	178.59	0.6	10.09	4.1	61.98	2.5
B 2.8	REF	Pine Bark	B2	27.07.2016	2.10	1.0	417.57	0.5	10.78	2.6	127.30	3.0
B 3.8	REF	Pine Bark	B3	29.07.2016	0.99	1.1	657.26	1.6	8.14	3.6	280.35	0.9
SIM 1.1.8	REF	Pine Bark	SIM 1	04.08.2016	3.18	2.3	631.01	1.1	19.74	2.4	295.84	1.2
SIM 2.1.8	REF	Pine Bark	SIM 2	05.08.2016	4.18	3.3	717.34	2.0	18.88	2.6	363.66	2.3
SIM 3.1.8	REF	Pine Bark	SIM 3	08.08.2016	4.21	1.7	1 455.24	2.8	28.69	1.3	1 270.09	0.5
SIM 4.1.8	REF	Pine Bark	SIM 4	09.08.2016	7.34	1.4	821.30	0.7	27.04	3.2	492.26	1.1
SIM 5.1.8	REF	Pine Bark	SIM 5	10.08.2016	4.19	1.0	806.2	0.8	21.7	1.4	446.2	0.3
SIM 6.1.8	REF	Pine Bark	SIM 6	11.08.2016	21.96	2.4	1 079.4	0.2	62.4	3.3	980.9	1.7
SIM 7.1.8	REF	Pine Bark	SIM 7	12.08.2016	9.52	1.2	1 044.8	2.3	39.9	0.4	751.0	3.3
SIM 7.3.8	REF	Pine Bark	SIM 7	13.08.2016	26.86	0.8	1 191.5	2.4	68.2	0.8	1 098.6	0.6
SIM 8.1.8	REF	Pine Bark	SIM 8	15.08.2016	5.74	2.7	1 051.2	2.0	22.8	0.5	590.4	1.6

SIM 8.3.8	REF	Pine Bark	SIM 8	16.08.2016	4.00	0.6	713.7	1.7	14.1	1.7	325.2	1.5
SIM 9.1.8	REF	Pine Bark	SIM 9	19.08.2016	36.22	1.2	1 794.4	3.4	98.7	1.5	1 827.4	0.7
SIM 9.3.8	REF	Pine Bark	SIM 9	20.08.2016	6.56	1.2	1 011.0	3.9	29.7	0.4	669.0	2.3
SIM 10.1.8	REF	Pine Bark	SIM 10	22.08.2016	6.67	1.0	696.7	1.9	23.1	2.0	324.8	0.7
SIM 11.1.8	REF	Pine Bark	SIM 11	23.08.2016	5.48	2.5	901.8	1.0	21.8	2.8	354.6	1.7
SIM 12.1.8	REF	Pine Bark	SIM 12	24.08.2016	3.21	1.8	862.4	1.3	14.4	0.6	296.5	0.7
SIM 12.3.8	REF	Pine Bark	SIM 12	25.08.2016	33.99	2.4	1 197.0	2.3	86.8	1.2	1 095.0	1.8
SIM 13.3.8	REF	Pine Bark	SIM 13	02.09.2016	54.59	0.7	1 104.4	0.7	119.0	2.8	1 091.8	0.7
SIM 14.3.8	REF	Pine Bark	SIM 14	16.09.2016	8.84	1.5	837.4	1.1	29.0	0.7	606.9	2.2
SIM 15.3.8	REF	Pine Bark	SIM 15	07.10.2016	51.90	2.5	1 047.9	3.0	103.3	2.2	1 168.8	3.2
SIM 16.3.8	REF	Pine Bark	SIM 16	11.11.2016	52.45	0.5	914.3	2.6	104.8	1.7	1 021.4	1.3

Appendix F: Metal contents charcoal columns

Sample name	Type	Media	SIM#	Date SIM	Pb208(LR) Conc. µg/L	Pb208(LR) RSD, %	Ni60(MR) Conc. µg/L	Ni60(MR) RSD, %	Cu63(MR) Conc. µg/L	Cu63(MR) RSD, %	Zn66(MR) Conc. µg/L	Zn66(MR) RSD, %
B1.1	SIM	GAC-Sand	B1	25.07.2016	14.15	1.1	93.31	3.3	16.49	1.2	6.19	7.6
B2.1	SIM	GAC-Sand	B2	27.07.2016	4.19	1.6	748.67	1.1	4.22	0.8	114.94	1.2
B3.1	SIM	GAC-Sand	B3	29.07.2016	6.56	3.5	1261.45	3.3	11.58	0.9	801.26	0.7
SIM 1.1.1	SIM	GAC-sand	SIM 1	04.08.2016	86.33	2.0	1304.65	1.2	119.22	3.7	954.47	0.5
SIM 1.2.1	SIM	GAC-sand	SIM 1	04.08.2016	73.81	3.0	1232.03	3.0	81.51	3.3	575.74	1.8
SIM 2.1.1	SIM	GAC-sand	SIM 2	05.08.2016	2.39	3.3	655.71	0.4	1.65	3.4	65.30	2.8
SIM 2.2.1	SIM	GAC-sand	SIM 2	05.08.2016	30.55	2.1	789.96	2.3	12.07	2.4	162.99	0.6
SIM 3.1.1	SIM	GAC-sand	SIM 3	08.08.2016	1.69	2.3	1605.76	3.0	0.64	9.5	488.49	1.6
SIM 3.2.1	SIM	GAC-sand	SIM 3	08.08.2016	129.14	2.9	2018.91	1.6	137.83	1.2	3588.42	1.7
SIM 4.1.1	SIM	GAC-sand	SIM 4	09.08.2016	8.74	1.4	966.28	0.6	7.19	1.0	431.68	1.8
SIM 4.2.1	SIM	GAC-sand	SIM 4	09.08.2016	55.31	1.6	1 128.6	2.8	37.4	3.9	580.4	4.6
SIM 4.2.1	SIM	GAC-sand	SIM 4	09.08.2016	56.57	0.2	1 144.1	1.6	37.5	3.4	581.2	3.0
SIM 5.1.1	SIM	GAC-sand	SIM 5	10.08.2016	9.27	2.4	897.3	3.0	1.3	0.6	255.8	0.8
SIM 5.2.1	SIM	GAC-sand	SIM 5	10.08.2016	421.19	2.2	1 725.7	1.5	412.0	2.8	1 627.0	1.8
SIM 6.1.1	SIM	GAC-sand	SIM 6	11.08.2016	8.25	1.1	1 035.9	3.1	1.3	2.8	327.0	2.0
SIM 6.2.1	SIM	GAC-sand	SIM 6	11.08.2016	72.85	1.4	1 113.3	2.5	33.9	1.9	714.9	2.4
SIM 7.1.1	SIM	GAC-sand	SIM 7	12.08.2016	35.96	2.0	1 358.9	2.4	8.3	4.9	1 268.7	1.8
SIM 7.2.1	SIM	GAC-sand	SIM 7	12.08.2016	69.20	1.2	774.0	2.0	16.0	3.3	280.0	0.8
SIM 7.3.1	SIM	GAC-sand	SIM 7	13.08.2016	125.81	2.3	1 973.1	1.0	45.9	0.5	2 280.9	0.7
SIM 8.1.1	SIM	GAC-sand	SIM 8	15.08.2016	213.04	1.6	4 263.4	2.8	36.8	0.7	7 477.0	0.6

SIM 8.2.1	SIM	GAC-sand	SIM 8	15.08.2016	88.72	1.9	1 088.3	1.8	29.8	0.9	684.5	2.7
SIM 8.3.1	SIM	GAC-sand	SIM 8	16.08.2016	39.32	1.7	645.6	2.2	6.4	1.3	407.0	0.6
SIM 9.1.1	SIM	GAC-sand	SIM 9	19.08.2016	250.88	1.5	4 619.6	1.4	57.3	1.9	8 064.6	2.2
SIM 9.2.1	SIM	GAC-sand	SIM 9	19.08.2016	91.38	1.7	1 036.0	3.3	33.9	1.3	684.8	1.7
SIM 9.3.1	SIM	GAC-sand	SIM 9	20.08.2016	80.31	2.0	1 479.5	1.7	57.0	2.0	1 193.2	2.7
SIM 10.1.1	SIM	GAC-sand	SIM 10	22.08.2016	12.56	1.8	654.2	1.4	0.7	6.6	82.6	2.7
SIM 10.2.1	SIM	GAC-sand	SIM 10	22.08.2016	123.69	1.2	1 178.4	1.5	78.4	1.5	844.5	0.6
SIM 11.1.1	SIM	GAC-sand	SIM 11	23.08.2016	116.57	2.0	1 637.9	1.4	74.9	4.3	1 587.4	1.2
SIM 11.2.1	SIM	GAC-sand	SIM 11	23.08.2016	200.61	0.9	1 439.2	1.6	138.7	1.7	1 108.4	3.2
SIM 12.1.1	SIM	GAC-sand	SIM 12	24.08.2016	53.25	1.1	1 247.2	1.8	4.9	2.5	640.1	2.8
SIM 12.2.1	SIM	GAC-sand	SIM 12	24.08.2016	85.16	2.9	1 120.8	1.2	24.1	1.8	533.6	0.6
SIM 12.3.1	SIM	GAC-sand	SIM 12	25.08.2016	140.41	1.8	1 840.2	1.3	75.0	2.1	1 929.1	0.6
SIM 13.2.1	SIM	GAC-sand	SIM 13	01.09.2016	255.75	2.0	1 963.7	1.7	223.8	2.3	2 421.2	2.4
SIM 15.2.1	SIM	GAC-sand	SIM 15	06.10.2016	176.70	1.1	1 645.7	1.0	97.2	2.6	1 887.8	1.2
SIM 16.2.1	SIM	GAC-sand	SIM 16	10.11.2016	85.05	1.9	1 326.3	1.1	46.7	0.8	1 353.1	2.2
B1.5	REF	GAC-Sand	B1	25.07.2016	59.38	1.1	896.61	0.5	70.80	1.7	367.28	0.6
B2.5	REF	GAC-Sand	B2	27.07.2016	100.20	0.4	1 493.66	2.2	121.99	1.6	1 122.99	1.8
B3.5	REF	GAC-Sand	B3	29.07.2016	32.74	1.6	1 126.60	1.5	18.56	1.3	685.26	1.3
SIM 1.1.5	REF	GAC-sand	SIM 1	04.08.2016	295.96	0.8	1 518.80	2.2	292.26	0.9	1 337.45	0.5
SIM 2.1.5	REF	GAC-sand	SIM 2	05.08.2016	63.49	2.3	1 021.60	2.5	30.34	1.1	533.93	2.9
SIM 3.1.5	REF	GAC-sand	SIM 3	08.08.2016	47.06	1.6	1 849.81	0.3	11.68	1.9	1 373.73	1.7
SIM 4.1.5	REF	GAC-sand	SIM 4	09.08.2016	352.00	1.6	1 620.75	1.1	257.58	1.4	1 390.04	1.2
SIM 5.1.5	REF	GAC-sand	SIM 5	10.08.2016	434.74	1.8	1 772.6	1.3	295.0	3.8	1 816.1	0.8
SIM 7.1.5	REF	GAC-sand	SIM 7	12.08.2016	123.60	1.3	1 199.5	0.3	38.5	1.8	856.7	2.0
SIM 7.3.5	REF	GAC-sand	SIM 7	13.08.2016	121.61	1.3	1 344.4	2.4	35.3	1.5	923.9	1.8
SIM 8.1.5	REF	GAC-sand	SIM 8	15.08.2016	64.13	3.3	1 473.6	1.8	15.9	1.9	1 031.2	0.4

SIM 8.3.5	REF	GAC-sand	SIM 8	16.08.2016	51.88	0.2	585.1	2.2	18.8	1.7	257.0	2.9
SIM 9.1.5	REF	GAC-sand	SIM 9	19.08.2016	40.95	2.3	377.5	1.9	3.7	4.1	100.9	1.3
SIM 9.3.5	REF	GAC-sand	SIM 9	20.08.2016	88.69	0.9	850.0	2.4	15.1	2.4	279.3	0.6
SIM 10.1.5	REF	GAC-sand	SIM 10	22.08.2016	28.27	3.5	268.3	1.0	2.0	1.3	40.5	1.5
SIM 11.1.5	REF	GAC-sand	SIM 11	23.08.2016	158.07	1.8	1 389.6	1.9	133.9	1.8	1 132.4	3.5
SIM 12.1.5	REF	GAC-sand	SIM 12	24.08.2016	168.88	3.3	1 560.6	0.9	111.2	1.2	1 484.7	0.6
SIM 12.3.5	REF	GAC-sand	SIM 12	25.08.2016	80.42	0.9	1 043.2	0.6	14.0	1.8	367.4	1.0
SIM 13.3.5	REF	GAC-sand	SIM 13	02.09.2016	157.11	3.9	1 470.4	1.7	117.5	1.6	1 509.5	1.7
SIM 14.3.5	REF	GAC-sand	SIM 14	16.09.2016	128.83	3.1	1 631.0	0.3	143.4	2.2	1 711.5	0.8
SIM 15.3.5	REF	GAC-sand	SIM 15	07.10.2016	196.35	1.2	1 570.7	2.8	140.0	2.0	1 650.3	1.4
SIM 16.3.5	REF	GAC-sand	SIM 16	11.11.2016	141.09	1.6	1 487.2	2.8	114.1	0.6	1 554.8	0.9

Appendix G: Metal contents bottom ash columns

					Cd114(LR)		Hg202(LR)		Pb208(LR)		Na23(MR)	
					Conc. µg/L	RSD, %	Conc. µg/L	RSD, %	Conc. µg/L	RSD, %	Conc. µg/L	RSD, %
Sample name	Type	Media	SIM#	Date SIM								
B1.2	SIM	BA-Fe2O3	B1	25.07.2016	0.0014	81.3	0.001	6.7	0.80	2.0	5 409	0.8
B1.2	SIM	BA-Fe2O3	B1	25.07.2016	0.0024	44.3	0.001	14.5	0.77	1.1	5 409	2.0
B2.2	SIM	BA-Fe2O3	B2	27.07.2016	0.0017	22.0	0.002	15.6	0.91	0.8	5 159	0.6
B3.2	SIM	BA-Fe2O3	B3	29.07.2016	0.0007	9.2	0.001	11.2	0.32	5.4	4 544	1.2
B3.2	SIM	BA-Fe2O3	B3	29.07.2016	0.0022	35.2	0.002	2.9	0.33	1.6	4 476	2.3
SIM 1.1.2	SIM	BA-Fe2O3	SIM 1	04.08.2016	0.0000	64.0	0.006	14.5	3.48	2.4	4 715	1.0
SIM 1.2.2	SIM	BA-Fe2O3	SIM 1	04.08.2016	0.0032	33.3	0.001	17.5	127.05	3.3	4 779	1.5
SIM 2.1.2	SIM	BA-Fe2O3	SIM 2	05.08.2016	0.0012	28.9	0.001	22.3	1.18	0.3	4 744	1.4
SIM 2.1.2	SIM	BA-Fe2O3	SIM 2	05.08.2016	0.0004	32.5	0.001	10.2	1.15	1.9	4 612	2.6
SIM 2.2.2	SIM	BA-Fe2O3	SIM 2	05.08.2016	0.0048	12.8	0.006	16.2	196.74	1.2	4 521	2.2
SIM 3.1.2	SIM	BA-Fe2O3	SIM 3	08.08.2016	0.0001	19.9	0.002	17.0	1.40	0.7	5 303	2.4
SIM 3.2.2	SIM	BA-Fe2O3	SIM 3	08.08.2016	0.0030	4.0	0.006	33.6	266.11	0.7	5 055	1.2
SIM 4.1.2	SIM	BA-Fe2O3	SIM 4	09.08.2016	0.0014	37.3	0.007	20.5	3.43	3.7	4 650	2.5
SIM 4.2.2	SIM	BA-Fe2O3	SIM 4	09.08.2016	0.0003	46.2	0.003	22.0	23.88	1.5	4 353	0.7
SIM 5.1.2	SIM	BA-Fe2O3	SIM 5	10.08.2016	0.0024	45.6	0.008	20.5	43.27	1.1	4 755	1.5
SIM 5.2.2	SIM	BA-Fe2O3	SIM 5	10.08.2016	0.0010	35.5	0.004	19.6	25.37	3.2	4 394	0.9
SIM 6.1.2	SIM	BA-Fe2O3	SIM 6	11.08.2016	0.0018	8.2	0.007	10.2	4.65	2.3	4 779	2.4
SIM 6.2.2	SIM	BA-Fe2O3	SIM 6	11.08.2016	0.0064	34.8	0.001	22.4	208.68	1.7	4 375	1.9
SIM 7.1.2	SIM	BA-Fe2O3	SIM 7	12.08.2016	0.0014	27.4	0.003	15.3	6.81	3.4	4 502	1.3
SIM 7.2.2	SIM	BA-Fe2O3	SIM 7	12.08.2016	0.0010	32.2	0.003	19.7	43.32	2.0	4 347	1.1
SIM 7.3.2	SIM	BA-Fe2O3	SIM 7	13.08.2016	0.0006	28.1	0.008	23.4	2.79	1.0	4 641	3.1
SIM 8.1.2	SIM	BA-Fe2O3	SIM 8	15.08.2016	0.0037	27.7	0.007	24.7	8.95	0.6	7 216	0.8
SIM 8.2.2	SIM	BA-Fe2O3	SIM 8	15.08.2016	0.0064	27.7	0.000	9.3	212.48	1.6	4 682	2.3
SIM 8.3.2	SIM	BA-Fe2O3	SIM 8	16.08.2016	0.0015	11.9	0.003	21.8	6.48	2.3	4 617	2.7

SIM 9.1.2	SIM	BA-Fe2O3	SIM 9	19.08.2016	0.0031	13.7	0.002	5.6	43.66	2.2	6 485	0.4
SIM 9.2.2	SIM	BA-Fe2O3	SIM 9	19.08.2016	0.0021	46.1	0.001	10.7	26.30	1.9	4 540	3.0
SIM 9.3.2	SIM	BA-Fe2O3	SIM 9	20.08.2016	0.0007	21.8	0.003	29.3	5.32	0.6	4 539	1.8
SIM 10.1.2	SIM	BA-Fe2O3	SIM 10	22.08.2016	0.0001	54.9	0.000	34.5	4.10	4.8	6 054	2.7
SIM 10.2.2	SIM	BA-Fe2O3	SIM 10	22.08.2016	0.0024	31.0	0.011	6.2	54.39	2.9	4 589	1.0
SIM 11.1.2	SIM	BA-Fe2O3	SIM 11	23.08.2016	0.0011	50.3	0.001	34.3	7.44	1.3	4 619	1.7
SIM 11.2.2	SIM	BA-Fe2O3	SIM 11	23.08.2016	0.0034	30.3	0.002	4.1	45.00	4.3	4 341	0.4
SIM 12.1.2	SIM	BA-Fe2O3	SIM 12	24.08.2016	0.0005	45.3	0.001	10.7	2.08	1.4	4 472	1.6
SIM 12.2.2	SIM	BA-Fe2O3	SIM 12	24.08.2016	0.0011	36.6	0.007	3.6	25.12	1.5	4 464	0.6
SIM 12.3.2	SIM	BA-Fe2O3	SIM 12	25.08.2016	0.0006	17.9	0.003	6.9	8.52	3.6	4 682	1.7
SIM 13.2.2	SIM	BA-Fe2O3	SIM 13	01.09.2016	0.0033	16.6	0.002	17.8	56.01	1.9	4 969	1.6
SIM 14.2.2	SIM	BA-Fe2O3	SIM 14	15.09.2016	0.0046	20.3	0.006	31.7	40.95	2.0	4 750	0.8
SIM 15.2.2	SIM	BA-Fe2O3	SIM 15	06.10.2016	0.0061	15.2	0.001	4.3	187.87	2.8	4 810	0.4
SIM 16.2.2	SIM	BA-Fe2O3	SIM 16	10.11.2016	0.0037	46.5	0.012	2.7	129.85	0.9	4 591	3.9

					Mg25(MR) Conc. µg/L	Mg25(MR) RSD, %	Al27(MR) Conc. µg/L	Al27(MR) RSD, %	Si29(MR) Conc. µg/L	Si29(MR) RSD, %	P31(MR) Conc. µg/L	P31(MR) RSD, %
Sample name	Type	Media	SIM#	Date SIM								
B1.2	SIM	BA-Fe2O3	B1	25.07.2016	1 073	2.5	812.3	0.3	1 309	0.9	49.1	5.2
B1.2	SIM	BA-Fe2O3	B1	25.07.2016	1 060	0.8	812.0	3.4	1 282	0.8	48.0	2.7
B2.2	SIM	BA-Fe2O3	B2	27.07.2016	1 054	2.1	207.2	3.0	468	0.6	37.9	2.3
B3.2	SIM	BA-Fe2O3	B3	29.07.2016	1 083	1.5	133.3	1.3	577	1.4	30.9	1.8
B3.2	SIM	BA-Fe2O3	B3	29.07.2016	1 077	1.0	133.3	1.7	573	2.2	31.1	3.0
SIM 1.1.2	SIM	BA-Fe2O3	SIM 1	04.08.2016	944	2.4	70.8	2.8	581	1.0	29.5	2.1
SIM 1.2.2	SIM	BA-Fe2O3	SIM 1	04.08.2016	1 062	1.0	269.3	2.8	1 605	1.4	34.9	5.3
SIM 2.1.2	SIM	BA-Fe2O3	SIM 2	05.08.2016	1 078	0.8	106.9	2.2	963	1.7	33.4	3.6
SIM 2.1.2	SIM	BA-Fe2O3	SIM 2	05.08.2016	1 082	2.6	106.9	2.1	961	0.5	32.2	3.1

SIM 2.2.2	SIM	BA-Fe2O3	SIM 2	05.08.2016	1 059	1.3	140.6	2.1	1 315	0.6	32.0	2.0
SIM 3.1.2	SIM	BA-Fe2O3	SIM 3	08.08.2016	800	0.9	64.4	1.5	365	0.6	32.6	1.3
SIM 3.2.2	SIM	BA-Fe2O3	SIM 3	08.08.2016	1 068	2.6	322.0	3.0	1 745	1.5	41.0	0.6
SIM 4.1.2	SIM	BA-Fe2O3	SIM 4	09.08.2016	1 098	1.9	26.3	3.1	742	1.1	35.0	0.6
SIM 4.2.2	SIM	BA-Fe2O3	SIM 4	09.08.2016	1 003	1.4	9.4	0.8	460	2.2	24.4	1.6
SIM 5.1.2	SIM	BA-Fe2O3	SIM 5	10.08.2016	1 133	0.9	384.2	2.2	2 175	0.5	52.8	0.9
SIM 5.2.2	SIM	BA-Fe2O3	SIM 5	10.08.2016	1 021	1.3	11.9	3.1	551	0.3	24.5	1.4
SIM 6.1.2	SIM	BA-Fe2O3	SIM 6	11.08.2016	1 101	2.1	18.7	0.9	770	2.4	30.9	5.3
SIM 6.2.2	SIM	BA-Fe2O3	SIM 6	11.08.2016	1 002	1.2	69.9	2.6	1 332	2.4	28.7	1.9
SIM 7.1.2	SIM	BA-Fe2O3	SIM 7	12.08.2016	1 022	2.2	9.0	0.9	742	2.8	29.9	4.2
SIM 7.2.2	SIM	BA-Fe2O3	SIM 7	12.08.2016	992	2.2	7.0	1.6	659	0.7	25.9	4.2
SIM 7.3.2	SIM	BA-Fe2O3	SIM 7	13.08.2016	1 023	2.0	34.6	0.7	1 195	1.9	31.1	1.0
SIM 8.1.2	SIM	BA-Fe2O3	SIM 8	15.08.2016	1 539	2.0	337.0	1.4	2 432	1.8	54.8	2.5
SIM 8.2.2	SIM	BA-Fe2O3	SIM 8	15.08.2016	1 042	2.2	101.0	0.5	1 515	1.6	31.8	1.2
SIM 8.3.2	SIM	BA-Fe2O3	SIM 8	16.08.2016	1 045	3.0	26.8	0.5	1 144	2.7	34.6	2.4
SIM 9.1.2	SIM	BA-Fe2O3	SIM 9	19.08.2016	1 284	3.1	400.0	3.6	2 369	2.2	56.6	2.7
SIM 9.2.2	SIM	BA-Fe2O3	SIM 9	19.08.2016	1 055	4.2	24.0	4.5	821	1.3	29.0	4.7
SIM 9.3.2	SIM	BA-Fe2O3	SIM 9	20.08.2016	1 115	2.6	22.4	0.5	981	1.0	32.7	2.5
SIM 10.1.2	SIM	BA-Fe2O3	SIM 10	22.08.2016	1 221	1.6	45.9	2.6	1 017	1.4	31.9	3.6
SIM 10.2.2	SIM	BA-Fe2O3	SIM 10	22.08.2016	1 106	1.5	11.8	0.6	866	1.9	27.7	2.7
SIM 11.1.2	SIM	BA-Fe2O3	SIM 11	23.08.2016	1 083	1.2	18.5	3.7	1 275	1.3	34.8	2.9
SIM 11.2.2	SIM	BA-Fe2O3	SIM 11	23.08.2016	995	2.5	8.2	0.8	812	1.1	24.3	5.6
SIM 12.1.2	SIM	BA-Fe2O3	SIM 12	24.08.2016	1 083	1.3	20.2	1.4	1 267	2.6	33.8	0.8
SIM 12.2.2	SIM	BA-Fe2O3	SIM 12	24.08.2016	987	0.7	5.9	3.0	583	1.7	22.2	2.7
SIM 12.3.2	SIM	BA-Fe2O3	SIM 12	25.08.2016	1 026	1.9	6.8	4.0	1 194	2.5	32.0	1.1
SIM 13.2.2	SIM	BA-Fe2O3	SIM 13	01.09.2016	1 092	4.0	10.6	2.9	679	1.9	26.7	1.5
SIM 14.2.2	SIM	BA-Fe2O3	SIM 14	15.09.2016	1 155	0.7	8.9	2.2	552	2.7	25.7	2.9
SIM 15.2.2	SIM	BA-Fe2O3	SIM 15	06.10.2016	1 145	2.1	134.81	1.2	1 472	2.1	38	2.3
SIM 16.2.2	SIM	BA-Fe2O3	SIM 16	10.11.2016	1 138	2.6	50.58	1.6	777	2.8	29	2.6

					S34(MR)		Cl35(MR)		K39(MR)		Ca44(MR)	
					Conc. µg/L	RSD, %	Conc. µg/L	RSD, %	Conc. µg/L	RSD, %	Conc. µg/L	RSD, %
Sample name	Type	Media	SIM#	Date SIM								
B1.2	SIM	BA-Fe2O3	B1	25.07.2016	16 998	0.6	18 806	1.7	7 443	3.6	42 560	1.1
B1.2	SIM	BA-Fe2O3	B1	25.07.2016	16 740	0.9	18 793	1.2	7 246	2.1	41 405	0.8
B2.2	SIM	BA-Fe2O3	B2	27.07.2016	6 461	0.3	15 293	2.1	2 017	4.8	22 127	1.8
B3.2	SIM	BA-Fe2O3	B3	29.07.2016	3 436	0.5	16 105	0.6	1 253	2.6	17 908	1.8
B3.2	SIM	BA-Fe2O3	B3	29.07.2016	3 493	2.8	15 728	0.6	1 252	1.4	17 999	1.7
SIM 1.1.2	SIM	BA-Fe2O3	SIM 1	04.08.2016	2 416	3.6	14 776	3.3	1 694	2.8	15 488	2.8
SIM 1.2.2	SIM	BA-Fe2O3	SIM 1	04.08.2016	1 600	1.2	16 438	3.0	1 267	1.0	26 762	2.8
SIM 2.1.2	SIM	BA-Fe2O3	SIM 2	05.08.2016	2 020	1.8	14 115	0.1	1 148	1.9	15 061	1.8
SIM 2.1.2	SIM	BA-Fe2O3	SIM 2	05.08.2016	2 027	1.3	14 555	1.3	1 156	2.8	14 608	2.3
SIM 2.2.2	SIM	BA-Fe2O3	SIM 2	05.08.2016	1 222	3.1	14 149	1.8	907	1.8	26 441	1.7
SIM 3.1.2	SIM	BA-Fe2O3	SIM 3	08.08.2016	7 765	1.5	13 297	4.7	1 604	3.6	18 847	1.7
SIM 3.2.2	SIM	BA-Fe2O3	SIM 3	08.08.2016	2 291	0.9	14 385	2.2	1 294	3.5	26 301	1.1
SIM 4.1.2	SIM	BA-Fe2O3	SIM 4	09.08.2016	1 788	1.6	14 096	1.0	1 126	2.6	15 517	1.9
SIM 4.2.2	SIM	BA-Fe2O3	SIM 4	09.08.2016	809	4.1	13 574	1.3	795	0.6	13 122	0.0
SIM 5.1.2	SIM	BA-Fe2O3	SIM 5	10.08.2016	2 148	2.8	14 443	3.6	1 131	2.8	28 668	0.7
SIM 5.2.2	SIM	BA-Fe2O3	SIM 5	10.08.2016	848	0.5	14 073	3.2	724	1.2	14 739	1.6
SIM 6.1.2	SIM	BA-Fe2O3	SIM 6	11.08.2016	1 656	0.5	14 316	1.9	1 028	1.8	18 702	1.6
SIM 6.2.2	SIM	BA-Fe2O3	SIM 6	11.08.2016	1 018	6.8	13 871	3.1	691	4.2	26 298	1.6
SIM 7.1.2	SIM	BA-Fe2O3	SIM 7	12.08.2016	1 552	1.7	13 791	1.2	956	5.5	16 035	1.0
SIM 7.2.2	SIM	BA-Fe2O3	SIM 7	12.08.2016	868	5.3	13 884	3.5	764	1.1	16 353	2.1
SIM 7.3.2	SIM	BA-Fe2O3	SIM 7	13.08.2016	1 391	2.1	13 961	1.7	757	2.4	16 701	3.2
SIM 8.1.2	SIM	BA-Fe2O3	SIM 8	15.08.2016	12 779	1.3	20 731	1.2	1 373	3.5	39 658	1.5
SIM 8.2.2	SIM	BA-Fe2O3	SIM 8	15.08.2016	1 185	3.2	14 203	2.4	802	4.4	25 481	3.4

SIM 8.3.2	SIM	BA-Fe2O3	SIM 8	16.08.2016	1 515	2.8	14 206	2.8	997	4.9	20 283	1.6
SIM 9.1.2	SIM	BA-Fe2O3	SIM 9	19.08.2016	6 743	2.0	16 068	2.3	1 385	5.1	31 247	0.9
SIM 9.2.2	SIM	BA-Fe2O3	SIM 9	19.08.2016	1 114	0.2	14 122	1.6	966	1.1	16 065	2.8
SIM 9.3.2	SIM	BA-Fe2O3	SIM 9	20.08.2016	1 271	1.5	14 217	1.9	908	0.8	15 222	2.6
SIM 10.1.2	SIM	BA-Fe2O3	SIM 10	22.08.2016	4 971	2.5	15 257	2.7	1 296	0.8	17 940	1.5
SIM 10.2.2	SIM	BA-Fe2O3	SIM 10	22.08.2016	922	2.6	14 477	0.8	923	5.1	17 011	2.9
SIM 11.1.2	SIM	BA-Fe2O3	SIM 11	23.08.2016	1 361	3.6	14 185	3.1	1 015	2.8	18 684	1.2
SIM 11.2.2	SIM	BA-Fe2O3	SIM 11	23.08.2016	774	0.3	13 975	2.6	885	2.3	14 078	0.7
SIM 12.1.2	SIM	BA-Fe2O3	SIM 12	24.08.2016	1 160	1.4	14 309	2.2	735	3.1	18 345	1.3
SIM 12.2.2	SIM	BA-Fe2O3	SIM 12	24.08.2016	708	5.5	14 500	2.1	669	2.8	13 549	3.6
SIM 12.3.2	SIM	BA-Fe2O3	SIM 12	25.08.2016	1 355	7.6	14 557	5.3	1 097	2.6	21 045	1.3
SIM 13.2.2	SIM	BA-Fe2O3	SIM 13	01.09.2016	1 615	1.4	14 455	5.0	994	3.7	16 267	2.0
SIM 14.2.2	SIM	BA-Fe2O3	SIM 14	15.09.2016	1 312	0.8	14 369	0.7	870	5.3	16 454	3.7
SIM 15.2.2	SIM	BA-Fe2O3	SIM 15	06.10.2016	1 641	1.8	15 353	4.4	1 024	0.7	24 171	0.3
SIM 16.2.2	SIM	BA-Fe2O3	SIM 16	10.11.2016	1 506	2.4	14 717	4.6	1 028	5.1	20 775	2.7

					Cr53(MR)		Mn55(MR)		Fe56(MR)		Ni60(MR)	
					Conc. µg/L	RSD, %	Conc. µg/L	RSD, %	Conc. µg/L	RSD, %	Conc. µg/L	RSD, %
Sample name	Type	Media	SIM#	Date SIM								
B1.2	SIM	BA-Fe2O3	B1	25.07.2016	1.82	12.4	3.34	140.3	1.49	8.7	2.23	7.4
B1.2	SIM	BA-Fe2O3	B1	25.07.2016	2.00	6.1	0.55	8.8	1.46	2.7	2.26	13.9
B2.2	SIM	BA-Fe2O3	B2	27.07.2016	0.24	9.3	0.53	9.5	1.29	2.6	4.58	5.4
B3.2	SIM	BA-Fe2O3	B3	29.07.2016	0.09	27.7	0.38	7.9	0.12	3.4	3.48	2.7
B3.2	SIM	BA-Fe2O3	B3	29.07.2016	0.16	20.4	0.38	4.2	0.14	5.7	3.52	8.1
SIM 1.1.2	SIM	BA-Fe2O3	SIM 1	04.08.2016	0.13	8.9	0.27	2.2	0.49	7.6	3.56	5.3
SIM 1.2.2	SIM	BA-Fe2O3	SIM 1	04.08.2016	0.32	12.0	1.67	0.7	0.52	0.9	57.66	1.5
SIM 2.1.2	SIM	BA-Fe2O3	SIM 2	05.08.2016	0.08	11.0	0.39	3.2	0.83	5.1	9.91	3.6

SIM 2.1.2	SIM	BA-Fe2O3	SIM 2	05.08.2016	0.08	22.6	0.38	10.6	0.78	4.8	9.96	3.2
SIM 2.2.2	SIM	BA-Fe2O3	SIM 2	05.08.2016	0.16	25.5	2.53	1.4	0.87	2.2	154.89	3.5
SIM 3.1.2	SIM	BA-Fe2O3	SIM 3	08.08.2016	0.42	8.7	0.26	6.3	0.18	8.8	3.93	4.6
SIM 3.2.2	SIM	BA-Fe2O3	SIM 3	08.08.2016	0.44	9.0	1.51	3.6	3.48	0.5	46.52	0.9
SIM 4.1.2	SIM	BA-Fe2O3	SIM 4	09.08.2016	0.09	11.6	0.38	3.3	0.22	8.9	11.58	4.1
SIM 4.2.2	SIM	BA-Fe2O3	SIM 4	09.08.2016	0.06	25.0	0.91	7.7	0.28	10.2	125.03	0.9
SIM 5.1.2	SIM	BA-Fe2O3	SIM 5	10.08.2016	0.39	29.4	1.23	1.9	1.17	5.5	21.81	1.6
SIM 5.2.2	SIM	BA-Fe2O3	SIM 5	10.08.2016	0.07	19.9	1.10	1.8	0.21	6.8	141.74	1.8
SIM 6.1.2	SIM	BA-Fe2O3	SIM 6	11.08.2016	0.23	20.5	0.64	2.5	0.15	6.7	23.76	3.2
SIM 6.2.2	SIM	BA-Fe2O3	SIM 6	11.08.2016	0.11	2.8	3.64	1.7	0.38	7.1	301.16	0.9
SIM 7.1.2	SIM	BA-Fe2O3	SIM 7	12.08.2016	0.07	21.8	0.63	4.5	0.32	6.6	29.21	2.5
SIM 7.2.2	SIM	BA-Fe2O3	SIM 7	12.08.2016	0.05	16.7	1.79	4.1	0.40	4.4	228.33	1.7
SIM 7.3.2	SIM	BA-Fe2O3	SIM 7	13.08.2016	0.06	31.5	0.77	6.5	0.30	2.1	38.41	1.3
SIM 8.1.2	SIM	BA-Fe2O3	SIM 8	15.08.2016	3.00	7.0	2.00	1.0	0.73	3.4	31.53	2.7
SIM 8.2.2	SIM	BA-Fe2O3	SIM 8	15.08.2016	0.19	9.7	4.66	51.4	0.44	2.8	242.56	0.6
SIM 8.3.2	SIM	BA-Fe2O3	SIM 8	16.08.2016	0.08	3.2	0.88	2.8	1.00	2.7	26.64	1.3
SIM 9.1.2	SIM	BA-Fe2O3	SIM 9	19.08.2016	1.74	6.7	1.03	8.7	0.57	7.6	18.32	2.4
SIM 9.2.2	SIM	BA-Fe2O3	SIM 9	19.08.2016	0.03	37.7	0.72	3.3	0.36	12.0	44.96	1.0
SIM 9.3.2	SIM	BA-Fe2O3	SIM 9	20.08.2016	0.02	22.2	0.50	3.0	0.20	1.6	18.53	2.9
SIM 10.1.2	SIM	BA-Fe2O3	SIM 10	22.08.2016	0.29	4.6	0.25	9.0	0.10	4.9	10.38	3.6
SIM 10.2.2	SIM	BA-Fe2O3	SIM 10	22.08.2016	0.05	27.7	1.35	1.7	0.40	5.2	138.40	1.2
SIM 11.1.2	SIM	BA-Fe2O3	SIM 11	23.08.2016	0.13	15.8	0.57	1.9	0.16	7.5	24.05	2.7
SIM 11.2.2	SIM	BA-Fe2O3	SIM 11	23.08.2016	0.03	24.0	1.18	3.1	0.37	1.3	175.09	3.0
SIM 12.1.2	SIM	BA-Fe2O3	SIM 12	24.08.2016	0.11	18.2	0.76	5.9	0.27	8.0	43.82	4.5
SIM 12.2.2	SIM	BA-Fe2O3	SIM 12	24.08.2016	0.00	23.1	1.40	4.8	0.30	2.5	292.00	4.1
SIM 12.3.2	SIM	BA-Fe2O3	SIM 12	25.08.2016	0.10	10.1	1.03	5.2	0.26	4.0	55.79	0.4
SIM 13.2.2	SIM	BA-Fe2O3	SIM 13	01.09.2016	0.04	27.9	0.60	5.1	0.41	7.1	61.07	2.1
SIM 14.2.2	SIM	BA-Fe2O3	SIM 14	15.09.2016	0.08	11.6	0.66	4.8	0.42	3.6	145.10	2.2
SIM 15.2.2	SIM	BA-Fe2O3	SIM 15	06.10.2016	0.24	10.1	0.73	4.3	1.30	6.0	165.52	2.1

SIM 16.2.2	SIM	BA-Fe2O3	SIM 16	10.11.2016	0.10	10.2	0.39	5.1	0.30	2.9	198.26	0.4

					Cu63(MR)		Zn66(MR)		Sb121(MR)		As75(HR)	
					Conc. µg/L	RSD, %	Conc. µg/L	RSD, %	Conc. µg/L	RSD, %	Conc. µg/L	RSD, %
Sample name	Type	Media	SIM #	Date SIM								
B1.2	SIM	BA-Fe2O3	B1	25.07.2016	6.44	7.5	1.18	20.1	11.05	3.2	1.78	16.0
B1.2	SIM	BA-Fe2O3	B1	25.07.2016	6.78	4.0	1.23	3.2	10.80	2.7	1.71	4.4
B2.2	SIM	BA-Fe2O3	B2	27.07.2016	15.85	1.8	1.63	11.6	4.83	4.2	1.12	8.0
B3.2	SIM	BA-Fe2O3	B3	29.07.2016	6.16	2.1	0.78	17.2	3.07	1.2	0.98	9.3
B3.2	SIM	BA-Fe2O3	B3	29.07.2016	6.19	3.1	0.87	7.7	3.09	1.8	1.08	5.6
SIM 1.1.2	SIM	BA-Fe2O3	SIM 1	04.08.2016	21.44	4.1	1.19	15.8	3.32	3.9	1.00	10.2
SIM 1.2.2	SIM	BA-Fe2O3	SIM 1	04.08.2016	145.14	1.4	16.39	4.5	2.24	1.0	0.95	9.2
SIM 2.1.2	SIM	BA-Fe2O3	SIM 2	05.08.2016	16.17	1.7	0.41	28.1	2.11	3.0	0.78	4.4
SIM 2.1.2	SIM	BA-Fe2O3	SIM 2	05.08.2016	16.02	3.2	0.52	20.4	2.19	3.4	0.81	14.2
SIM 2.2.2	SIM	BA-Fe2O3	SIM 2	05.08.2016	114.03	0.6	20.61	4.6	1.22	7.1	0.58	7.8
SIM 3.1.2	SIM	BA-Fe2O3	SIM 3	08.08.2016	13.24	1.9	0.56	16.0	5.79	0.4	0.78	2.4
SIM 3.2.2	SIM	BA-Fe2O3	SIM 3	08.08.2016	325.90	1.8	20.24	3.4	3.76	2.6	1.09	7.9
SIM 4.1.2	SIM	BA-Fe2O3	SIM 4	09.08.2016	26.34	1.8	1.13	3.9	2.33	3.5	0.82	14.4
SIM 4.2.2	SIM	BA-Fe2O3	SIM 4	09.08.2016	89.81	7.6	10.82	6.0	0.69	3.0	0.25	10.1
SIM 5.1.2	SIM	BA-Fe2O3	SIM 5	10.08.2016	86.32	4.2	5.19	7.1	3.85	4.0	1.42	8.7
SIM 5.2.2	SIM	BA-Fe2O3	SIM 5	10.08.2016	66.44	3.0	6.69	6.5	0.73	8.1	0.27	23.9
SIM 6.1.2	SIM	BA-Fe2O3	SIM 6	11.08.2016	32.82	1.7	2.24	10.1	2.32	4.4	0.84	6.8
SIM 6.2.2	SIM	BA-Fe2O3	SIM 6	11.08.2016	92.39	2.0	39.09	2.2	0.82	5.1	0.42	9.5
SIM 7.1.2	SIM	BA-Fe2O3	SIM 7	12.08.2016	37.48	1.5	1.82	10.8	1.96	1.2	0.71	9.5
SIM 7.2.2	SIM	BA-Fe2O3	SIM 7	12.08.2016	108.32	2.4	20.27	5.2	0.70	1.8	0.27	23.8
SIM 7.3.2	SIM	BA-Fe2O3	SIM 7	13.08.2016	20.52	2.8	0.95	29.3	1.72	4.7	0.59	14.9
SIM 8.1.2	SIM	BA-Fe2O3	SIM 8	15.08.2016	33.51	3.5	5.29	5.9	10.81	3.2	1.64	9.9
SIM 8.2.2	SIM	BA-Fe2O3	SIM 8	15.08.2016	127.48	1.3	36.49	2.2	1.59	1.2	0.45	3.1

SIM 8.3.2	SIM	BA-Fe2O3	SIM 8	16.08.2016	41.08	2.5	2.28	3.9	3.13	1.2	0.88	12.1
SIM 9.1.2	SIM	BA-Fe2O3	SIM 9	19.08.2016	80.35	1.5	6.35	0.7	11.38	2.1	1.84	1.3
SIM 9.2.2	SIM	BA-Fe2O3	SIM 9	19.08.2016	80.28	2.4	5.77	14.2	1.75	6.7	0.52	13.0
SIM 9.3.2	SIM	BA-Fe2O3	SIM 9	20.08.2016	32.06	2.1	1.98	6.9	1.92	4.1	0.64	11.5
SIM 10.1.2	SIM	BA-Fe2O3	SIM 10	22.08.2016	24.64	2.6	1.68	8.0	7.22	1.1	1.01	9.3
SIM 10.2.2	SIM	BA-Fe2O3	SIM 10	22.08.2016	135.04	3.7	17.11	2.3	1.42	2.7	0.40	6.0
SIM 11.1.2	SIM	BA-Fe2O3	SIM 11	23.08.2016	40.24	4.1	2.70	10.1	2.81	2.0	0.89	14.9
SIM 11.2.2	SIM	BA-Fe2O3	SIM 11	23.08.2016	120.22	0.9	17.20	5.0	0.76	5.8	0.21	40.5
SIM 12.1.2	SIM	BA-Fe2O3	SIM 12	24.08.2016	17.60	3.1	1.39	8.9	1.64	6.4	0.66	11.7
SIM 12.2.2	SIM	BA-Fe2O3	SIM 12	24.08.2016	54.58	2.5	18.40	1.0	0.44	8.3	0.18	25.3
SIM 12.3.2	SIM	BA-Fe2O3	SIM 12	25.08.2016	42.57	1.0	3.94	8.6	2.25	1.5	0.69	12.3
SIM 13.2.2	SIM	BA-Fe2O3	SIM 13	01.09.2016	185.25	1.9	23.85	3.3	2.62	4.7	0.36	18.4
SIM 14.2.2	SIM	BA-Fe2O3	SIM 14	15.09.2016	102.00	0.9	12.05	1.6	1.80	3.2	0.42	1.5
SIM 15.2.2	SIM	BA-Fe2O3	SIM 15	06.10.2016	150.3	2.8	21.6	2.2	71.3	1.9	0.801	14.1
SIM 16.2.2	SIM	BA-Fe2O3	SIM 16	10.11.2016	163.1	3.0	26.1	4.6	61.8	1.3	0.650	8.0

					Cd114(LR)		Hg202(LR)		Pb208(LR)		Na23(MR)	
					Conc.		Conc.		Conc.		Conc.	
Sample name	Type	Media	SIM#	Date SIM	µg/L	RSD, %	µg/L	RSD, %	µg/L	RSD, %	µg/L	RSD, %
B1.6	REF	BA-Fe2O3	B1	25.07.2016	0.0009	3.2	0.0031	8.4	0.75	4.7	5 323	3.8
B2.6	REF	BA-Fe2O3	B2	27.07.2016	0.0009	41.3	0.0002	17.6	1.86	0.5	5 057	0.5
B3.6	REF	BA-Fe2O3	B3	29.07.2016	0.0005	16.0	0.0001	5.8	0.71	3.6	3 996	0.2
SIM 1.1.6	REF	BA-Fe2O3	SIM 1	04.08.2016	0.0001	41.0	0.0096	21.9	5.39	1.1	5 181	1.7
SIM 2.1.6	REF	BA-Fe2O3	SIM 2	05.08.2016	0.0011	59.6	0.0046	10.4	3.35	0.4	4 728	2.3
SIM 3.1.6	REF	BA-Fe2O3	SIM 3	08.08.2016	0.0028	19.6	0.0089	4.3	42.44	2.3	6 684	2.3
SIM 4.1.6	REF	BA-Fe2O3	SIM 4	09.08.2016	0.0019	30.1	0.0001	11.0	14.60	1.1	4 707	0.7
SIM 5.1.6	REF	BA-Fe2O3	SIM 5	10.08.2016	0.0014	50.4	0.0085	9.0	18.94	0.9	4 669	0.2
SIM 6.1.6	REF	BA-Fe2O3	SIM 6	11.08.2016	0.0022	40.2	0.0042	23.1	17.76	0.4	4 657	1.8
SIM 7.1.6	REF	BA-Fe2O3	SIM 7	12.08.2016	0.0008	45.0	0.0043	13.0	12.40	0.3	4 689	1.7

SIM 7.3.6	REF	BA-Fe2O3	SIM 7	13.08.2016	0.0004	87.4	0.0092	16.7	2.97	1.7	2 928	2.4
SIM 8.1.6	REF	BA-Fe2O3	SIM 8	15.08.2016	0.0009	50.3	0.0089	6.8	7.26	2.2	5 902	1.3
SIM 8.3.6	REF	BA-Fe2O3	SIM 8	16.08.2016	0.0030	45.5	0.0074	10.7	9.94	2.8	4 683	3.0
SIM 9.1.6	REF	BA-Fe2O3	SIM 9	19.08.2016	0.0019	46.3	0.0001	9.1	11.27	1.3	5 814	2.7
SIM 9.3.6	REF	BA-Fe2O3	SIM 9	20.08.2016	0.0020	18.9	0.0018	7.2	6.10	3.2	4 662	3.4
SIM 10.1.6	REF	BA-Fe2O3	SIM 10	22.08.2016	0.0008	42.6	0.0012	21.4	11.65	3.2	5 139	1.0
SIM 11.1.6	REF	BA-Fe2O3	SIM 11	23.08.2016	0.0001	64.1	0.0000	9.5	10.99	2.4	4 481	2.4
SIM 12.1.6	REF	BA-Fe2O3	SIM 12	24.08.2016	0.0012	64.6	0.0014	5.4	8.39	1.1	4 482	2.2
SIM 12.3.6	REF	BA-Fe2O3	SIM 12	25.08.2016	0.0012	15.5	0.0018	19.7	15.97	2.0	4 622	1.5
SIM 13.3.6	REF	BA-Fe2O3	SIM 13	02.09.2016	0.0011	12.6	0.0076	2.8	21.73	0.6	4 777	4.9
SIM 14.3.6	REF	BA-Fe2O3	SIM 14	16.09.2016	0.0011	24.1	0.0021	11.9	12.53	2.0	4 085	2.7
SIM 15.3.6	**REF**	BA-Fe2O3	SIM 15	07.10.2016	0.0037	23.0	0.0001	7.4	88.28	1.1	4 720	1.5
SIM 15.3.6	**REF**	BA-Fe2O3	SIM 15	07.10.2016	0.0025	12.1	0.0001	1.9	90.45	2.9	4 680	0.6
SIM 16.3.6	REF	BA-Fe2O3	SIM 16	11.11.2016	0.0044	25.0	0.0001	6.4	88.92	1.8	4 487	0.7

Sample name	Type	Media	SIM#	Date SIM	Mg25(MR) Conc. µg/L	Mg25(MR) RSD, %	Al27(MR) Conc. µg/L	Al27(MR) RSD, %	Si29(MR) Conc. µg/L	Si29(MR) RSD, %	P31(MR) Conc. µg/L	P31(MR) RSD, %
B1.6	REF	BA-Fe2O3	B1	25.07.2016	1 065	1.6	209.5	1.8	302	1.7	35.1	3.9
B2.6	REF	BA-Fe2O3	B2	27.07.2016	1 082	1.2	175.2	0.6	482	1.6	31.3	3.1
B3.6	REF	BA-Fe2O3	B3	29.07.2016	822	2.3	57.8	1.4	407	1.5	26.6	1.4
SIM 1.1.6	REF	BA-Fe2O3	SIM 1	04.08.2016	1 104	2.4	96.0	2.2	660	1.1	31.6	3.7
SIM 2.1.6	REF	BA-Fe2O3	SIM 2	05.08.2016	1 079	1.3	130.2	1.0	1 070	1.6	31.6	2.6
SIM 3.1.6	REF	BA-Fe2O3	SIM 3	08.08.2016	1 290	1.0	390.2	2.0	2 096	0.5	47.5	1.5
SIM 4.1.6	REF	BA-Fe2O3	SIM 4	09.08.2016	1 100	0.2	41.6	1.5	868	1.2	27.5	3.1
SIM 5.1.6	REF	BA-Fe2O3	SIM 5	10.08.2016	1 056	0.6	13.2	2.0	781	0.8	30.8	3.3
SIM 6.1.6	REF	BA-Fe2O3	SIM 6	11.08.2016	1 027	1.2	25.6	1.9	1 007	0.7	30.3	1.1
SIM 7.1.6	REF	BA-Fe2O3	SIM 7	12.08.2016	1 047	3.5	30.5	1.6	906	0.1	29.0	2.2
SIM 7.3.6	REF	BA-Fe2O3	SIM 7	13.08.2016	680	3.1	32.6	0.6	857	2.1	27.5	2.5

SIM 8.1.6	REF	BA-Fe2O3	SIM 8	15.08.2016	1 205	1.0	53.4	0.8	988	1.7	33.9	1.9
SIM 8.3.6	REF	BA-Fe2O3	SIM 8	16.08.2016	1 079	3.6	22.1	2.6	1 111	2.1	31.9	2.9
SIM 9.1.6	REF	BA-Fe2O3	SIM 9	19.08.2016	1 161	2.2	20.4	2.1	855	3.3	30.3	1.8
SIM 9.3.6	REF	BA-Fe2O3	SIM 9	20.08.2016	1 106	2.8	59.9	2.4	1 125	1.3	27.2	2.9
SIM 10.1.6	REF	BA-Fe2O3	SIM 10	22.08.2016	1 136	1.6	35.2	2.2	909	0.7	31.9	2.5
SIM 11.1.6	REF	BA-Fe2O3	SIM 11	23.08.2016	1 071	1.7	33.7	1.3	1 155	0.3	27.6	7.2
SIM 12.1.6	REF	BA-Fe2O3	SIM 12	24.08.2016	1 047	1.2	18.8	1.2	1 079	2.1	24.5	1.3
SIM 12.3.6	REF	BA-Fe2O3	SIM 12	25.08.2016	1 046	2.0	6.9	0.5	788	3.5	28.4	1.4
SIM 13.3.6	REF	BA-Fe2O3	SIM 13	02.09.2016	1 062	2.8	5.9	0.5	701	1.7	26.8	2.0
SIM 14.3.6	REF	BA-Fe2O3	SIM 14	16.09.2016	1 007	2.3	21.9	1.0	895	1.1	31.2	3.0
SIM 15.3.6	**REF**	BA-Fe2O3	SIM 15	07.10.2016	1 132	1.8	241.64	2.1	2 069	1.3	46	0.7
SIM 15.3.6	**REF**	BA-Fe2O3	SIM 15	07.10.2016	1 168	2.0	245.98	1.4	2 102	0.7	47	4.4
SIM 16.3.6	REF	BA-Fe2O3	SIM 16	11.11.2016	1 142	2.7	241.35	2.5	2 082	0.8	45	1.5

					S34(MR)		Cl35(MR)		K39(MR)		Ca44(MR)	
					Conc.		Conc.		Conc.		Conc.	
Sample name	Type	Media	SIM#	Date SIM	µg/L	RSD, %	µg/L	RSD, %	µg/L	RSD, %	µg/L	RSD, %
B1.6	REF	BA-Fe2O3	B1	25.07.2016	17 398	1.7	14 449	0.5	2 703	2.2	33 993	2.2
B2.6	REF	BA-Fe2O3	B2	27.07.2016	8 403	1.7	15 742	1.0	1 880	2.5	24 788	0.8
B3.6	REF	BA-Fe2O3	B3	29.07.2016	3 322	1.9	14 051	1.9	1 214	4.3	16 773	2.2
SIM 1.1.6	REF	BA-Fe2O3	SIM 1	04.08.2016	3 338	1.0	16 411	1.7	1 811	5.3	17 916	2.1
SIM 2.1.6	REF	BA-Fe2O3	SIM 2	05.08.2016	2 379	1.1	14 457	3.9	1 164	1.3	15 885	1.0
SIM 3.1.6	REF	BA-Fe2O3	SIM 3	08.08.2016	13 552	0.6	15 600	2.0	2 359	2.4	37 498	1.1
SIM 4.1.6	REF	BA-Fe2O3	SIM 4	09.08.2016	2 226	2.3	13 930	1.9	1 105	1.9	17 914	2.0
SIM 5.1.6	REF	BA-Fe2O3	SIM 5	10.08.2016	1 938	1.6	13 853	1.6	972	4.6	18 614	2.2
SIM 6.1.6	REF	BA-Fe2O3	SIM 6	11.08.2016	1 725	4.8	13 728	2.5	973	2.0	19 074	1.9
SIM 7.1.6	REF	BA-Fe2O3	SIM 7	12.08.2016	1 788	2.6	14 210	1.9	1 011	4.1	17 752	1.7
SIM 7.3.6	REF	BA-Fe2O3	SIM 7	13.08.2016	1 016	1.3	9 157	0.8	549	0.7	12 449	1.2
SIM 8.1.6	REF	BA-Fe2O3	SIM 8	15.08.2016	5 159	1.2	15 232	1.6	1 394	0.7	19 609	3.0

SIM 8.3.6	REF	BA-Fe2O3	SIM 8	16.08.2016	1 581	3.3	14 251	0.5	990	1.9	18 956	0.8
SIM 9.1.6	REF	BA-Fe2O3	SIM 9	19.08.2016	4 851	2.6	15 166	2.9	1 383	2.5	15 514	0.3
SIM 9.3.6	REF	BA-Fe2O3	SIM 9	20.08.2016	1 307	0.9	14 318	1.2	885	4.2	15 034	1.1
SIM 10.1.6	REF	BA-Fe2O3	SIM 10	22.08.2016	2 336	2.5	14 453	1.8	1 192	7.3	15 013	2.0
SIM 11.1.6	REF	BA-Fe2O3	SIM 11	23.08.2016	1 304	2.6	14 446	1.1	949	3.7	15 583	2.4
SIM 12.1.6	REF	BA-Fe2O3	SIM 12	24.08.2016	1 110	2.4	14 161	2.0	685	2.2	15 648	0.6
SIM 12.3.6	REF	BA-Fe2O3	SIM 12	25.08.2016	1 168	2.0	14 080	3.9	860	2.8	17 280	1.6
SIM 13.3.6	REF	BA-Fe2O3	SIM 13	02.09.2016	1 185	2.3	14 278	2.6	982	3.8	15 233	2.4
SIM 14.3.6	REF	BA-Fe2O3	SIM 14	16.09.2016	953	0.6	12 186	1.5	842	3.6	16 444	1.0
SIM 15.3.6	**REF**	BA-Fe2O3	SIM 15	07.10.2016	1 372	3.6	14 725	7.2	1 019	4.0	24 617	2.0
SIM 15.3.6	**REF**	BA-Fe2O3	SIM 15	07.10.2016	1 364	1.9	15 031	2.3	1 012	2.3	24 841	3.3
SIM 16.3.6	REF	BA-Fe2O3	SIM 16	11.11.2016	1 309	2.7	14 469	3.8	1 164	1.8	23 583	1.5

Sample name	Type	Media	SIM#	Date SIM	Cr53(MR) Conc. µg/L	Cr53(MR) RSD, %	Mn55(MR) Conc. µg/L	Mn55(MR) RSD, %	Fe56(MR) Conc. µg/L	Fe56(MR) RSD, %	Ni60(MR) Conc. µg/L	Ni60(MR) RSD, %
B1.6	REF	BA-Fe2O3	B1	25.07.2016	0.75	4.5	0.32	13.0	0.18	2.8	2.89	8.5
B2.6	REF	BA-Fe2O3	B2	27.07.2016	0.29	12.9	0.46	7.4	0.26	8.3	8.00	2.0
B3.6	REF	BA-Fe2O3	B3	29.07.2016	0.14	20.4	0.38	6.6	0.24	1.5	8.00	0.9
SIM 1.1.6	REF	BA-Fe2O3	SIM 1	04.08.2016	0.07	10.2	0.42	2.0	0.36	2.1	10.89	2.6
SIM 2.1.6	REF	BA-Fe2O3	SIM 2	05.08.2016	0.10	21.7	0.77	6.8	0.25	3.9	19.02	1.3
SIM 3.1.6	REF	BA-Fe2O3	SIM 3	08.08.2016	1.75	3.5	1.67	4.4	0.52	4.1	23.53	2.5
SIM 4.1.6	REF	BA-Fe2O3	SIM 4	09.08.2016	0.24	11.7	0.91	3.3	0.44	5.2	56.32	2.0
SIM 5.1.6	REF	BA-Fe2O3	SIM 5	10.08.2016	0.11	16.0	1.04	2.3	0.42	3.2	44.16	3.0
SIM 6.1.6	REF	BA-Fe2O3	SIM 6	11.08.2016	0.21	11.5	1.11	4.6	0.30	2.9	51.17	1.5
SIM 7.1.6	REF	BA-Fe2O3	SIM 7	12.08.2016	0.10	43.8	0.85	4.7	0.18	5.7	37.68	2.9
SIM 7.3.6	REF	BA-Fe2O3	SIM 7	13.08.2016	0.02	18.2	0.55	1.6	0.17	3.6	37.95	4.2
SIM 8.1.6	REF	BA-Fe2O3	SIM 8	15.08.2016	0.67	7.5	0.55	4.7	0.23	2.8	14.62	3.0

SIM 8.3.6	REF	BA-Fe2O3	SIM 8	16.08.2016	0.18	10.0	1.09	3.9	0.38	4.6	34.52	2.3
SIM 9.1.6	REF	BA-Fe2O3	SIM 9	19.08.2016	0.19	6.9	0.25	2.2	0.28	6.8	10.34	3.4
SIM 9.3.6	REF	BA-Fe2O3	SIM 9	20.08.2016	0.04	34.6	0.45	2.2	0.14	9.3	31.65	4.5
SIM 10.1.6	REF	BA-Fe2O3	SIM 10	22.08.2016	0.10	31.5	0.33	3.3	0.18	3.4	12.66	8.2
SIM 11.1.6	REF	BA-Fe2O3	SIM 11	23.08.2016	0.04	2.6	0.44	5.9	0.19	5.0	24.32	5.4
SIM 12.1.6	REF	BA-Fe2O3	SIM 12	24.08.2016	0.03	42.3	0.87	2.6	0.23	11.2	80.98	1.3
SIM 12.3.6	REF	BA-Fe2O3	SIM 12	25.08.2016	0.05	14.9	1.09	8.6	0.27	3.3	70.14	1.9
SIM 13.3.6	REF	BA-Fe2O3	SIM 13	02.09.2016	0.09	16.1	0.54	5.1	6.68	2.4	30.78	0.3
SIM 14.3.6	REF	BA-Fe2O3	SIM 14	16.09.2016	0.11	13.1	0.55	10.2	0.97	2.7	51.11	2.9
SIM 15.3.6	**REF**	BA-Fe2O3	SIM 15	07.10.2016	0.24	18.3	0.65	2.2	1.07	2.0	71.81	1.1
SIM 15.3.6	**REF**	BA-Fe2O3	SIM 15	07.10.2016	0.23	8.7	0.65	0.9	1.14	2.0	72.48	1.3
SIM 16.3.6	REF	BA-Fe2O3	SIM 16	11.11.2016	0.21	21.8	0.44	4.5	0.69	7.7	58.06	1.0

s

Sample name	Type	Media	SIM#	Date SIM	Cu63(MR) Conc. µg/L	Cu63(MR) RSD, %	Zn66(MR) Conc. µg/L	Zn66(MR) RSD, %	Sb121(MR) Conc. µg/L	Sb121(MR) RSD, %	As75(HR) Conc. µg/L	As75(HR) RSD, %
B1.6	REF	BA-Fe2O3	B1	25.07.2016	7.91	2.6	0.78	24.3	8.35	1.4	1.30	7.3
B2.6	REF	BA-Fe2O3	B2	27.07.2016	16.75	5.1	0.65	11.5	5.04	1.2	1.19	3.8
B3.6	REF	BA-Fe2O3	B3	29.07.2016	6.53	1.4	0.43	3.6	2.76	2.5	0.57	7.1
SIM 1.1.6	REF	BA-Fe2O3	SIM 1	04.08.2016	51.46	2.2	1.08	7.8	4.21	4.2	1.06	0.9
SIM 2.1.6	REF	BA-Fe2O3	SIM 2	05.08.2016	21.47	3.5	0.52	25.8	2.81	4.8	0.71	9.6
SIM 3.1.6	REF	BA-Fe2O3	SIM 3	08.08.2016	80.04	0.6	9.10	10.6	11.80	4.4	1.95	0.4
SIM 4.1.6	REF	BA-Fe2O3	SIM 4	09.08.2016	68.30	2.4	7.53	5.6	3.12	3.2	0.70	20.5
SIM 5.1.6	REF	BA-Fe2O3	SIM 5	10.08.2016	82.37	1.6	5.31	8.3	2.71	4.0	0.67	12.5
SIM 6.1.6	REF	BA-Fe2O3	SIM 6	11.08.2016	64.48	2.0	3.93	9.0	2.48	0.2	0.72	3.7
SIM 7.1.6	REF	BA-Fe2O3	SIM 7	12.08.2016	49.07	2.6	2.15	5.8	2.69	3.6	0.74	6.8
SIM 7.3.6	REF	BA-Fe2O3	SIM 7	13.08.2016	18.84	2.6	0.83	20.7	1.78	3.0	0.38	18.2
SIM 8.1.6	REF	BA-Fe2O3	SIM 8	15.08.2016	35.29	1.2	4.30	7.9	8.11	2.7	1.14	14.5
SIM 8.3.6	REF	BA-Fe2O3	SIM 8	16.08.2016	54.83	1.7	3.69	13.8	2.83	5.3	0.80	14.9

SIM 9.1.6	REF	BA-Fe2O3	SIM 9	19.08.2016	50.57	1.5	3.86	7.6	8.26	6.1	0.78	8.3
SIM 9.3.6	REF	BA-Fe2O3	SIM 9	20.08.2016	27.08	6.2	1.14	25.8	1.99	5.0	0.55	11.0
SIM 10.1.6	REF	BA-Fe2O3	SIM 10	22.08.2016	42.33	1.7	2.65	15.2	4.71	5.1	0.98	12.6
SIM 11.1.6	REF	BA-Fe2O3	SIM 11	23.08.2016	40.14	2.6	1.68	13.8	2.57	1.4	0.68	7.9
SIM 12.1.6	REF	BA-Fe2O3	SIM 12	24.08.2016	37.48	2.1	2.56	8.4	1.42	7.1	0.38	28.1
SIM 12.3.6	REF	BA-Fe2O3	SIM 12	25.08.2016	59.69	2.3	4.52	3.7	1.73	3.6	0.49	15.5
SIM 13.3.6	REF	BA-Fe2O3	SIM 13	02.09.2016	85.36	4.9	9.89	8.5	2.16	5.9	0.55	12.9
SIM 14.3.6	REF	BA-Fe2O3	SIM 14	16.09.2016	46.81	4.8	2.85	2.0	2.29	3.8	0.58	3.0
SIM 15.3.6	**REF**	BA-Fe2O3	SIM 15	07.10.2016	139.7	2.3	9.7	2.3	78.5	0.5	1.039	9.5
SIM 15.3.6	**REF**	BA-Fe2O3	SIM 15	07.10.2016	140.5	1.1	9.6	2.2	79.9	1.9	1.133	6.7
SIM 16.3.6	REF	BA-Fe2O3	SIM 16	11.11.2016	128.1	2.8	10.2	3.7	78.1	0.9	1.059	5.5